Universidade Federal Fluminense
Instituto de Física

# *Effective models for confining strings*

Gustavo M. Simões
Niterói, 2022

GUSTAVO M. SIMÕES

# Effective models and confining strings

A thesis submitted to the Physics
Departament - UFF in partial fulfillment
of the requirements for the degree
of Doctor in Sciences (Physics).

Advisor: Prof. Dr. Luis Esteban Oxman

Niterói-RJ
2022

Ficha catalográfica automática - SDC/BIF
Gerada com informações fornecidas pelo autor

S593e Simões, Gustavo Moreira
Effective models and confining strings / Gustavo Moreira Simões ; Luis Esteban Oxman, orientador. Niterói, 2022.
118 f. : il.

Tese (doutorado)-Universidade Federal Fluminense, Niterói, 2022.

DOI: http://dx.doi.org/10.22409/PPGF.2022.d.14752105748

1. Teoria quântica de campos. 2. Confinamento (Física). 3. Produção intelectual. I. Oxman, Luis Esteban, orientador. II. Universidade Federal Fluminense. Instituto de Física. III. Título.

CDD -

Bibliotecário responsável: Debora do Nascimento - CRB7/6368

# Acknowledgments

Four people deserve my special love and gratitude for their immense support and care in the past five years.

Both of my parents, to whom I own everything, from my values in life to my life itself. They are my cornerstone, my foundation.

My advisor, who I could just as easily call mentor or close friend. He has been guiding me through my academic life with zeal and thoughtfulness. Thank you for all your tactful and often humorous directions.

My boyfriend, who has been my light in dark places, even when all the other lights went out. Your emotional support gave me the strength to overcome many hardships in the last few years.

I would like to thank the many friends I made along the way. I thank you for the voyage we shared. Finally, I would like to thank the CNPq for all the funding in the past years. I tried my best to honor this investment and will continue to contribute to the development of science even in these times of turmoil.

*"They asked me how well I understood theoretical physics. I said I had a theoretical degree in physics. They said welcome aboard"*

-Fantastic

**Abstract**

In this thesis, we study confining strings in effective field models of percolating center vortices, which have been observed in lattice simulations of pure Yang-Mills theory. This analysis is based on three main pillars: modelling the ensemble components detected in the lattice, deriving effective field representations, and contrasting the associated properties with Monte Carlo lattice results. The integration of the present knowledge about these areas is essential to get closer to a unified physical picture for confinement. Our findings point to the importance of including the nonoriented center-vortex component and non-Abelian degrees when modelling the center-vortex ensemble measure. These inputs are responsible for the emergence of topological solitons and the possibility of accommodating the asymptotic scaling properties of the confining string tension.

In particular, in a three-dimensional spacetime, we derive an effective field description for the center-element average where center vortices get represented by $N$ flavors of effective Higgs fields transforming in the fundamental representation. This field content is required to accommodate fusion rules where $N$ vortices can be created out of the vacuum. The inclusion of a nonoriented sector, formed by center-vortex worldlines attached to pointlike defects, leads to a discrete set of $Z(N)$ vacua. This type of SSB pattern supports the formation of a stable domain wall between quarks, thus accommodating not only a linear potential but also the Lüscher term. Moreover, after a detailed analysis of the associated field equations, the asymptotic string tension turns out to scale with the quadratic Casimir of the antisymmetric quark representation. These behaviors reproduce those derived from Monte Carlo simulations in $SU(N)$ $3D$ Yang-Mills theory, which lacked understanding in the framework of confinement as due to percolating magnetic defects.

In a four-dimensional spacetime, we explore vortex solutions for a class of effective $SU(N)$ Yang-Mills models with $N^2-1$ Higgs fields in the adjoint representation. Initially, we show that there is a collective behavior that can be expressed in terms of a small $N$-independent number of field profiles. Then, we find a region in parameter space where the nontrivial profiles coincide with those of the Nielsen-Olesen vortex, and the energy scales exactly with the quadratic Casimir. Out of this region, we solve the ansatz equations numerically and find very small deviations from the Casimir law. The coexistence of Abelian-like string profiles and non-Abelian scaling features is welcome, as these properties have been approximately observed in pure YM lattice simulations. At a particular point in parameter space, the stability of this scaling law is supported by a set of BPS equations that provide vortex solutions and their energies for arbitrary representations.

At a fundamental level, we explore a recent approach where the gauge fields are mapped into an auxiliary space. This space can be used to initially determine sectors labeled by center vortices, and then separately fix the gauge on each one of them. In this

thesis, we study this procedure in more detail. We provide examples of configurations belonging to these sectors and discuss the existence of nonabelian degrees of freedom. Then, we discuss the importance of the mapping injectivity, and show that this property holds infinitesimally for typical configurations of the vortex-free sector and for the simplest example in the one-vortex sector. Finally, we show that these examples are free from Gribov copies.

# List of publications

- L. E. Oxman and G. M. Simões, *$k-$strings with exact Casimir law and Abelian-like profiles*, Phys. Rev. D 99 (2019) 016011.

- D. R. Junior, L. E. Oxman, G. M. Simões, *BPS strings and the stability of the asymptotic Casimir law in adjoint flavor-symmetric Yang-Mills-Higgs models*, Phys. Rev. D 102 (2020) 074005.

- D. R. Junior, L. E. Oxman, and G. M. Simões, *3D Yang-Mills confining properties from a non-Abelian ensemble perspective*, JHEP 1 (2020) 180.

- D. Fiorentini, D. R. Junior, L. E. Oxman, G. M. Simões, R. F. Sobreiro, *Study of Gribov copies in a Yang-Mills ensemble*, Phys. Rev. D 103 (2021) 114010.

- David R. Junior, Luis E. Oxman, and Gustavo M. Simões, *From Center-Vortex Ensembles to the Confining Flux Tube*, Universe 7(8) (2021) 253.

# Contents

# Chapter 1

# Introduction

Our knowledge about the elementary particles, as well as three of the four known fundamental interactions, is successfully described by the standard model of particle physics. In particular, the quantitative behavior of the electromagnetic, weak, and strong interactions is encoded in the common language of gauge theories. In the strong sector, an important and intriguing phenomenon regarding the possible asymptotic particle states takes place. When quarks and gluons are created in a collision, they cannot move apart. Instead, they give rise to jets of colorless particles (hadrons) formed by confined quark and gluon degrees of freedom. Although confinement is key for the existence of protons and neutrons, a first-principles understanding of the mechanism underlying this phenomenon is still lacking. At high energies, the detailed scattering properties between quarks and gluons are successfully reproduced by QCD perturbative calculations in the continuum, which are possible thanks to asymptotic freedom. This is in contrast with the status at low-energies, where the validity of quantum chromodynamics (QCD) is well-established from sucessfull computer simulations of the hadron spectrum. This thesis focuses on this type of non-perturbative problem in pure $SU(N)$ Yang–Mills (YM) theory, which is a challenging open problem in contemporary physics. Here again, Monte Carlo simulations provide a direct way to deal with the large quantum fluctuations and compute averages of observables such as the Wilson loop, which is an order parameter for confinement in pure YM theories. As usual, the lattice calculations, as well as the center-vortex ensembles we shall discuss, consider an Euclidean (3d or 4d) spacetime. Unless explicitly stated, this is the metric that will be used throughout this work. For heavy quark probes in an irreducible representation D, the Wilson loop is given by:

$$\mathcal{W}_{\mathrm{D}}(\mathcal{C}_{\mathrm{e}}) = \frac{1}{\mathscr{D}} \operatorname{tr} \mathrm{D} \left( P \left\{ e^{i \int_{\mathcal{C}_{\mathrm{e}}} dx_\mu \, A_\mu(x)} \right\} \right) \ , \tag{1.1}$$

where $\mathscr{D}$ is the dimensionality of D. The closed path $\mathcal{C}_{\mathrm{e}}$ can be thought of as associated to the creation, propagation, and annihilation of a pair of quark/antiquark probes. From a rectangular path, with sides $T$ and $R$, information about the static interquark potential

was obtained from the large $T$ behavior $\langle \mathcal{W}_{\rm D}(\mathcal{C}_{\rm e})\rangle \sim e^{-T\,V_{\rm D}(R)}$. An area law, given by the propagation time $T$ multiplied by the interquark distance $R$, corresponds to a linear confining potential [1] (for a review, see Ref. [2]).

There are many model-independent facts that point to the importance of $Z(N)$, the center of the group $SU(N)$, to describe the confining properties of YM theory. This subgroup elements are given by

$$Z(N) = \left\{ z\,\mathbb{I}_N |\, z \in \mathbb{C},\, z^N = 1 \right\} \ . \tag{1.2}$$

In this regard, the first ideas relating the possible phases to the $Z(N)$ properties of the vacuum were developed in [3]. There, disorder vortex field and string field operators were introduced in (2 + 1)d and (3 + 1)d Minkowski spacetime, respectively. At equal time, they satisfy

$$\hat{\mathcal{W}}_{\rm F}(\mathcal{C}_{\rm e})\,\hat{V}(\mathbf{x}) = e^{i2\pi\,L(\mathbf{x},\mathcal{C}_{\rm e})/N}\,\hat{V}(\mathbf{x})\,\hat{\mathcal{W}}_{\rm F}(\mathcal{C}_{\rm e})\ , \qquad \text{in } (2+1)\text{d}, \tag{1.3}$$

$$\hat{\mathcal{W}}_{\rm F}(\mathcal{C}_{\rm e})\,\hat{V}(\mathcal{C}) = e^{i2\pi\,L(\mathcal{C},\mathcal{C}_{\rm e})/N}\,\hat{V}(\mathcal{C})\,\hat{\mathcal{W}}_{\rm F}(\mathcal{C}_{\rm e})\ , \qquad \text{in } (3+1)\text{d}, \tag{1.4}$$

where the subindex F denotes the fundamental representation, $\mathbf{x} \in \mathbb{R}^2$ ($\mathcal{C} \in \mathbb{R}^3$) is a point (curve) in real space where a thin pointlike (looplike) thin center vortex is created in three (four) dimensional spacetime. $L(\mathbf{x},\mathcal{C}_{\rm e})$ and $L(\mathcal{C},\mathcal{C}_{\rm e})$ are the corresponding linking numbers. An explicit realization of $\hat{V}$ was given by the action $\hat{V}|A\rangle = |A^S\rangle$, where $|A\rangle$ are quantum states with well-defined shape $A_0 = 0, A_i$ $(i = 1, 2, 3)$ at a given time. The field $A^S_\mu$ has the form of a gauge transformation, but performed with a singular phase $S \in SU(N)$. To define the operator $\hat{V}(\mathbf{x})$ (respectively $\hat{V}(\mathcal{C})$), $S$ must change by a center element when going around any spatial closed loop that links $\mathbf{x}$ (respectively $\mathcal{C}$). Spurious singularities may be eliminated by using the adjoint representation $\mathrm{Ad}(S)$, which leaves a physical effect only at the point $\mathbf{x}$, or closed path $\mathcal{C}$, where $\mathrm{Ad}(S)$ is multivalued. Arguments in favor of characterizing confinement as a *magnetic* $Z(N)$ spontaneous symmetry breaking phase (center-vortex condensate),

$$\langle \hat{V}(\mathbf{x})\rangle \neq 0 \quad , \quad \langle \hat{V}(\mathcal{C})\rangle \sim e^{-\mu\,\mathrm{Perimeter}(\mathcal{C})}\ , \tag{1.5}$$

were also given in that work. The lattice also provides direct information about the role played by $Z(N)$ in the confinement/deconfinement phase transition [4]. This is observed in the fundamental Polyakov loops $P_{\mathbf{x}}(\not{\mathcal{A}})$, which are given by Eq. (1.1) computed on a straight path located at a spatial coordinate $\mathbf{x}$ and extending along the Euclidean time-direction. Due to the finite-temperature periodicity conditions, these segments can be thought of as circles. When changing from higher to lower temperatures, the distribution

of the phase factors of $P_{\mathbf{x}}(\mathscr{A})$, for typical Monte Carlo configurations, shows a phase transition. At higher temperatures, for most $\mathbf{x}$, the phase factors are close to one of the center elements $e^{i2\pi k/N}$, $k = 0, \ldots, N-1$. On the other hand, below the transition, they are equally distributed on $Z(N)$, as a function of the spatial site $\mathbf{x}$. As a result, the Monte Carlo calculation gives a transition from a non-vanishing to a vanishing gauge-field average $\langle P_{\mathbf{x}} \rangle$, which is in fact $\mathbf{x}$-independent, where the *electric* $Z(N)$ symmetry is not broken. This corresponds to a transition from a deconfined phase at higher $T$, where the quark free energy is finite, to a confined phase below $T_c$, where the free energy diverges.

The chromoelectric flux tube between external quarks [5, 6, 7, 8, 9, 10, 11, 12] also displays many interesting properties. At intermediate distances, the lattice string tension $\sigma_{\rm I}(\mathrm{D})$, derived from the Wilson loop average $\langle W_{\mathcal{C}} \rangle$[1], scales with the quadratic Casimir $C_2(\mathrm{D})$ of the $SU(N)$ quark representation $D(\cdot)$, see Ref. [13]. That is,

$$\frac{\sigma_{\rm I}(\mathrm{D})}{\sigma_{\rm I}(\mathrm{F})} = \frac{C_2(\mathrm{D})}{C_2(\mathrm{F})} \, , \tag{1.6}$$

where F stands for the fundamental representation. In this work, we will be mainly interested in the behavior at asymptotic distances. In this regime, full Monte Carlo simulations showed the relevance of $Z(N)$ in general Wilson loop simulations. Namely, the string tension only depends on the $N$-ality $k$ of D, which determines how the center $Z(N)$ of $SU(N)$ is realized in the given quark representation [14] ($\mathbb{I}_{\mathcal{D}}$ is a $\mathcal{D} \times \mathcal{D}$ identity)

$$\mathrm{D}\left(e^{i\frac{2\pi}{N}} I\right) = \left(e^{i\frac{2\pi}{N}}\right)^k \mathbb{I}_{\mathscr{D}} \, . \tag{1.7}$$

Regarding the confinement mechanism, lattice calculations aimed at determining the relevant degrees of freedom have been performed for many years. In particular, procedures have been constructed to analyze Monte Carlo $U_\mu(x) \in SU(N)$ link-configurations and extract center projected configurations $Z_\mu(x) \in Z(N)$ [15, 16, 17, 18] (for recent techniques to improve the detection of center vortices, see [19]). A given plaquette is then said to be pierced by a thin center vortex if the product of these center elements along the corresponding links is nontrivial. Observables may then be evaluated by considering vortex-removed and vortex-only configurations. The confining properties are only well described in the latter case [15, 16, 20, 21, 22, 23, 24, 25, 26, 27], [28]-[34]. In the lattice, the analysis and visualization of center-vortex configurations [35] led to important insights regarding the origin of the topological charge density in the YM vacuum. In 3d (4d), thin center vortices are localized on worldlines (worldsheets) $\omega$. In this case, the Wilson loop in Eq. (1.1) yields a center element

$$\mathcal{W}_{\rm D}(\mathcal{C}_{\rm e}) = \mathcal{Z}_{\rm D}(\mathcal{C}_{\rm e}) = \frac{1}{\mathscr{D}} \, \mathrm{tr} \, \left[\mathrm{D}\left(e^{i\frac{2\pi}{N}} I\right)\right]^{\mathrm{L}(\omega, \mathcal{C}_{\rm e})} \, , \tag{1.8}$$

[1] $\mathcal{C}$ is the closed worldline associated with the external quark/antiquark pair.

where $\mathrm{L}(\omega, \mathcal{C}_\mathrm{e})$ is the total linking number between $\omega$ and $\mathcal{C}_\mathrm{e}$. This also applies to thick center vortices, when their cores are completely linked by $\mathcal{C}_\mathrm{e}$. In this case, $\omega$ refers to the thick center-vortex guiding centers. In the scaling limit, where the lattice calculations make contact with the continuum, the density of thin center vortices detected at low temperatures is finite [16, 36]. Furthermore, center vortices percolate and have positive stiffness [37, 38], while the fundamental Wilson loop average over $Z_\mu(x)$ displays an area law. This is in accordance with center-vortex condensation and the Wilson loop confinement criteria. For $SU(2)$, a model based on the projected thin center-vortex ensemble captures 97.7% of the fundamental string tension. On the other hand, the percentage drops to $\sim 62\%$ for $SU(3)$ [39]. One of the most important features of the center-vortex scenario is that it naturally explains asymptotic $N$-ality: the center element contribution in Eq. (1.8) only depends on the $N$-ality of D. For these reasons, it is believed that the confinement mechanism should involve these degrees of freedom. For a recent discussion about this area of research, see [40].

When it comes to accommodating the model-independent full Monte Carlo calculations, some questions arise. In 3d, the full asymptotic string tension dependence on D is very well fitted by the Casimir law [41]

$$\sigma_k^{(3)} = \frac{k(N-k)}{N-1} = \frac{C_2(k\text{-A})}{C_2(\mathrm{F})} \,, \tag{1.9}$$

which is proportional to the lowest quadratic Casimir among those representations with the same $N$-ality $k$ of D, which corresponds to the antisymmetric representation $k$-A. In addition, it is precisely at asymptotic interquark distances where a model based on an ensemble of thin objects should be more reliable. This is different at intermediate distances, where finite-size effects allowed for an explanation of the observed scaling with the Casimir of D [42, 43]. Then, one question is: how to capture the asymptotic law in Eq. (1.9) from an average over percolating thin center-vortices? In 4d, where the available data cannot tell between a Casimir or a Sine law [6]

$$\sigma_k^{(4)} = \frac{k(N-k)}{N-1} \quad \text{vs.} \quad \sigma_k^{(4)} = \frac{\sin k\pi/N}{\sin \pi/N} \,, \tag{1.10}$$

is there any ensemble based on center-vortices that could reproduce one of these behaviors? More importantly, how can one explain this together with the formation of the confining flux tube observed in the lattice? This means reproducing the Lüscher term [5, 7, 8] and the observed transverse field distributions (see [9, 10, 11], and references therein). In this thesis, we shall present some developments aimed at providing a possible answer to these questions.

# Chapter 2

# Context and Motivations

The idea that center vortices are the dominant degrees of freedom in the infrared regime means, in practice, that the Wilson loop average at asymptotic distances may well be captured by modeling the average of the center-elements in Eq. (1.8). This line of research was mainly explored in the lattice [44] by considering an ensemble of fluctuating worldlines (in 3d) or worldsurfaces (in 4d) with tension and stiffness (see also the discussion at the beginning of 2.1.2). For example, in 4d, a theory of fluctuating center-vortex worldsurfaces in four dimensions was introduced by considering the lattice action [44]

$$S_{\rm latt}(\omega) = \mu \mathcal{A}(\omega) + c N_p \ , \tag{2.1}$$

where $\mathcal{A}(\omega)$ is the area of the vortex closed worldsurface $\omega$, formed by a set of plaquettes, and $N_p$ is the number of pairs of neighboring plaquettes of the surface lying on different planes. The latter term, as well as the lattice regularization, contribute to the stiffness of the vortices. This model, initially introduced for $SU(2)$, and then generalized for $SU(3)$ [45], is able to describe important features, such as the confining string tension for fundamental quarks and the order of the deconfinement transition. This type of model can be also formulated in the continuum. The objective is the same, that is, looking for natural ensemble measures to compute center-element averages and compare them with the asymptotic information extracted from the full Monte Carlo average $\langle \mathcal{W}_{\rm D}(\mathcal{C}_e) \rangle$. A successful comparison is expected to give important clues about the underlying mechanism of confinement. When computing center-element averages in the continuum, the simplest model has the form:

$$\langle \mathcal{Z}_{\rm D}(\mathcal{C}_e) \rangle = \mathcal{N} \sum_{\omega} e^{-S(\omega)} \frac{1}{\mathscr{D}} \, {\rm tr} \, \left[ {\rm D} \left( e^{i \frac{2\pi}{N} I} \right) \right]^{{\rm L}(\omega, \mathcal{C}_{\rm e})} \ , \tag{2.2}$$

where $\sum_\omega$ represents the sum over different configurations in a diluted gas of closed worldlines (in 3d) or worldsurfaces (in 4d). The weight factor $e^{-S(\omega)}$ implements the

effect of center-vortex tension ($\mu$) and stiffness ($1/\kappa$) observed in the lattice [37, 38]. More precisely, $S(\omega)$ contains a term proportional to the length or area of $\omega$, and another one proportional to a power of the absolute value of the curvature of $\omega$. See Eq. (D.3) for an explicit formula in 3 dimensions. $S(\omega)$ could also contain interactions with a scalar field $\psi$ that, when integrated with a corresponding weight $W(\psi)$, generates interactions among the variables $\omega$.

Extended models can also be introduced where the defining elements are not only given by $\omega$ but also by additional labels. At the level of the gauge field variables $A_\mu$, the center-vortex sectors can be characterized by different mappings $S_0 \in SU(N)$ containing defects (see 2.2.2). A center vortex with guiding center $\omega$ and magnetic weight $\beta$ is characterized by $S_0 = e^{-i\chi\beta\cdot T}$, $\beta \cdot T \equiv \beta|_q T_q$, where $\chi$ is a multivalued angle that changes by $2\pi$ when going around $\omega$, and $T_q$, $q = 1, \ldots, N-1$ are the Cartan generators. Magnetic weights are defined as $2N\lambda$, where $\lambda$ are weights of the $\mathfrak{su}(N)$ Lie algebra.[1] The general properties of the $\mathfrak{su}(N)$ Lie algebra, associated roots, and weights are summarized in the Appendices A and B. For elementary center vortices, the tuple $\beta$ is one of the magnetic weights $\beta_i$ ($i = 1, \ldots, N$) of the fundamental representation. In the region outside the vortex cores, $A_\mu$ is locally a pure gauge configuration constructed with $S_0$. Then, for fundamental quarks, the contribution to a large loop contained in that region is $i$-independent and given by the elementary center-element $(1/N)\,\mathrm{tr}\left(e^{-i2\pi\beta_i\cdot T}\right) = e^{i2\pi/N}$ to the power $\mathrm{L}(\omega, \mathcal{C}_\mathrm{e})$. Different elementary fluxes may join to form more complex configurations, provided this is done in a way that conserves the flux. For example, $N$ center-vortex guiding centers associated with different magnetic weights $\beta_i$ can be matched. For simplicity, let us consider the $SU(3)$ case in three dimensions and a configuration characterized by $S_0 = e^{i\chi_1\beta_1\cdot T} e^{i\chi_2\beta_2\cdot T}$, where $\chi_1$ and $\chi_2$ are multivalued when going around the closed worldlines $\omega_1$ and $\omega_2$, respectively. These worldlines could meet at a point, then follow a common open line $\gamma$, and again bifurcate to close the corresponding loops. In this case, we would have a pair of fluxes entering the initial point, carrying the fundamental weights $\beta_1, \beta_2$, and a flux leaving along $\gamma$, carrying the weight $\beta_1 + \beta_2$. In $SU(3)$, this sum is an antifundamental weight $-\beta_3$. In other words, there are three fluxes entering the initial point, which carry the three different fundamental weights $\beta_1, \beta_2, \beta_3$. This can be readily generalized to $SU(N)$, where $N$ fluxes carrying the different fundamental weights can meet at a point, as these weights satisfy $\sum_i \beta_i = 0$. Vortices may also be nonoriented [46], in the sense that they may be described by two or more weights. In this case, the center-vortex components with different fundamental weights are interpolated by instantons in 3d and monopole worldlines in 4d. These lower dimensional junctions, which carry a flux of the form $\beta_i - \beta_j$, should be weighted with additional phenomenological terms in $S(\omega)$. Furthermore, in the 4d case, three monopole worldlines carrying fluxes $\beta_i - \beta_j$, $\beta_j - \beta_k$, $\beta_k - \beta_i$ can be matched at a spacetime point. Similar higher-order matching rules are

[1] As they carry a single weight, these vortices are known as oriented in the Cartan subalgebra.

also possible. In what follows, we shall discuss the different ensembles, starting with the simplest possibilities in 3d and 4d (for a brief review, see Ref. [47]).

## 2.1 Abelian effective description of center vortices

In this section, we shall briefly discuss center-vortex ensembles formed by diluted closed worldlines in 3d (see 2.1.1) or worldsurfaces in 4d (see 2.1.2), characterized by no other properties than tension, stiffness, and vortex–vortex interactions. No additional degrees of freedom, matching rules or correlations with lower dimensional objects will be considered here.

### 2.1.1 Three dimensions

In a planar system, thin center vortices are localized on points, so they are created or annihilated by a field operator $\hat{V}(x)$. The emergence of this order parameter can be clearly seen by applying polymer techniques to center-vortex worldlines [48]. In [49], the center-element average for fundamental quarks, over all possible diluted loops, was initially represented in the form

$$\langle \mathcal{Z}_{\rm F}(\mathcal{C}_e)\rangle = \mathcal{N}\int [D\psi]\, e^{-W[\psi]}\, e^{\int_0^\infty \frac{dL}{L}\ \int dx \int du\, Q(x,u,x,u,L)}\ , \tag{2.3}$$

where $Q(x,u,x_0,u_0,L)$ is the integral over all paths with length $L$, starting (ending) at $x_0$ ($x$) with unit tangent vector $u_0$ ($u$), in the presence of scalar and vector sources $\psi$ and $\frac{2\pi}{N}s_\mu$, and weighted by tension and stiffness. The factor $W[\psi] = \frac{\zeta}{2}\int d^3x\, \psi^2(x)$ generates, upon integration of the auxiliary scalar field $\psi$, repulsive contact interactions between the loops with strength given by the parameter $\frac{1}{\zeta}$. Indeed, as in the exponential we have $x = x_0$, $u = u_0$, its expansion generates the diluted loop ensemble. As usual, the factor $1/L$ is to avoid loop overcounting when choosing $x_0$ on a given loop. The external source $s_\mu$ is localized on a surface $S(\mathcal{C}_{\rm e})$ whose border is the Wilson loop. As a consequence, it generates the intersection numbers between the loop-variables in $Q$ and $S(\mathcal{C}_{\rm e})$, which coincide with the different linking-numbers. Using the large-distance behavior of $Q(x,u,x_0,u_0,L)$, which satisfies a Fokker–Planck diffusion equation (given by Eqs. (D.1) and (D.7), with $b_\mu$ Abelian, and $D(\Gamma_\gamma[b_\mu])$ being the complex number $\Gamma_\gamma[b_\mu]$) it was shown that the ensemble average of center elements becomes represented by a complex scalar field $V(x)$,

$$\langle \mathcal{Z}_{\rm F}(\mathcal{C}_e)\rangle \approx \mathcal{N}\int [\mathcal{D}V][\mathcal{D}\bar{V}]\, e^{-\int d^3x \left[\frac{1}{3\kappa}\,\overline{D_\mu V} D_\mu V + \frac{1}{2\zeta}\,(\overline{V}V - v^2)^2\right]}\ ,$$
$$v^2 \propto -\mu\kappa > 0\quad ,\quad D_\mu = \partial_\mu - i\frac{2\pi}{N}s_\mu\ . \tag{2.4}$$

This was obtained for small (positive) stiffness $1/\kappa$ and repulsive contact interactions. The scalar field $V$ is originated due to the approximate behavior of $Q(x, u, x_0, u_0, L)$ in Eq. (D.12), which turns the exponential in Eq. (2.3) into a functional determinant. The squared mass parameter of this field is proportional to $\kappa\mu$, where $\mu$ is the center-vortex tension. For percolating objects ($\mu < 0$), the $U(1)$ symmetry of the effective field theory is spontaneously broken ($\kappa\mu < 0$). Among the consequences, it was obtained that:

1. In the center-vortex condensate, the effective description is dominated by the soft Goldstone modes, $V(x) \sim v\, e^{i\phi(x)}$. Then, the calculation of the center-element average is neither Gaussian nor dominated by a saddle-point, as it involves a compact scalar field $\phi$ and large fluctuations;

2. This is better formulated in the lattice, where the Goldstone mode sector is governed by a 3d XY model with frustration

$$S^{(3)}_{\text{latt}} = \tilde{\beta} \sum_{x,\mu} \text{Re}\left[1 - e^{i\gamma(x+\hat{\mu})} e^{-i\gamma(x)} e^{-i\alpha_\mu(x)}\right] \ . \tag{2.5}$$

   The external source in Eq. (2.4) translates into the frustration $e^{i\alpha_\mu(\mathbf{x})} = e^{i\frac{2\pi}{N}}$ if $S(\mathcal{C}_{\text{e}})$ is crossed by the link and is trivial otherwise;

3. In the expansion of the partition function, due to the measure $\prod_x \int_{-\pi}^{\pi} d\gamma(x)$, the terms that contribute contain products of the composite $e^{i\gamma(x+\hat{\mu})} e^{-i\gamma(x)}$ (or its conjugate) over links organized forming loops. Otherwise, the integrals over the site variables at the line edges vanish (see Figure 2.1);

4. Due to frustration, every time $\mathcal{C}_{\text{e}}$ is linked, a center element is generated. Then, in the lattice, the closed center-vortex worldlines in the initial ensemble, which led to Eq. (2.3) and gave origin to the effective description (2.4), are represented by the loops of item 3.

This point of view was useful to propose other ensemble measures relying on lattice models, as in the case where the derivation of the effective description is not known, see for example 2.1.2 and 4.1. The initial ensemble properties encoded in Eq. (2.3) are recovered close to the 3d XY model critical point, as expected. Indeed, using the same techniques reviewed in [50] for the case without frustration, the partition function may be formulated in terms of integer-valued divergenceless currents, originated after using the Fourier decomposition

$$e^{\beta\cos\gamma} = \sum_{b=-\infty}^{\infty} I_b(\beta) e^{ib\gamma} \ , \tag{2.6}$$

at every lattice link. The resulting expression turns out to be equivalent to a grand canonical ensemble of non-backtracking closed loops formed by currents of strength $|b_\mu| = 1$. In the model without frustration, close to the critical point $\beta_c \approx 0.454$ (continuum limit), the relevant configurations are known to be formed by large loops rather than by multiple small loops, and multiple occupation of links is disfavored, thus making contact with the initial properties parametrized in the ensemble (see Table 2.1 below).

Table 2.1: The correspondence between the effective field and the 3d XY model representations of the Abelian center−vortex ensemble.

| **3d XY** | **Effective Fields** |
|---|---|
| large loops are favored | negative tension $\mu$ |
| multiple small loops are disfavored | positive stiffness $1/\kappa$ |
| multiple occupation of links is disfavored | repulsive interactions |

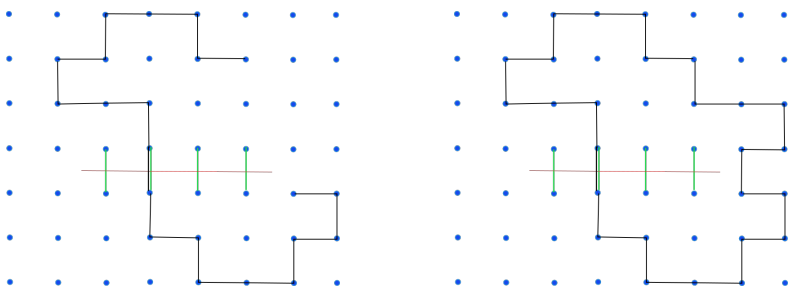

(**a**) (**b**)

Figure 2.1: The Wilson loop and the frustration are represented in red and green, respectively. Configurations of type (**a**), which involve sites joined by open lines, do not contribute to the partition function. Only site configurations joined by loops, like the one in (**b**), contribute (with a center-element).

### 2.1.2 Four dimensions

Regarding the effective description of 4d ensembles based on random surfaces, as in the 3 + 1 dimensional world center vortices are one-dimensional objects spanning closed worldsurfaces, the emergent order parameter would be a *string field*. However, unlike the 3d case, a derivation starting from the ensemble of closed worldsurfaces with stiffness is still lacking. Such generalization should initially describe a growth process where a surface is generated, and then a Fokker–Planck equation for the lattice loop-to-loop probability should be derived. Similarly to what happens with end-to-end probabilities for polymers, where stiffness is essential to get a continuum limit when the monomer size goes to zero [51, 52], curvature effects are expected to be essential for the continuum limit of triangulated random surfaces. Indeed, ensembles of surfaces which consider only the Polyakov (or Nambu-Goto) action leads to a phase of branched polymers [53, 54]. On the

other hand, in [55], the phase fluctuations of an Abelian string field with frozen modulus were approximated by a lattice *field* theory: the $U(1)$ gauge-invariant Abelian Wilson action. In other words, the Goldstone modes for a condensate of one-dimensional objects are gauge fields. Motivated by this enormous simplification and by an analogy with the 3d case, in Ref. [56] a Wilson action with frustration was proposed as a starting point to define a measure for percolating center vortices in four dimensions. This proposal will be discussed in section 4.1. For the time being, we summarize the main initial steps, which are analogous to items 1–4 in 2.1.1:

1. In the center-vortex condensate, the effective theory is dominated by the soft Goldstone modes, which are represented by an emergent compact Abelian gauge field $V_\mu \in U(1)$. In the center-vortex context, another natural model based on $V_\mu \in SU(N)$ was also proposed (see Sec. 4.1);

2. The lattice version of the Goldstone mode sector is given by a Wilson action with frustration;

3. In the expansion of the partition function, the relevant configurations to compute the gauge model correspond to link-variables on the edges of plaquettes organized on closed surfaces (see Figure 2.2);

4. The frustration is nontrivial on plaquettes $x, \mu, \nu$ that intersect $S(\mathcal{C}_{\rm e})$. Every time a closed surface links $\mathcal{C}_{\rm e}$, a center-element for quarks in the representation D is generated.

Thus, the main simplification in 4d is that, in a condensate, the effective description can be captured by a local field. Similarly to 3d, where the soft modes can be read in the phase of the vortex field $V(x) \sim v\, e^{i\gamma(x)}$, the natural soft modes in 4d are given by a compact gauge field,

$$V(C) \sim v\, e^{i\gamma_\Lambda(C)} \quad , \quad \gamma_\Lambda(C) = \oint_C dx_\mu\, \Lambda_\mu \; . \tag{2.7}$$

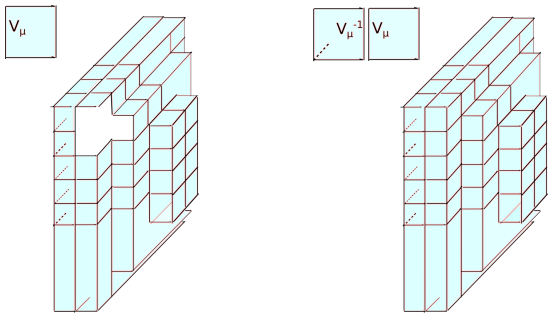


(**a**) (**b**)

Figure 2.2: (**a**) Configurations formed by link variables distributed on plaquettes organized on an open surface do not contribute, as the $V_\mu$ link−variables at the surface edges cannot form singlets; (**b**) when they are organized on closed surfaces, singlets can be formed and the group−integral is nontrivial.

## 2.2 Center-vortices, matching rules, and correlations

The simplest center-vortex ensembles discussed in Sec. 2.1 could provide an important basis to understand the confinement mechanism at asymptotic distances. However, they do not contain enough ingredients to reproduce more intricate properties. In this section, we shall discuss the center-vortex gauge fields and typically non-Abelian elements that could characterize the associated ensembles.

### 2.2.1 Thick center vortices and intermediate Casimir scaling

Before discussing generalized center-vortex ensembles with matching rules and nonoriented components, let us recall how the consideration of center-vortex thickness and the natural non-Abelian orientations in the gauge group can account for the observed Casimir scaling at intermediate distances. Some ideas along this line were initially pursued in [57]. In [42, 43] (see also [58]), a simple model was put forward in the lattice, where the contribution to a planar Wilson loop along a curve $\mathcal{C}_{\rm e}$ was modeled. The starting point is to postulate an ensemble of thick center vortices whose total flux, as measured by a fundamental holonomy, have different possibilities $z^j = e^{i2\pi j/N}$, $j = 1, \ldots, N-1$. When a thick center vortex is partially linked, the contribution to the Wilson loop is given by the insertion of a group element $G_j(x, S)$ that depends on the location $(x)$ of the center-vortex midpoint (or guiding center) with respect to $\mathcal{C}_{\rm e}$. It also depends on a group orientation $S$,

$$G_j(x, S) = S\mathcal{G}_j(x)S^\dagger \,, \tag{2.8}$$

where $\mathcal{G}_j = \exp\left[i\,\alpha_j \cdot T\right]$ is in the Cartan subgroup and the tuples $\alpha_j$ are formed by model-dependent scalar profiles. These profiles implement the natural condition that

$G_j(x, I) = z^j I_N$, if the thick center vortex is fully enclosed by $\mathcal{C}_{\rm e}$, it is $I_N$ if it is not enclosed at all, and it gives an interpolating value otherwise. After averaging over random group orientations in [42, 43], they arrived at

$$\sigma_{\mathcal{C}_{\rm e}}({\rm D}) \equiv -\sum_x \frac{1}{A} \ln(1 - \sum_{j=0}^{N-1} f_j (1 - \frac{1}{\mathscr{D}} {\rm Tr}\, {\rm D}\,(\,\mathcal{G}_j))) \,, \tag{2.9}$$

where $f_j$ is the probability that a given plaquette of the planar surface enclosed by $\mathcal{C}_{\rm e}$ be pierced by the midpoint of a center-vortex of type $j$, $\sigma_{\mathcal{C}_e}({\rm D})$ is the string tension in representation D, and $A$ is the minimal area of $\mathcal{C}_{\rm e}$. At intermediate distances, after some natural approximations, an appropriate choice of profiles, and using the key formula

$${\rm Tr}\,({\rm D}(T_q){\rm D}(T_p)) = \mathscr{D}\,\delta_{qp} \frac{C_2({\rm D})}{N^2-1} \,, \tag{2.10}$$

the Casimir Scaling (recall Eq. (1.6)) was obtained. In [42, 43], based on a specific choice of probabilities and profiles, it was also possible to reproduce different asymptotic behaviors, such as the Casimir and the Sine law. In Sec. 2.3, we shall review a different line based on oriented and nonoriented center vortices, which naturally lead to an asymptotic Casimir law. As these models are generated from weighted center-element averages, they are expected to be applicable in the asymptotic region.

### 2.2.2 Center-vortex sectors in continuum YM theory

Center vortex correlations were considered for the first time in [3]. In $(2+1)$d Minkowski spacetime, the order–disorder algebra in Eq. (1.3) says that the action of $\hat{V}(\mathbf{x})$ on $|A\rangle$ gives

$$\hat{\mathcal{W}}_{\rm F}(\mathcal{C}_{\rm e}) \left(\hat{V}(\mathbf{x})|A\rangle\right) = e^{i\frac{2\pi}{N}}\, \mathcal{W}_{\rm F}(\mathcal{C}_{\rm e}) \left(\hat{V}(\mathbf{x})|A\rangle\right) \,, \tag{2.11}$$

if $\mathbf{x}$ is encircled by $\mathcal{C}_{\rm e}$, and it leaves the state $|A\rangle$ unaltered otherwise. Here, $|A\rangle$ is a state with well-defined shape in the Weyl gauge $A_0 = 0$, That is, $\hat{V}(\mathbf{x})|A\rangle$ is a state where a thin center-vortex is created on top of $A_i$. In particular, the action of $\hat{V}^N(\mathbf{x})$ is trivial. Then, the possible phases were effectively described by a model with magnetic $Z(N)$ symmetry

$$\mathcal{L} = \partial^\mu \bar{V}\, \partial_\mu V + m^2\, \bar{V} V + \frac{\lambda}{2}\, (\bar{V} V)^2 + \xi\, (V^N + \bar{V}^N) \,. \tag{2.12}$$

This includes quadratic and quartic correlations, as well as the $N$-th order terms that capture the possibility that $N$ vortices may annihilate. The case $m^2 > 0$ would correspond to a Higgs phase where center vortices are in the spectrum of asymptotic states. The case $m^2 < 0$ corresponds to a center-vortex condensate, with $N$ degenerate classical vacua, so that $Z(N)$ is spontaneously broken. For a detailed analysis of this effective description,

see [59, 60]. In [3], based on the center-vortex operator definition $\hat{V}(\mathbf{x})|A\rangle = |A^S\rangle$, discussed in Chapter 1, 3d Euclidean vortex Green's functions $\langle \bar{V}(y)V(x)\rangle$ were defined. This was done by considering the YM path-integral over configurations $A_\mu$ with boundary conditions around the pair of points $x, y \in \mathbb{R}^3$, such that a vortex is created at $x$, it is then propagated, and finally annihilated at $y$. When $|x-y| \to \infty$, an exponential decay would correspond to a Higgs phase and $\langle V\rangle = 0$, because of the clustering property. This agrees with the discussion above, where the Higgs phase $m^2 > 0$ is characterized by a $Z(N)$ symmetric vacuum. On the other hand, a condensate would correspond to a Green's function that tends to a constant.

Now, from the definition of the operator $\hat{V}(\mathbf{x})$, it is clear that it introduces singularities in the gauge fields. If $A$ is smooth, the configuration $A^S$ is singular, with a field strength containing a delta-singularity at the center vortex location $\mathbf{x}$. As pointed out by 't Hooft, the operator's definition could be made more precise by smearing the singularities over an infinitesimal region around $\mathbf{x}$. Otherwise, we would be working with singular infinite action gauge fields. Although this direction was not pursued in that work, the smeared Green's functions could depend on the choice of boundary conditions, for the mapping $S \in SU(N)$, around $x$ and $y$. In other words, the vortex field $\hat{V}$ could hide non-Abelian degrees of freedom which are not evidenced by the algebra in Eq. (1.3), which only depends on properties with respect to the Wilson loop.

In Chapter 6, we will analyze the procedure given in Ref. [61], proposed for quantizing Yang-Mills theories in the continuum. In that work, the authors introduced a partition of the full configuration space of *smooth* gauge fields $\{A_\mu\}$ into sectors $\mathcal{V}(S_0) \subset \{A_\mu\}$ characterized by topological labels $S_0$. These labels $S_0$ are characterized by the location of oriented and nonoriented center-vortex guiding centers, with all possible matching rules. While a possible label for an oriented center-vortex would be $S_0 = e^{i\chi\beta\cdot T}$, a typical nonoriented configuration is characterized by $S_0 = e^{i\chi\beta\cdot T}W$. In 3d, close to some points (instantons) on the center-vortex worldline generated by $e^{i\chi\beta\cdot T}$, the mapping $W$ behaves as a Weyl transformation that changes the fundamental weight $\beta$ to $\beta'$. Similarly, in 4d, the change occurs at some monopole worldlines on the center-vortex worldsurfaces generated by $e^{i\chi\beta\cdot T}$ (see [56]). The full YM partition function and averages of observables were then represented by a sum over partial contributions,

$$Z_{\rm YM} = \sum_{S_0} Z_{(S_0)} \quad , \quad \langle O\rangle_{\rm YM} = \frac{1}{Z_{\rm YM}} \sum_{S_0} \int_{\mathcal{V}(S_0)} [D\mathcal{A}_\mu]\, O\, e^{-S_{\rm YM}} \, . \tag{2.13}$$

Here, $\sum_{S_0}$ is a short-hand notation for the contribution originated from the continuum of labels $S_0$. In Ref. [62], this quantization procedure was shown to be renormalizable in the vortex-free sector. Furthermore, the extension of the renormalization proof to sectors labeled by center vortices was done in Ref. [63]. These ideas provided a glimpse of a path connecting first principles Yang–Mills theory to an ensemble containing all possible

center-vortex configurations. In addition to addressing this important conceptual issue, the partition into sectors may circumvent the well-known Gribov problem when fixing the gauge in non-Abelian gauge theories, as Singer's no go theorem [64] only applies to global gauges in configuration space (see [65] for a detailed discussion). An interesting consequence of this construction is that a new label may be generated by the right multiplication, $S_0 \to S_0\tilde{U}^{-1}$, with regular $\tilde{U}$, which is not necessarily connected to $S_0$ by a regular gauge transformation. That is, given a center-vortex sector, there is a continuum of physically inequivalent sectors characterized by non-Abelian d.o.f. where the defects are located at the same spacetime points. In the context of effective Yang–Mills–Higgs models, which describe the confining string as a smooth topological classical vortex solution, the presence of similar internal d.o.f. was previously noted in a large class of color-flavor symmetric theories [66, 67, 68, 69, 70, 71, 72, 73, 74, 75].

## 2.3 Mixed ensembles of oriented and nonoriented center vortices

The general properties of center vortices discussed so far motivate the search for a natural ensemble that captures all the asymptotic properties of confinement. Among them, the formation of a confining flux tube is the most elusive one in this scenario. The formation of this object would also explain the Lüscher term, which has not been observed in projected center-vortex ensembles. Furthermore, the asymptotic Casimir law (cf. Eq. (1.9)) should be reproduced in 3d, while in 4d we would like to understand the coexistence of $N$-ality with the Abelian-like flux tube profiles [9, 10, 11]. It is clear that a confining flux tube requires an ensemble whose effective description contains topological solitons, namely, a confining domain wall in $(2 + 1)$d and a vortex in $(3 + 1)$d. However, the simple models of oriented and uncorrelated center vortices discussed in Sec. 2.1 do not have the conditions to support these topological objects[2]. In Chapters 3 and 4, we will explain how the inclusion of center-vortex matching rules and a nonoriented component, where lower dimensional defects are attached to center vortices (see Sec. 2.2.2), could fill the gap between center-vortex ensembles and the formation of a flux tube. In [76, 77], lattice studies showed that the 4d Abelian-projected lattice is not represented by a monopole Coulomb gas, but rather by monopoles attached to collimated fluxes (for a scenario only relying on monopole ensembles, see [78, 79, 80]). In 3d, the attached lower dimensional defects are instantons. The relevance of nonoriented center vortices to generate a nonvanishing Pontryagin index was shown in [46]. We also note that although oriented and nonoriented center vortices, located at the same place, would contribute to a large

[2]Namely, a SSB pattern with discrete classical vacua in $(2 + 1)$d and multiple connected vacua in $(3 + 1)$d.

Wilson loop with the same center-element, it is natural to weight them with different effective actions. In the second case, the measure should also depend on the location of the lower-dimensional defects.

# Chapter 3

# 3d Ensemble with Asymptotic Casimir Law

Understanding the mechanism behind the nonperturbative asymptotic Casimir scaling in Eq. (1.9) is a challenging problem. Until now, a picture for Casimir scaling as due to percolating magnetic defects was only given at intermediate distances [42], however these arguments rely on the finite thickness of center vortices, so they cannot be extended to the asymptotic region. In order to incorporate this non-Abelian feature, it is natural to equip the ensemble with non-Abelian d.o.f. Indeed, in the continuum, the presence of these degrees in Yang-Mills theories was brought up in Ref. [56], noting that the definition of a path-integral measure that detects magnetic defects contains, for every realization of their locations, a continuum of physically inequivalent sectors. In this chapter, we shall initially propose an ensemble measure where center-vortex worldlines equipped with non-Abelian d.o.f. can be attached to pointlike defects (instantons). This will be an extension of the center vortex measure in Ref. [49] (see also Refs. [48, 81]), where a $3D$ ensemble of Abelian loops was considered. In that case, in the percolating phase, the effective theory is equivalent to an XY model with topological frustration, which implies an area law for the center-element average. For the extended measure, we will derive an effective field description where the vortices, carrying fundamental weights, get naturally represented by $N$ flavors of effective Higgs fields transforming in the fundamental representation. Up to this point, in the center-vortex condensate, the vacuum manifold has an $SU(N)$ degeneracy. However, the instanton sector is manifested as an additional interaction, which replaces this continuum of possibilities by a discrete set of $Z(N)$ vacua. This gives rise to the formation of a stable domain wall whose border is given by the quark loop. Thus, besides a linear term, the potential will contain a subleading Lüscher term originated, as usual, from the fluctuation of collective coordinates around the saddle-point. Finally, after a detailed analysis of the associated field equations, we will show that the string tension turns out to scale with the sought-after asymptotic Casimir law.

## 3.1 Center-vortices with non-Abelian d.o.f.

In Ref. [3], an Abelian model to describe center vortices in $(2+1)$D was proposed. For this aim, center-vortex operators $\hat{V}(x)$ were defined in $SU(N)$ pure YM theory. In this case, the nontrivial correlators are not only of the form

$$\langle\Omega|T\{\hat{V}^\dagger\hat{V}\}|\Omega\rangle \quad , \quad \langle\Omega|T\{\hat{V}^\dagger\hat{V}\hat{V}^\dagger\hat{V}\}|\Omega\rangle \quad , \quad \dots$$

but also those involving $N$ elementary operators of the same type,

$$\langle\Omega|T\{\hat{V}\dots\hat{V}\}|\Omega\rangle \quad , \quad \langle\Omega|T\{\hat{V}^\dagger\dots\hat{V}^\dagger\}|\Omega\rangle \ .$$

This is due to the fact that $N$ center-vortex operators have trivial total $Z(N)$ charge, so they can connect vacuum to vacuum amplitudes. Based on these physical inputs, the effective model given by Eq. (2.12) was then introduced which captures the correlators mentioned above. When a condensate is formed ($m^2 < 0$), the $Z(N)$ symmetry is spontaneously broken, thus leading to classical topological solutions (one-dimensional domain walls) on the physical $\mathbb{R}^2$-plane, with finite energy per unit length. As discussed in Ref. [3], these line defects can end at a pair of heavy quark-antiquark probes. That is, a confining string is formed in this phase.

In Ref. [48], the application of polymer techniques to vortex loops with stiffness $1/\kappa$ and tension $\mu$, coupled to an external vector field, made it possible to think of the end-to-end probability of a vortex worldline as a solution to a diffusion equation in 3D. In this manner, the $N = 2$ model in Eq. (2.12) was associated with the large distance effective description of an ensemble where vortex pairs are created/annihilated via pointlike correlated defects. In Ref. [49], an ensemble measure to compute center-element averages was clearly related with the first three $U(1)$-symmetric terms in Eq. (2.12), with a covariant derivative in the place of $\partial_\mu$. This derivative depends on the external field used to represent linking numbers between center vortices and the Wilson loop in the initial ensemble. The $U(1)$-symmetric sector is dominated by Goldstone modes in a 3d XY model with topological frustration. For large $N$, an analysis based on the associated critical properties led to a *squared* sine (area) law. Here, the inclusion of $N$-line correlations is expected to reproduce the complete model in Eq. (2.12); however, this cannot accommodate the asymptotic Casimir law either.

In order to describe this type of scaling, which involves a non-Abelian property, it is natural to improve the ensemble with non-Abelian information. Indeed, as discussed in Ref. [61], the inequivalent sectors of magnetic defects in Yang-Mills theories are naturally labeled by these degrees. Therefore, we shall initially consider the center-vortex loop ensemble of Ref. [49] embedded in a non-Abelian setting. The Wilson Loop associated to

a quark worldline $\mathcal{C}$ carrying an irreducible $\mathscr{D}$-dimensional representation $D$ is given by

$$W_{\mathcal{C}}[A_\mu] = \frac{1}{\mathscr{D}} \operatorname{tr} \mathrm{D}\left(P\left\{e^{i \oint_{\mathcal{C}} dx_\mu \, A_\mu(x)}\right\}\right) \ . \tag{3.1}$$

The contribution of an elementary center vortex configuration $A_\mu = \beta \cdot T \, \partial_\mu \chi$, whose field strength is localized on a loop $l$, is the center element

$$W_{\mathcal{C}}[A_\mu] = \left(e^{i\, 2\pi\, \beta \cdot w_{\mathrm{e}}}\right)^{L(\mathcal{C},l)} = \left(e^{i 2\pi k/N}\right)^{L(\mathcal{C},l)} \quad , \quad \beta = 2Nw \ , \tag{3.2}$$

where $L(\mathcal{C}, l)$ is the linking number between $\mathcal{C}$ and $l$. The tuple $\beta$ is a (magnetic) weight of the defining representation, corresponding to unit-flux vortices (there are $N$ possibilities $\beta_i = 2Nw_i$), and $\chi$ is a multivalued angle that changes by $2\pi$ when we go around $l$. These weights can be ordered as $w_1 > w_2 > ... > w_N$. They satisfy

$$w_q \cdot w_p = \frac{N\delta_{qp} - 1}{2N^2} \ . \tag{3.3}$$

In addition, $w_{\mathrm{e}}$ is an electric weight of the quark representation D.[1] This contribution can be rewritten in the form

$$W_{\mathcal{C}}[A_\mu] = W_l[b_\mu^{\mathcal{C}}] = \frac{1}{N} \mathrm{tr} P\left(e^{i \oint_l dx_\mu \, b_\mu^{\mathcal{C}}(x)}\right) \quad , \quad A_\mu = \beta \cdot T \, \partial_\mu \chi \ , \tag{3.4}$$

where $b_\mu^{\mathcal{C}}(x) \equiv 2\pi \beta_e \cdot T \, s_\mu$, $\beta_{\mathrm{e}} = 2Nw_{\mathrm{e}}$, and $s_\mu$ is concentrated on a surface $S(\mathcal{C})$ whose border is $\mathcal{C}$

$$s_\mu = \frac{1}{2} \int_{S(C)} d\sigma_1 d\sigma_2 \, \epsilon_{\mu\nu\rho} \frac{\partial x^\nu}{\partial \sigma_1} \frac{\partial x^\rho}{\partial \sigma_2} \delta(\bar{x}(\sigma_1, \sigma_2) - x) \ . \tag{3.5}$$

In this respect, note that the circulation of $s_\mu$ along $l$ gives the intersection number between $l$ and $S(\mathcal{C})$,

$$\oint_l dx_\mu s_\mu = I(S(\mathcal{C}), l) \ , \tag{3.6}$$

which coincides with the linking number $L(\mathcal{C}, l)$.

The contribution to the Wilson Loop originated from $n$ center vortices is the product of the corresponding center elements. Then, including the property of stiffness, observed in the lattice [44, 45, 82], as well as tension $\mu$, the ensemble average becomes $Z_{\mathrm{loops}}[b_\mu^{\mathcal{C}}]$,

[1] For a general representation, a weight $\lambda$ is an $(N-1)$-tuple formed by the eigenvalues $\lambda|_q$ of simultaneous eigenvectors of the Cartan generators $\mathrm{D}(T_q)$, that is, $\mathrm{D}(T_q)|\lambda\rangle = \lambda|_q|\lambda\rangle$, $q = 1, \ldots, N-1$. We also defined $\beta \cdot T = \beta|_q T_q$.

where

$$Z_{\rm loops}[b_\mu] = \sum_{n=0}^{\infty} \frac{1}{n!} \prod_{k=1}^{n} \int_0^\infty \frac{dL_k}{L_k} \int dv_k \int [dx^{(k)}]_{v_k,v_k}^{L_k} e^{-\int_0^{L_k} ds_k \left[\frac{1}{2\kappa}\dot{u}_\mu^{(k)}\dot{u}_\mu^{(k)} + \mu\right]} W_{l_k}[b_\mu] \quad (3.7)$$

is the ensemble partition function in the presence of a general external source $b_\mu \in \mathfrak{su}(N)$. For each closed worldline $x^{(k)}(s)$, $u_\mu^{(k)}$ is its tangent vector

$$u_\mu(s) = \frac{dx_\mu}{ds} \in S^2 \quad , \quad \dot{u}_\mu(s) = \frac{du_\mu}{ds} \, . \quad (3.8)$$

The loops start and end at some point $x_k \in \mathbb{R}^3$ where the tangent is $u_k \in S^2$. $[dx]_{v,v}^L$ path-integrates over loops with length $L$ starting and ending at $v$, $v = (x,u)$. This partition function may be rewritten as

$$Z_{\rm loops}[b_\mu] = e^{\int_0^\infty \frac{dL}{L} \int dv \, {\rm tr}\, Q(v,v,L)} \, , \quad (3.9)$$

$$Q(x,u,x_0,u_0,L) = \int [dx(s)]_{v,v_0}^L \, e^{-\int_0^L ds \left[\frac{1}{2\kappa}\dot{u}_\mu \dot{u}_\mu + \mu\right]} \, \Gamma_\gamma[b_\mu] \, , \quad (3.10)$$

$$\Gamma_\gamma[b_\mu] = P\left\{ e^{i\int_\gamma dx_\mu \, b_\mu(x)} \right\} \, . \quad (3.11)$$

We can use the methods of Refs. [52, 81] to obtain the non-Abelian difusion equation

$$\left(\partial_L - \frac{\kappa}{2}\hat{L}_u^2 + \mu + u_\mu(\partial_\mu - i b_\mu)\right) Q(x,u,x_0,u_0,L) = 0 \, , \quad (3.12)$$

to be solved with the initial condition $Q(x,u,x_0,u_0,0) = \delta^{(3)}(x-x_0)\delta^{(2)}(u-u_0) I_N$. These methods are briefly reviewed in Appendix D. In particular, $Q(x,u,x_0,u_0,L)$ is given by Eq. (D.1) computed with the fundamental representation of $SU(N)$. In the small stiffness limit (large $\kappa$), the solution can be approximated by

$$Q(x,u,x_0,u_0,L) \approx \langle x | e^{-LO} | x_0 \rangle \quad , \quad O = -\frac{1}{3\kappa}(\partial_\mu - i b_\mu)^2 + \mu I_N \, , \quad (3.13)$$

thus leading to

$$Z_{\rm loops}[b_\mu] \approx e^{-{\rm Tr}\,\ln O} = ({\rm det}\; O)^{-1} = \int [d\phi] \, e^{-\int d^3x \, \phi^\dagger O \phi} \, , \quad (3.14)$$

where $\phi$ is a complex field in the fundamental representation.

## 3.2 $N$-worldline matching rules

The ensemble above can be further improved by including matching rules where $N$ elementary center vortices carrying different weights $\beta_i$, $\sum_i^N \beta_i = 0$, can be created at a point out of the vacuum, then propagated along the lines $\gamma_1, \ldots, \gamma_N$, and finally annihilated.

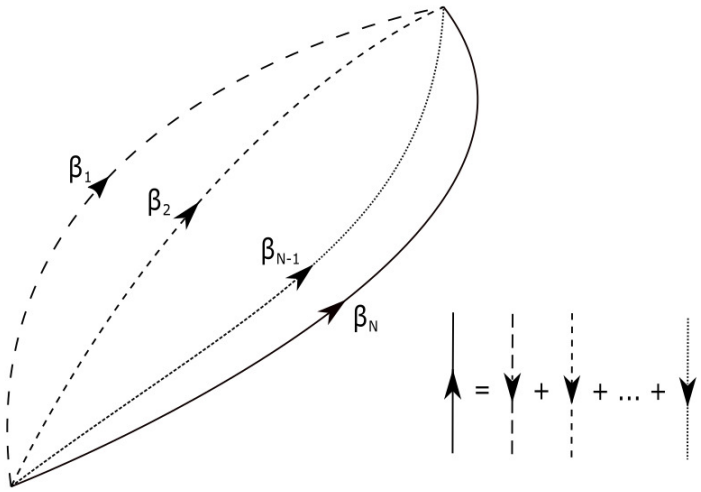


Figure 3.1: An $N$ center-vortex creation-annihilation process can be thought of as $N-1$ correlated loops. The loop $l_i$ is formed by joining $\gamma_i$ with $-\gamma_N$.

Since the weights sum to zero, we can think of this configuration as $N-1$ correlated loops $l_i = \gamma_i - \gamma_N$ with a common line $-\gamma_N$ (see Fig. 3.1), carrying magnetic weights $\beta_i$, $i = 1, \ldots, N-1$, respectively. For this configuration, the gauge field can be written as $A_\mu = \sum_{i=1}^{N-1} \beta_i \cdot T\, \partial_\mu \chi_i$, where $\chi_i$ changes by $2\pi$ when we go around $l_i$. The corresponding contribution to the Wilson Loop is

$$W_{\mathcal{C}}[A_\mu] = \left(e^{i\,2\pi\,\beta_1 \cdot w_{\rm e}}\right)^{L(S(\mathcal{C}),l_1)} \ldots \left(e^{i\,2\pi\,\beta_{N-1} \cdot w_{\rm e}}\right)^{L(S(\mathcal{C}),l_{(N-1)})} . \tag{3.15}$$

This is a product of center elements that can be rewritten as

$$W_{\mathcal{C}}[A_\mu] = \frac{1}{N!}\,\epsilon_{i_1 \ldots i_N} \epsilon_{i'_1 \ldots i'_N} \Gamma_{\gamma_1}[b^{\mathcal{C}}_\mu]|_{i_1 i'_1} \ldots \Gamma_{\gamma_N}[b^{\mathcal{C}}_\mu]|_{i_N i'_N} \quad , \quad A_\mu = \sum_{i=1}^{N-1} \beta_i \cdot T\, \partial_\mu \chi_i \, . \tag{3.16}$$

In this regard, since $\langle w_i | \beta_e . T | w_j \rangle = w_{\rm e} \cdot \beta_i\, \delta_{ij}$, we have $e^{2\pi i \int_\gamma dx_\mu w_{\rm e} \cdot T\, s_\mu}|_{ij} = e^{2\pi i \int_\gamma dx_\mu w_{\rm e} \cdot \beta_i\, s_\mu} \delta_{ij}$, so that the right-hand side in Eq. (3.16) becomes,

$$\begin{aligned} \frac{1}{N!}\,\epsilon_{i_1 \ldots i_N} \epsilon_{i'_1 \ldots i'_N} e^{2\pi i \int_{\gamma_1} dx_\mu w_{\rm e} \cdot \beta_{i_1}\, s_\mu} \delta_{i_1 i'_1} \ldots e^{2\pi i \int_{\gamma_N} dx_\mu w_{\rm e} \cdot \beta_{i_N}\, s_\mu} \delta_{i_N i'_N} \\ = e^{2\pi i \int_{\gamma_1} dx_\mu w_{\rm e} \cdot \beta_1\, s_\mu} \ldots e^{2\pi i \int_{\gamma_N} dx_\mu w_{\rm e} \cdot \beta_N\, s_\mu} \\ = e^{2\pi i \oint_{l_1} dx_\mu w_{\rm e} \cdot \beta_1\, s_\mu} \ldots e^{2\pi i \oint_{l_{N-1}} dx_\mu w_{\rm e} \cdot \beta_{N-1}\, s_\mu} , \end{aligned} \tag{3.17}$$

which coincides with the right-hand side in Eq. (3.15). Including the phenomenological properties of center vortices, the $N$-line configuration gives a contribution:

$$C_N \propto \int d^4x\, d^4x_0 \prod_{j=1}^{N} \int dL_j du^j du_0^j \int [Dx^{(j)}]_{v_0^j\, v^j}^{L_j} e^{-\int_0^{L_j} ds_j \left[\frac{1}{2\kappa}\, \dot{u}_\mu^{(j)} \dot{u}_\mu^{(j)} + \mu\right]} D_N \ , \tag{3.18}$$

$$D_N = \epsilon_{i_1 \ldots i_N} \epsilon_{j_1 \ldots j_N} \Gamma_{\gamma_1}[b_\mu]_{i_1 j_1} \ldots \Gamma_{\gamma_N}[b_\mu]_{i_N j_N} \ . \tag{3.19}$$

To proceed, using Eqs. (3.10) and (3.13), for every line we can use

$$\int dL\, du\, du_0 \int [Dx]_{v_0\, v}^{L} e^{-\int_0^L ds \left[\frac{1}{2\kappa}\, \dot{u}_\mu \dot{u}_\mu + \mu\right]} \Gamma[b_\mu] = \int_0^\infty dL\, du\, du_0\, Q(x, u, x_0, u_0, L) \sim G(x, x_0) \ , \tag{3.20}$$

where $O\, G(x, x_0) = \delta(x - x_0)\, I_{\mathscr{N}}$ (see Appendix D). In other words,

$$C_N \propto \int d^4x\, d^4x_0\, \epsilon_{i_1 \ldots i_N} \epsilon_{j_1 \ldots j_N} G(x, x_0)_{i_1 j_1} \ldots G(x, x_0)_{i_N j_N} \ . \tag{3.21}$$

The field representation (3.14) and the discussion above clearly suggest the consideration of $N$ flavors of fundamental fields, one for each fundamental weight, and an appropriate interaction to accomodate the possible $N$-line matchings by means of the generated Feynman diagrams in an effective field theory. Indeed, all possibilities for this type of corelation can be generated from the following field partition function

$$\int [D\Phi^\dagger][D\Phi]\, e^{-\int d^3x \left(\frac{1}{3\kappa} \mathrm{Tr}((D_\mu \Phi)^\dagger D_\mu \Phi) + \mu\, \mathrm{Tr}(\Phi^\dagger \Phi) - \xi_0 (\det \Phi + \det \Phi^\dagger)\right)} \ , \tag{3.22}$$

where $D_\mu \Phi \equiv (\partial_\mu - i b_\mu)\Phi$ and we defined a matrix with components $\Phi_i^j = \phi^j|_i$, where $\phi^j$, $j = 1, \ldots, N$ are complex fields in the fundamental representation. A perturbative expansion reads

$$\int [D\Phi^\dagger][D\Phi] \left(1 + \xi_0^2 \int d^3x \int d^3x_0 \right.$$
$$\left. \epsilon_{i_1 \ldots i_N} \epsilon_{i'_1 \ldots i'_N}\, \phi^{i'_1}|_{i_1} \ldots \phi^{i'_N}|_{i_N} \epsilon_{j_1 \ldots j_N} \epsilon_{j'_1 \ldots j'_N}\, \bar{\phi}^{j'_1}|_{j_1} \ldots \bar{\phi}^{j'_N}|_{j_N} + \ldots \right) e^{-\int d^3x\, \bar{\phi}^j|_i O_{ii'}^{jj'} \phi^{j'}|_{i'}} \ . \tag{3.23}$$

Clearly, the first term is $Z_{\mathrm{loops}}^N$, the contribution to the ensemble of the uncorrelated $N$ copies of loop types. In addition, multiplying and dividing the $\xi_0^2$-term by

$$(\det O)^{-N} = \int [D\Phi^\dagger][D\Phi]\, e^{-\int d^3x\, \bar{\phi}^j|_i O_{ii'}^{jj'} \phi^{j'}|_{i'}} \quad , \quad O_{ii'}^{jj'} \equiv \delta^{jj'} O_{i'i} \ ,$$

and using Wick's theorem, we get

$$\begin{aligned}
&\tfrac{\xi_0^2}{(N!)^2}\int[D\Phi^\dagger][D\Phi]\int d^3x\int d^3x_0\,\epsilon_{i_1\ldots i_N}\epsilon_{i'_1\ldots i'_N}\phi^{i'_1}|_{i_1}(x)\ldots\phi^{i'_N}|_{i_N}(x)\\
&\qquad\times\epsilon_{j_1\ldots j_N}\epsilon_{j'_1\ldots j'_N}\bar\phi^{j'_1}|_{j_1}(x_0)\ldots\bar\phi^{j'_N}|_{j_N}(x_0)e^{-\int d^3x\,\bar\phi^j|_i O^{jj'}_{ii'}\phi^{j'}|_{i'}}\\
&=Z^N_{\rm loops}\xi_0^2\int d^3x\int d^3x_0\,\epsilon_{i_1\ldots i_N}\epsilon_{j_1\ldots j_N}G_{i_1j_1}(x,x_0)\ldots G_{i_Nj_N}(x,x_0)\;. \qquad (3.24)
\end{aligned}$$

Therefore, due to Eqs. (3.14) and (3.20), we can write this partial contribution as

$$\begin{aligned}
&\xi_0^2\prod_{j=1}^N\int d^4x\,d^4x_0\,\epsilon_{i_1\ldots i_N}\epsilon_{k_1\ldots k_N}\int dL_j du^j du_0^j\int[Dx^{(j)}]^{L_j}_{v_0^j\,v^j}\,e^{-\int_0^{L_j}ds_j\left[\frac{1}{2\kappa}\dot u_\mu^{(j)}\dot u_\mu^{(j)}+\mu\right]}\Gamma^{(j)}_{i_jk_j}[b_\mu]\\
&\qquad\left(\sum_n\frac{1}{n!}\prod_{k=1}^n\int_0^\infty\frac{dL_k}{L_k}\int dv_k\int[dx^{(k)}]^{L_k}_{v_k,v_k}\,e^{-\int_0^{L_k}ds_k\left[\frac{1}{2\kappa}\dot u_\mu^{(k)}\dot u_\mu^{(k)}+\mu\right]}W_{l_k}[b_\mu]\right)^N\;. \qquad (3.25)
\end{aligned}$$

This represents the mixing of the uncorrelated loop configurations and a single correlated two-point component (cf. Fig. 3.1). Proceeding similarly with the other terms, the perturbative series can be identified with all possible configurations with $N$-line correlations. At this point, the effective model in Eq. (3.22) is invariant under (magnetic) local color and global flavor transformations

$$\Phi\to S_c(x)\Phi\quad,\quad b_\mu\to S_cb_\mu S_c^{-1}+iS_c\partial_\mu S_c^{-1}\quad,\quad\Phi\to\Phi S_f\;. \qquad (3.26)$$

Other possible correlations among center vortices, with the same symmetry, can be introduced by means of new terms in the exponent of Eq. (3.22). For example we may consider the center-element average generated by $Z_{\rm v}[b_\mu^{\mathcal C}]$ where

$$Z_{\rm v}[b_\mu]=\int[D\Phi^\dagger][D\Phi]\,e^{-\int d^3x\,\mathcal L_{\rm v}}\;, \qquad (3.27)$$

$$\mathcal L_{\rm v}=\frac{1}{3\kappa}{\rm Tr}((D_\mu\Phi)^\dagger D_\mu\Phi)+\mu\,{\rm Tr}(\Phi^\dagger\Phi)+\lambda_0{\rm Tr}(\Phi^\dagger\Phi)^2-\xi_0(\det\Phi+\det\Phi^\dagger) \qquad (3.28)$$

also contains quartic correlations whose importance is weighted by $\lambda$ ($>0$). This effective description has some similarities with the 't Hooft model (cf. Eq. (2.12)). More specifically, they coincide for configurations of the type $\Phi=VI_N$. Indeed, the $\det\Phi$ and $V^N$ terms have a similar physical origin. However, there is no reason for the path-integral to favor this type of restricted configuration. Up to this point, in the percolating phase ($\mu<0$), the quadratic and quartic terms tend to produce a manifold of classical vacua labeled by $U(N)$, while the addition of the $\det\Phi$-interaction reduces this manifold to $SU(N)$. Then, unlike the 't Hooft model, in the SSB phase this effective description has a continuum set of classical vacua which precludes the formation of the stable domain wall. In Sec. 3.3, this situation will be modified after introducing the possibility of correlated

instantons on top of center vortices.

It is interesting to formulate the Goldstone modes $V(x) \in SU(N)$ in the lattice, which leads to

$$S^{(3)}_{\rm latt}(b^{\mathcal{C}_e}_\mu) = \tilde{\beta} \sum_{x,\mu} {\rm Re}\ \left[\mathbb{I} - \bar{U}_\mu V(x+\hat{\mu}) V^\dagger(x))\right]\ , \tag{3.29}$$

where $U_\mu(x) = e^{i2\pi\beta_{\rm e}\cdot T} \in Z(N)$, if the link $x,\mu$ crosses $S(\mathcal{C}_{\rm e})$, and it is the identity otherwise. As expected, in the expansion of the partition function, besides the contribution of sites distributed on links that form loops, there is also one originated from $N$ lines that start or end at a common site $x$. In the former case, the singlets are included in $N \otimes \bar{N}$, while in the latter they are in the products of $N$ $V(x)$ or $V^\dagger(x)$ (compare with the Abelian case in 2.1.1). In this way, the rules originating Eq. (3.28) can be recovered in the lattice. This type of cross-checking is useful to better understand proposals of lattice ensemble measures in situations where it is harder to derive the effective field description, like in 4d spacetime.

## 3.3 Center vortices with attached instantons

In the lattice, most center vortices contain defects, thus forming chains or nonoriented center vortices [46]. It is therefore reasonable to expect that they might play an important role for describing all the properties of confinement in a satisfactory way. Similarly to the center-vortex configuration $A_\mu$ in Eq. (3.4) (resp. (3.16)), which can be written locally (but not globally) as a pure gauge using the singular phase $S = e^{i\chi\,\beta\cdot T}$ (resp. $e^{i\sum_{i=1}^{N-1}\chi_i\,\beta_i\cdot T}$), a chain can also be locally introduced as a transformation with phase

$$S = e^{i\chi\,\beta\cdot T}\,W(x)\ . \tag{3.30}$$

Because of the multivalued phase, the Cartan factor creates a thin center vortex, while $W(x)$ creates lower dimensional defects (see for example [46, 83, 84]). In 3D, these are pointlike (instanton) defects on the center-vortex worldlines, where the Lie algebra orientation changes. These orientations can be associated with two different fundamental weights $w$, $w'$, while $W(x)$ is a different Weyl transformation on each side of the instanton, at the center-vortex branches.

The properties of each type of defect are reflected in the gauge-invariant dual field strength $f_\mu(A) = \epsilon_{\mu\nu\rho} S^{-1} F_{\nu\rho}(A) S$. Considering a more general case where the mappings $S$ are multiplied on the right by a regular map, $S \to S\tilde{U}^{-1}(x)$, the field strengths for a thin center-vortex loop and $N$ matched center-vortex lines in Fig. 3.1 are respectively

given by

$$f_\mu(A) = f_\mu(l, g(s), \beta) \quad , \quad f_\mu(A) = \sum_{i=1}^{N} f_\mu(\gamma_i, g_i(s_i), \beta_i) \; . \tag{3.31}$$

where

$$f_\mu(\gamma, g(s), \beta) = \int_\gamma ds \frac{dx_\mu}{ds} \delta(x - x(s))\, g(s) \beta \cdot T g(s)^{-1} \quad , \quad g(s) \equiv \tilde{U}(x(s)) \; , \tag{3.32}$$

In addition, for a chain with a pair of instantons, $f_\mu(A)$ is given by

$$f_\mu(A) = f_\mu(\gamma, g(s), \beta) + f_\mu(\gamma', g'(s'), \beta') \; , \tag{3.33}$$

and, for $N \geq 3$, the three instanton contribution can be written as

$$f_\mu(A) = f_\mu(\gamma, g(s), \beta) + f_\mu(\gamma', g'(s'), \beta') + f_\mu(\gamma'', g''(s''), \beta'') \; . \tag{3.34}$$

## 3.4 Introducing correlated pointlike defects

Now, we would like to incorporate in the ensemble the possibility of nonoriented center-vortices. In Sec. 3.1, to derive the effective model, we used as starting point that the center elements $W_{\mathcal{C}}[A_\mu]$, obtained for a thin center-vortex loop and $N$ matched center-vortex lines, can be respectively cast in the form (cf. Eqs. (3.4) and (3.16))

$$W_l[b_\mu^{\mathcal{C}}] \quad \text{and} \quad \frac{1}{N!}\, \epsilon_{i_1 \ldots i_N} \epsilon_{i'_1 \ldots i'_N} \Gamma_{\gamma_1}[b_\mu^{\mathcal{C}}]|_{i_1 i'_1} \ldots \Gamma_{\gamma_N}[b_\mu^{\mathcal{C}}]|_{i_N i'_N} \; . \tag{3.35}$$

In order to identify correlators analogous to those in Eq. (3.35), while keeping in the ensemble the information about the attached instantons, we shall need the concept of Gilmore-Perelemov group coherent states (for a detailed discussion, see Refs. [87]-[91]).

Given a $\mathscr{D}$-dimensional irreducible representation D of a compact Lie Group $G$ over a vector space $V$, and a reference state $|\lambda\rangle \in V$, we may define the subgroup $H$ whose elements leave $|\lambda\rangle$ invariant up to a phase. The Gilmore-Perelemov group coherent states are then given by $|\xi, \lambda\rangle = \xi|\lambda\rangle$, where $\xi \in G$ is a choice of representatives (labels) for the equivalence classes in the coset space $G/H$. In particular, there is a unique decomposition $g = \xi h$, $g \in G$, $h \in H$. Then, as $G$ is transitive over $V$, the coherent states span this vector space, but they are not orthogonal, $\langle \xi, \lambda | \xi', \lambda \rangle \neq 0$. In addition, by using the invariance of the appropriately normalized measures in the group and the coset

$$\int d\mu(g) = 1 \quad , \quad \int d\mu(\xi) = \mathscr{D} \; , \tag{3.36}$$

as well as Schur's lemma, it is possible to show that the following relation holds:

$$\int d\mu(\xi)|\xi,\lambda\rangle\langle\xi,\lambda| = I_{\mathscr{D}} \ . \tag{3.37}$$

Therefore, the Gilmore-Perelemov states form an over-complete basis in $V$.

For elementary center vortices, we are interested in the coherent states $|g,w\rangle = g|w\rangle$, where $|w\rangle$ is any weight vector of the fundamental representation. In this case, Eq. (3.37) allows us to write

$$W_l[b_\mu] = \int d\mu(g)\, \langle g,w|\Gamma_l[b_\mu]|g,w\rangle \ . \tag{3.38}$$

Furthermore, the identity [92]

$$\int d\mu(g)\, g_{i_1 j_1}\dots g_{i_N j_N} = \frac{1}{N!}\epsilon_{i_1\dots i_N}\epsilon_{j_1\dots j_N} \tag{3.39}$$

leads to

$$\int d\mu(g)\, |g,w_1\rangle|_{i_1}\dots|g,w_N\rangle|_{i_N} = \int d\mu(g)\, g_{i_1 j_1}\dots g_{i_N j_N}|w_1\rangle|_{j_1}\dots|w_N\rangle|_{j_N} = \frac{1}{N!}\epsilon_{i_1\dots i_N} \ . \tag{3.40}$$

That is, for every $N$-line factor appearing in the ensemble, like the one in Eq. (3.19), we can use the representation

$$D_N[b_\mu] = (N!)^2 \int d\mu(g)d\mu(g_0)\langle g,w_1|\Gamma_{\gamma_1}[b_\mu]|g_0,w_1\rangle\dots\langle g,w_N|\Gamma_{\gamma_N}[b_\mu]|g_0,w_N\rangle \ . \tag{3.41}$$

The Eqs. (3.38) and (3.41) can be interpreted as associating each loop with a weight and each matched line as corresponding to a different weight.

Then, given that the center-vortex weight changes at the instantons, to include the effect of chains with $n$ pointlike defects into the ensemble, we may propose the contribution

$$\begin{aligned} &\langle g_1,w'|\Gamma_{\gamma_n}[b_\mu]|g_n,w\rangle\dots\langle g_3,w'|\Gamma_{\gamma_2}[b_\mu]|g_2,w\rangle\langle g_2,w'|\Gamma_{\gamma_1}[b_\mu]|g_1,w\rangle \\ &= \mathrm{Tr}\left(|\Gamma_{\gamma_n}[b_\mu]|g_n,w\rangle\langle g_n,w'|\dots|\Gamma_{\gamma_2}[b_\mu]|g_2,w\rangle\langle g_2,w'|\Gamma_{\gamma_1}[b_\mu]|g_1,w\rangle\langle g_1,w'|\right) \end{aligned} \tag{3.42}$$

to be integrated over the group elements. However, the integrals of $g_i|w\rangle\langle w'|g_i^\dagger$ vanish. This follows from the formula

$$\int d\mu(g)\, \mathrm{D}^{(i)}(g)|_{ab}\, \mathrm{D}^{(j)}(g^{-1})|_{\beta\alpha} = \delta_{ij}\delta_{a\alpha}\delta_{b\beta} \ , \tag{3.43}$$

where $\mathrm{D}^{(i)}$ and $\mathrm{D}^{(j)}$ are unitary irreps [93], applied to the adjoint and trivial irreps. Moreover, chains also contribute to the Wilson loop $W_{\mathcal{C}}[A_\mu]$ with a center element [20, 46, 83, 84]. This comes about as the $W(x)$-factor in Eq. (3.30) is single-valued when we go

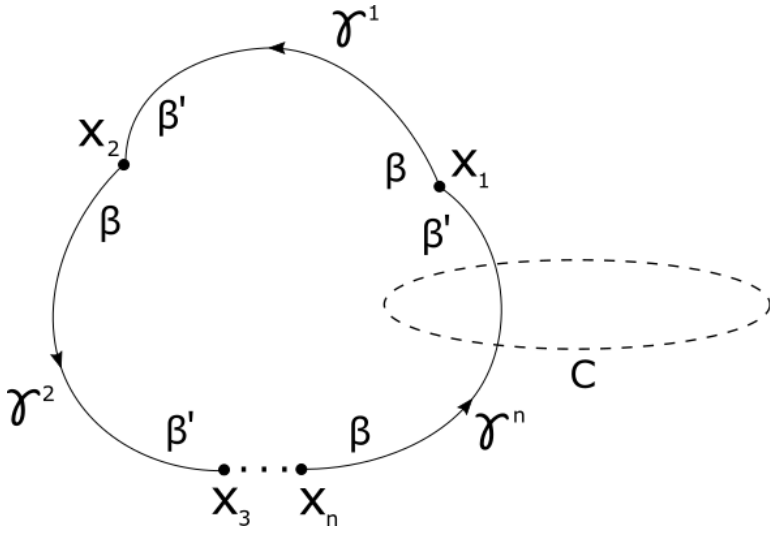


Figure 3.2: A chain configuration, with n correlated instantons, linking a Wilson Loop $\mathcal{C}$.

around the chain, so that the Wilson loop is only affected by the first factor, which gives the center element in Eq. (3.2). On the other hand, replacing $b_\mu \to b_\mu^{\mathcal{C}}$ in Eq. (3.42), we get a center element times additional overlaps which contain a nontrivial phase. To make sure that the only phases are associated with center elements, we shall include appropriate overlaps, defining the chain variable (see Fig. 3.2)

$$\int d\mu(g_1)\dots d\mu(g_n)\,\langle g_1,w|g_2,w'\rangle\langle g_2,w|g_3,w'\rangle\dots\langle g_n,w|g_1,w'\rangle$$
$$\times\langle g_1,w'|\Gamma_{\gamma_n}[b_\mu]|g_n,w\rangle\dots\langle g_3,w'|\Gamma_{\gamma_2}[b_\mu]|g_2,w\rangle\langle g_2,w'|\Gamma_{\gamma_1}[b_\mu]|g_1,w\rangle \tag{3.44}$$
$$=\int d\mu(g_1)\dots d\mu(g_n)\,\mathrm{Tr}\big(|g_n,w'\rangle\langle g_n,w|\dots|g_2,w'\rangle\langle g_2,w|\,|g_1,w'\rangle\langle g_1,w|\big)$$
$$\times\mathrm{Tr}\left(|\Gamma_{\gamma_n}[b_\mu]|g_n,w\rangle\langle g_n,w'|\dots|\Gamma_{\gamma_2}[b_\mu]|g_2,w\rangle\langle g_2,w'|\Gamma_{\gamma_1}[b_\mu]|g_1,w\rangle\langle g_1,w'|\right). \tag{3.45}$$

In this manner, for $b_\mu \to b_\mu^{\mathcal{C}}$, when the chain links $\mathcal{C}$, one of the center-vortex lines will intersect the surface $S(\mathcal{C})$ giving a nontrivial contribution. The final result coincides with the Wilson loop computed for the chain configuration $A_\mu$, times a real and positive weight factor:

$$\left(e^{i2\pi k/N}\right)^{L(\mathcal{C},l)}\int d\mu(g_1)\dots d\mu(g_n)\,\left|\mathrm{Tr}\big(|g_n,w'\rangle\langle g_n,w|\dots|g_2,w'\rangle\langle g_2,w|\,|g_1,w'\rangle\langle g_1,w|\big)\right|^2\,. \tag{3.46}$$

To obtain an alternative interpretation of the chain and the other defects, we initially note that for, say, the $n=2$ case, we may change $g_2 \to g_2 W$, where $W$ is an odd Weyl

reflection that takes $w$ into $w'$ and $w'$ and $w$, to get the variable

$$\int d\mu(g_1)d\mu(g_2)\,\langle g_1,w|g_2,w\rangle\langle g_2,w'|g_1,w'\rangle\times\langle g_1,w'|\Gamma_{\gamma_2}[b_\mu]|g_2,w'\rangle\langle g_2,w|\Gamma_{\gamma_1}[b_\mu]|g_1,w\rangle\ . \tag{3.47}$$

Similarly, for $n=3$, $N>2$ we can make an even Weyl transformation that changes $g_2\to g_2P_A$, where $P_A$ permutes $w$, $w'$, $w''$ to $w''$, $w$, $w'$, and then $g_3\to g_3P_B$, where $P_B$ permutes $w$, $w'$, $w''$ to $w'$, $w''$, $w$, thus obtaining the variable

$$\begin{aligned}&\int d\mu(g_1)d\mu(g_2)d\mu(g_3)\,\langle g_1,w|g_2,w\rangle\langle g_2,w''|g_3,w''\rangle\langle g_3,w'|g_1,w'\rangle\\ &\times\langle g_1,w'|\Gamma_{\gamma_3}[b_\mu]|g_3,w'\rangle\langle g_3,w''|\Gamma_{\gamma_2}[b_\mu]|g_2,w''\rangle\langle g_2,w|\Gamma_{\gamma_1}[b_\mu]|g_1,w\rangle\ .\end{aligned} \tag{3.48}$$

Next, we can use the Gilmore-Perelemov representation,

$$\langle g,w|\Gamma_\gamma[b_\mu]|g_0,w\rangle=\int[dg(s)]\,e^{i\int ds\mathrm{Tr}\left(\left(g(s)^\dagger b(s)g(s)+ig^\dagger(s)\dot g(s)\right)w\cdot T\right)}\quad,\quad b(s)=b_\mu(x(s))\frac{dx_\mu}{ds}\ , \tag{3.49}$$

where the paths $g(s):[0,L]\to SU(N)$ satisfy the boundary conditions $g(0)=g_0$, $g(L)=g$. In principle, this applies when the reference state $|w\rangle$ is a highest weight vector. However, the center-vortex holonomy is in the fundamental representation, so the associated weights can be connected by Weyl transformations. Thus, this formula holds for any weight vector $|w_i\rangle$, $i=1,\dots,N$, which has components $|w_i\rangle|_j=\delta_{ij}$. As usual, the trace in the exponent of Eq. (3.49) can be rewritten in terms of non-Abelian d.o.f. $|z(s)\rangle=|g(s),w\rangle$ [95] (see also [91]),

$$\mathrm{Tr}\,(\dots)=b^A_\mu(x(s))T_A|_{ij}\,z_j\bar z_i\frac{dx_\mu}{ds}+\frac{i}{2}(\bar z_i\dot z_i-\dot{\bar z}_iz_i)\ , \tag{3.50}$$

where the last term can be interpreted as a kinetic term for these degrees (see Ref. [96]). Moreover, using Eq. (3.49) for each line defect, the $b_\mu$-coupling in the variables containing a loop, $N$ matched center vortex lines, and chains with two or three instantons (cf. Eqs. (3.38), (3.41), (3.47), and (3.48)), becomes

$$e^{i\int d^3x\,\frac{1}{2N}\mathrm{Tr}\left(b_\mu f_\mu(A)\right)}\ , \tag{3.51}$$

where $f_\mu(A)$ is the gauge-invariant field strength for the corresponding $A_\mu$-configurations equipped with non-Abelian d.o.f. (see Eqs. (3.31)-(3.34)), as described in Ref. [56] when dealing with nonoriented center vortices in $(3+1)$d. That is, the various dual variables, which are designed to reproduce $W[A_\mu]$, precisely couple the corresponding fields $f_\mu(A)$ to $b_\mu(x)$.

As already discussed, when immersed into the ensemble, the path-integral of the holonomies over paths with tension and stiffness will give rise to a Green's function (cf. Eq. (3.20)). In this manner, the chain contributions in Eq. (3.44) become generated by the new vertex

$$V_{\rm inst} \propto \int d\mu(g) \langle g, w'|\Phi^\dagger|g, w'\rangle\langle g, w|\Phi|g, w\rangle, \tag{3.52}$$

or, equivalently,

$$\begin{aligned} V_{\rm inst} &\propto \int d\mu(g) {\rm Tr}\, \left(|g, w\rangle\langle g, w'|\Phi^\dagger|g, w'\rangle\langle g, w|\Phi\right) \\ &= \int d\mu(g) {\rm Tr}\, \left(g|w\rangle\langle w'|g^\dagger\Phi^\dagger g|w'\rangle\langle w|g^\dagger\Phi\right). \end{aligned} \tag{3.53}$$

Notice that $|w'\rangle\langle w| = E_\alpha$ is a root vector characterized by the root $\alpha = w' - w$. We may write it in terms of the hermitian generators $T_\alpha$, $T_{\bar\alpha}$, defined by

$$E_\alpha = \frac{T_\alpha + iT_{\bar\alpha}}{\sqrt{2}}\,, \tag{3.54}$$

and use that $gT_Ag^\dagger$ is just the adjoint action of $g$ on $T_A$, $gT_Ag^\dagger = R_{AB}(g)T_B$. Then,

$$V_{\rm inst} \propto \frac{1}{2}\int d\mu(g)\, {\rm Tr}\left((R_{\alpha B}(g) + iR_{\bar\alpha B}(g))T_B\Phi^\dagger(R_{\alpha C}(g) - iR_{\bar\alpha C}(g))T_C\Phi\right)\,. \tag{3.55}$$

To perform the integrals, we can use Eq. (3.43) for the case where $i$ and $j$ stand for the adjoint representation,

$$\int d\mu(g)\, R_{AB}(g)\, R_{A'B'}(g) = \delta_{AA'}\delta_{BB'}\,. \tag{3.56}$$

The result is that the instanton-vertex turns out to be

$$V_{\rm inst} \propto {\rm Tr}(\Phi^\dagger T_A\Phi T_A)\,. \tag{3.57}$$

Summarizing, after the discussions in Sec. 3.1 and 3.3, we have shown that the center element average in the proposed 3D ensemble, which involves the linking-numbers between the Wilson loop and the mixture of center-vortex loops, correlated $N$-line center vortices and chains, can be effectively represented as

$$\langle W(\mathcal{C})\rangle = \frac{Z[b_\mu^{\mathcal{C}}]}{Z[0]} \quad , \quad Z[b_\mu] \equiv \int [D\Phi]\, e^{-S_{\rm eff}(\Phi, b_\mu)}\,, \tag{3.58}$$

where the partition function is governed by the large-distance effective action

$$S_{\rm eff}(\Phi, b_\mu) = \int d^3x \left( {\rm Tr}\,(D_\mu \Phi)^\dagger D^\mu \Phi + V(\Phi, \Phi^\dagger) \right) \quad , \quad D_\mu = \partial_\mu - i b_\mu \ ,$$
$$V(\Phi, \Phi^\dagger) = \frac{\lambda}{2} {\rm Tr}\,(\Phi^\dagger \Phi - a^2 I_N)^2 - \xi \big( \det \Phi + \det \Phi^\dagger \big) - \vartheta {\rm Tr}\,(\Phi^\dagger T_A \Phi T_A) + c \ . \qquad (3.59)$$

Here, we considered a negative tension $\mu$ in Eq. (3.28), which represents a phase where center vortices proliferate. This, together with a positive stiffness $1/\kappa$, implies $a^2 > 0$. This precisely corresponds to a center-vortex condensate. At this point, we notice that the initial color and flavour symmetries of the pure vortex model (c.f. Eq. (3.26)) are broken by the instanton term. However, a global color-flavor symmetry ($S_c = S_f^\dagger$) is preserved, as well as a (local) discrete $Z(N)$ symmetry $\Phi \to e^{i\theta_V(x)\beta\cdot T}\Phi$, where $\theta_V(x)$ is a Heaviside function, which is equal to $2\pi$ (resp. 0) inside (resp. outside) a volume $V$. The latter can be used to change the surface $S(\mathcal{C})$ when computing center-element averages. The constant $c$ is chosen such that the action at the vacua is zero. In addition, for later convenience, we shall consider a region in parameter space given by positive $\xi$ and $\vartheta$.

It is interesting to check in the lattice how the different configuration types are recovered. For example, in the parameter region $\lambda \ , \xi \ >> \ \vartheta$, the most relevant fluctuations will be parametrized by $\Phi \propto S$, $S \in SU(N)$. The additional nonoriented component in the discretized theory is generated from the product of an adjoint variable arising from the new term

$${\rm Tr}\left(\Phi^\dagger T_A \Phi T_A\right) \sim {\rm const.}\, {\rm Tr}\,({\rm Ad}(S)) \ , \qquad (3.60)$$

at a lattice site $x$, with the adjoint contribution in $N \otimes \bar{N}$ associated with $V(x)$ and $V^\dagger(x)$.

## 3.5 Domain walls with asymptotic Casimir scaling

In this section, we shall explore the physical consequences of the effective representation for the ensemble of magnetic defects (cf. Eqs. (3.58) and (3.59)). For this aim, we shall initially analyze the properties of the spontaneous symmetry breaking phase that the system undergoes. If $N > 4$, the potential does not have a lower bound and terms of order higher than $N$ should be included to stabilize it. When seeking a global minimum, we suppose these terms are present, although we do not include them explicitly. We shall consider a region in parameter space so that the potential is dominated by the $\lambda$ and $\xi$-terms. The polar decomposition $\Phi = PU$, where $P$ is a positive semidefinite hermitian matrix and $U \in U(N)$, can be used to write the potential as

$$V(P, U) = \frac{\lambda}{2} {\rm Tr}\ \left((P^2 - a^2 I_N)^2\right) - \xi \det P \,(\det U + \det U^\dagger) - \vartheta {\rm Tr}\ \left(P T_A P U T_A U^\dagger\right) \ . \ (3.61)$$

If the only terms were those associated with center-vortex correlations, namely the $\lambda$ and $\xi$-terms, then the global minima would certainly be achieved at $P$ proportional to the identity $I_N$. Due to the minus sign, the determinant term also forces $\det U = 1$, so that $U \in SU(N)$. Then, up to this point, the possible vacua would form a (continuum) connected manifold, thus precluding the formation of a stable domain wall sitting on the Wilson loop. In this case, the calculation of the partition function would involve large quantum fluctuations associated with the various Goldstone field modes. This type of problem was analyzed in an Abelian context in Ref. [49]. On the other hand, when the scenario above is corrected by the inclusion of pointlike defects on center vortices, which is represented by the $\vartheta$-term, the set of possible vacua becomes discrete. Indeed, because of our choice of sign for $\vartheta$, the minimum values of the potential require a maximum overlap between the basis $T_A$ and the rotated basis $n_A = UT_AU^{-1}$, which is attained when $U$ is in the center $Z(N)$ of $SU(N)$. More precisely, the global minima turn out to be

$$P = vI_N \ , \ U \in \mathcal{Z}_N = \left\{ e^{i\frac{2\pi n}{N}} I_N \,\middle|\, n = 0, 1, 2, ..., N-1 \right\} \ , \tag{3.62a}$$

$$2\lambda N(v^2 - a^2) - 2\xi N v^{N-2} - \vartheta \left(N^2 - 1\right) = 0 \ . \tag{3.62b}$$

Then, it is the presence of correlated instantons that grants the formation of stable domain walls. In a 3D spacetime, a disconnected set of vacua (with nontrivial homotopy group $\Pi_0$) enables a field configuration with different vacua on both sides of a surface, with a transition that necessarily implies an action cost localized on the surface. As we will see, in the presence of a Wilson loop, the surface will sit on the loop. Moreover, as the vacua are discrete, there are no Goldstone field modes, and the partition function will be evaluated by means of a saddle point corrected by low-action fluctuations around this point. The former will give rise to a confining area law, while the latter will correct the associated linear potential with the well-known universal Lüscher term. A similar situation was recently obtained in Ref. [56], when describing a mixed ensemble of center vortices and chains in 4D spacetime. In that reference, the inclusion of correlated monopole worldlines on center-vortex worldsurfaces led to a manifold of vacua with nontrivial first homotopy group $\Pi_1 = Z(N)$. This led to the formation of a confining center string between a quark-antiquark pair, which spans a surface whose border is the Wilson loop.

Our main objective is to determine the scaling law obeyed by the asymptotic string tension. The saddle-point $\Phi$ for the partition function $Z[b_\mu^{\mathcal{C}}]$ in Eq. (3.58) satisfies

$$D^2\Phi = \lambda\Phi(\Phi^\dagger\Phi - a^2) - \xi\, C[\Phi^*] - \vartheta T_A \Phi T_A \quad , \quad D_\mu = \partial_\mu - ib_\mu^{\mathcal{C}} \ . \tag{3.63}$$

In this respect, we recall that for small variations of the determinant, we have

$$\det(\Phi + \delta\Phi) \approx \det\Phi + \mathrm{Tr}\, \left(C[\Phi^T]\delta\Phi\right) \tag{3.64}$$

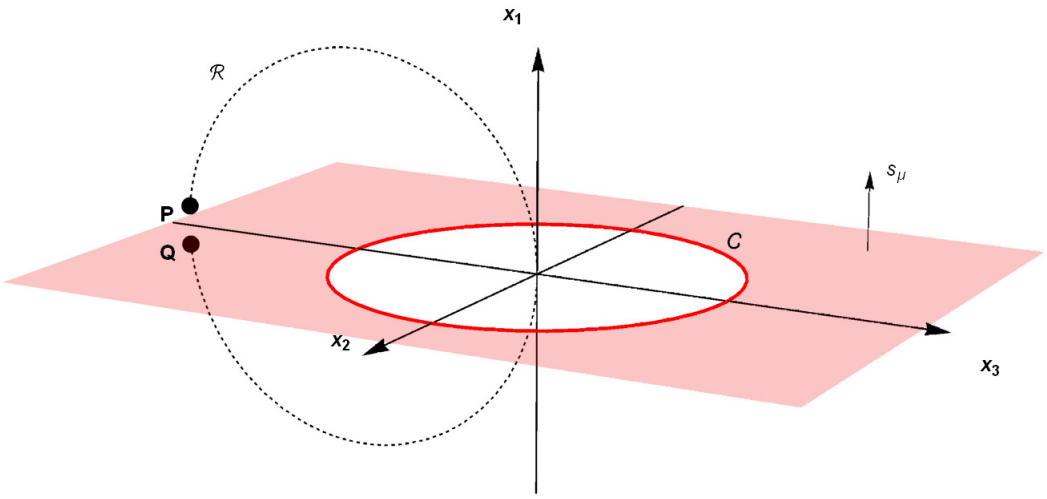


Figure 3.3: A ring $\mathcal{R}$ winding around the Wilson loop and passing through the origin. The surface where $s_\mu$ is concentrated is depicted in red.

where $C[\ ]$ stands for the cofactor matrix. Let us analyze how the field $\Phi$ must behave along an arbitrary circle $\mathcal{R}$ that links the loop $\mathcal{C}$. Take for example the loop shown in Fig. 3.3. From **Q** to **P**, points immediately below and above the intersection between $\mathcal{R}$ and the surface where $s_\mu$ is concentrated, the field $\Phi$ must 'jump' by a phase factor $e^{i2\pi\beta_e\cdot T}$ in order to cancel (the regularized form of) $b_\mu^C$ in the covariant derivative, and yield a finite action. This factor is an element of $Z(N)$ and, consequently, the action will be minimized if $\Phi$ is at a vacuum value at **Q**, say $vI_N$, and continuously changes to the vacuum $ve^{i2\pi\beta_e\cdot T}$ at **P**, as one goes around $\mathcal{R}$. With a discrete set of vacua, this is only possible if $\Phi$ leaves the vacuum somewhere. In general, the transition will be localized around the minimal surface (the disk **D**) whose border is $\mathcal{C}$. A finite action also requires that above and below the $x_1 = 0$ plane, and far from the Wilson loop $\mathcal{C}$, the field $\Phi$ must tend to two different vacua, given by the values at **P** and **Q**, respectively. In particular, if we follow the $x_1$-axis, or any other parallel line that intersects the disk **D** at coordinates $(0, x_2, x_3)$, the external source leaves a trace of its existence only in the boundary condition

$$\lim_{x_1\to-\infty}\Phi(x_1,x_2,x_3) = vI_N \quad , \quad \lim_{x_1\to+\infty}\Phi(x_1,x_2,x_3) = v\,e^{i2\pi\beta_e\cdot T} \quad , \quad (0,x_2,x_3)\in\mathbf{D}\ . \tag{3.65}$$

For an asymptotic Wilson loop, which is much larger than the localization scales in the effective model, the solution will be almost independent of $(x_2, x_3)$, as long as they remain away from $\mathcal{C}$. In other words, the saddle-point action can be approximated by

$$S_{\text{eff}} \approx \varepsilon A\ , \tag{3.66}$$

where $A$ is the area of the disk (plus a border effect that scales as the perimeter), and the

string tension is then obtained from the soliton solution $\Phi(x)$, ($x_1 \equiv x$) that minimizes

$$\varepsilon \;=\; \int dx \left( \mathrm{Tr}\,(\partial_x \Phi)^\dagger \partial_x \Phi + V(\Phi, \Phi^\dagger) \right) \;, \tag{3.67}$$

with $\Phi(-\infty) = v I_N$, $\Phi(+\infty) = v\, e^{i2\pi\beta_e \cdot T}$. This solution satisfies Eq. (3.63) with the replacement $D^2\Phi \to \partial_x^2 \Phi$. To close this equation with a simple ansatz, we need to discuss some properties of the weights of $\mathfrak{su}(N)$. For each $N-$ality $k$, we shall consider two types of irreps., called $k-$Symmetric and $k-$Antisymmetric. Their highest weights are $w_k^S = k w_1$ and $w_k^A = w_1 + w_2 + ... + w_k$, respectively. Note that, being the sum of $k$ weights of the defining representation, they yield the correct center element in Eq. (3.2).

In the asymptotic regime, gluon screening is expected to take place, bringing down the string tension of any irreducible representation to that of the lowest-dimensional one with the same $N-$ality $k$. The latter corresponds to the $k-$Antisymmetric irrep., $\beta_e = 2N w_k^A$, which we shall focus in what follows. In this case, a simple ansatz is motivated by the block-diagonal structure of $\beta_e \cdot T$. If we define $P_1 = \mathrm{Diag}(1, 1, ..., 0, 0, ....0)$ with the first $k$ entries being nonzero and $P_2 = I_N - P_1$, we can use Eq. (3.3) to write

$$\beta_e \cdot T = \mathrm{Diag}(\beta_e \cdot w_1, ..., \beta_e \cdot w_N) = \begin{pmatrix} \frac{N-k}{N} I_k & 0 \\ 0 & -\frac{k}{N} I_{N-k} \end{pmatrix} = \frac{N-k}{N} P_1 - \frac{k}{N} P_2 \;. \tag{3.68}$$

Because the product between any number of $P_1$ and $P_2$ is either $P_1$, $P_2$ or 0, an ansatz built upon $P_1$ and $P_2$ will close the equations of motion. Thus, we propose

$$\Phi = (h_1 P_1 + h_2 P_2)\, S \quad , \quad S = e^{i\theta_1 \frac{N-k}{N} P_1 - i\theta_2 \frac{k}{N} P_2} \;. \tag{3.69}$$

The phase can be factored in $U(1)$ and $SU(N)$ sectors

$$S = e^{i\alpha} e^{i\theta\beta\cdot T} \quad , \quad \theta = \frac{N-k}{N}\theta_1 + \frac{k}{N}\theta_2 \quad , \quad \alpha = \frac{k(N-k)(\theta_1 - \theta_2)}{N^2} \;. \tag{3.70}$$

In principle, as $e^{i2\pi\beta_e \cdot T} = e^{-i\frac{2k\pi}{N}}$, there are two ways to impose the boundary conditions (3.65): one where $\alpha$ (resp. $\theta$) undergoes a nontrivial transition and leaves the possibility of $\theta$ (resp. $\alpha$) to remain constant. The first possibility gives rise to a model closely related with the 't Hooft's model [3], for which a Casimir law is not observed, while the second,

$$h_1(-\infty) = h_2(-\infty) = h_0 \qquad , \qquad h_1(\infty) = h_2(\infty) = h_0 \;, \tag{3.71a}$$

$$\theta_1(-\infty) = \theta_2(-\infty) = 0 \qquad , \qquad \theta_1(\infty) = \theta_2(\infty) = 2\pi \;, \tag{3.71b}$$

$$\theta(-\infty) = 0 \;,\; \theta(\infty) = 2\pi \qquad , \qquad \alpha(-\infty) = 0 \;,\; \alpha(\infty) = 0 \;, \tag{3.71c}$$

which is consistent with our choice of external source $b_\mu^{\mathcal{C}}$, is the option we shall further explore. Moreover, we shall assume $\xi v^{N-2} >> \vartheta$, thus disfavoring $\alpha$ to leave its constant

value $\alpha = 0$. Plugging the ansatz in eq. (3.63) and equating to zero the coefficients of $P_1S$, $P_2S$ $iP_1S$ and $iP_2S$, we obtain

$$\partial_x^2 h_1 = \left(\frac{N-k}{N}\right)^2 (\partial_x\theta_1)^2 h_1 + \lambda h_1(h_1^2 - a^2) - \xi h_1^{k-1} h_2^{N-k} \cos\left(\frac{k(N-k)(\theta_1-\theta_2)}{N}\right) - \vartheta \frac{Nk-1}{2N^2} h_1 - \vartheta \frac{N-k}{2N} h_2 \cos\left(\frac{k}{N}\theta_2 + \frac{N-k}{N}\theta_1\right) , \tag{3.72a}$$

$$\partial_x^2 h_2 = \left(\frac{k}{N}\right)^2 (\partial_x\theta_2)^2 h_2 + \lambda h_2(h_2^2 - a^2) - \xi h_1^{k} h_2^{N-k-1} \cos\left(\frac{k(N-k)(\theta_1-\theta_2)}{N}\right) - \vartheta \frac{N(N-k)-1}{2N^2} h_2 - \vartheta \frac{k}{2N} h_1 \cos\left(\frac{k}{N}\theta_2 + \frac{N-k}{N}\theta_1\right) , \tag{3.72b}$$

$$\partial_x^2 \theta_1 = -2\partial_x \ln h_1 \, \partial_x\theta_1 + \xi \frac{N}{N-k} h_1^{k-2} h_2^{N-k} \sin\left(\frac{k(N-k)(\theta_1-\theta_2)}{N}\right) + \frac{\vartheta}{2}\frac{h_2}{h_1} \sin\left(\frac{k}{N}\theta_2 + \frac{N-k}{N}\theta_1\right) , \tag{3.72c}$$

$$\partial_x^2 \theta_2 = -2\partial_x \ln h_2 \, \partial_x\theta_2 - \xi \frac{N}{k} h_1^{k} h_2^{N-k-2} \sin\left(\frac{k(N-k)(\theta_1-\theta_2)}{N}\right) + \frac{\vartheta}{2}\frac{h_1}{h_2} \sin\left(\frac{k}{N}\theta_2 + \frac{N-k}{N}\theta_1\right) . \tag{3.72d}$$

The ansatz in Eq. (3.69) can be rewritten as

$$\Phi = (\eta I_N + \eta_0 \beta\cdot T)\, e^{i\theta\beta\cdot T} e^{i\alpha} \quad , \quad \eta = \frac{k}{N}h_1 + \frac{N-k}{N}h_2 \ , \ \eta_0 = h_1 - h_2 \, . \tag{3.73}$$

The equations for these profiles are a little bit more intricate to write down, but they are more meaningful. In particular, if we look at small perturbations around their vacuum value and keep up to linear terms, we get

$$\partial_x^2 \delta\eta = M_\eta^2 \delta\eta \quad , \quad M_\eta^2 = \lambda(3v^2 - a^2) - \xi(N-1)v^{N-2} - \vartheta\frac{N^2-1}{2N^2} \, , \tag{3.74a}$$

$$\partial_x^2 \delta\eta_0 = M_{\eta_0}^2 \delta\eta_0 \quad , \quad M_{\eta_0}^2 = \lambda(3v^2 - a^2) + \xi v^{N-2} + \frac{\vartheta}{2N^2} \, , \tag{3.74b}$$

$$\partial_x^2 \delta\alpha = M_\alpha^2 \delta\alpha \quad , \quad M_\alpha^2 = N\xi v^{N-2} \, , \tag{3.74c}$$

$$\partial_x^2 \delta\theta = M_\theta^2 \delta\theta \quad , \quad M_\theta^2 = \frac{\vartheta}{2} \, . \tag{3.74d}$$

These squared masses are non negative (cf. Eq. (3.62b)), with $M_\eta$, $M_{\eta_0}$ and $M_\alpha$ larger than $M_\theta$ due to our previous requirements $\lambda a^2$, $\xi v^{N-2} >> \vartheta$. In this region of parameter space, the functions $\eta$, $\eta_0$ and $\alpha$ are practically constant and $\theta$ is the only one that varies appreciably as it is compelled by the boundary conditions. If the instantons were absent ($\vartheta = 0$), the field $\theta$ would be a massless mode associated with the residual $SU(N)$ symmetry of the vacuum. On the other hand, their presence on top of center vortices to form nonoriented center vortices makes the profile $\theta$ to be governed by the Sine-Gordon

equation

$$\partial_x^2\,\theta = \frac{\vartheta}{2}\sin\theta\ . \tag{3.75}$$

For the soliton solution, we can use Derrick's theorem in Eq. (3.67) to equate its kinetic and potential contribution so that the string tension in the $k$-Antisymmetric representation is

$$\begin{aligned}\varepsilon_k = 2\int dx\,\Bigg(&\left(\frac{N-k}{N}\right)^2 h_1^2(\partial_x\theta_1)^2\,\mathrm{Tr}\,P_1\\ &+(\partial_x h_1)^2\,\mathrm{Tr}\,P_1+\left(\frac{k}{N}\right)^2 h_2^2(\partial_x\theta_2)^2\,\mathrm{Tr}\,P_2+(\partial_x h_2)^2\,\mathrm{Tr}\,P_2\Bigg)\ ,\end{aligned} \tag{3.76}$$

which can be approximated by

$$\varepsilon_k = \frac{k(N-k)}{N-1}\left(2v^2\frac{N-1}{N}\int(\partial_x\theta)^2dx\right) = \frac{k(N-k)}{N-1}\varepsilon_1\ . \tag{3.77}$$

where $\varepsilon_1$ is proportional to the Sine-Gordon parameter $\vartheta$. Therefore, the string tension follows a Casimir law. This result can be understood if one considers that, for $\alpha$, $\eta$ and $\eta_0$ frozen at their vacuum value, the only relevant mode is $\theta$ with $\Phi = ve^{i\theta\beta_e\cdot T}$. Consequently, since the total energy is twice the kinetic energy, we get[2]

$$\varepsilon_k = 2v^2\int \mathrm{Tr}\big(\partial_x S^\dagger\partial_x S\big)\,dx = v^2\frac{\beta_e\cdot\beta_e}{N}\int(\partial_x\theta)^2dx\ , \tag{3.78}$$

which, for the $k-$Antisymmetric representation, is proportional to the quadratic Casimir operator: $\beta_e\cdot\beta_e = 2k(N-k)$. For an arbitrary irrep., besides the mode along $\beta_e\cdot T$, additional soft modes in the Cartan sector are needed to close the equations of motion. In this case, a similar procedure can be followed, although it is difficult to analytically obtain the scaling. However, for the $k$-Symmetric representation, it is easy to see that the same ansatz works, and that the energy can be approximated by Eq. (3.78) with $\beta_e\cdot\beta_e = 2k^2(N-1)$. This is greater than $2k(N-k)$, the value obtained for the $k-$Antisymmetric case. Therefore, for a given $N$-ality $k$, it becomes clear that the latter possibility will be preferred, together with its ensuing Casimir law.

[2]Here, we use the normalization $\mathrm{Tr}\,(T_qT_p) = \frac{\delta_{qp}}{2N}$, which is consistent with Eq. (3.3).

# Chapter 4

# 4d Ensemble with Asymptotic Casimir Law

Although dual superconductor models have long been proposed as an effective description of color confinement [3, 85, 86], so far, no such model has been completely successful. The many candidates [66, 67, 68, 69, 70, 83, 97, 98, 99, 100, 101, 102, 103, 104, 105, 106, 107, 108, 109, 110] grasp some, but not all, of the rich confinement phenomenology obtained from the lattice. $N$-ality suggests that confining strings could be represented as stable topological vortices in a Yang-Mills-Higgs (YMH) field description. Models with fields transforming in the fundamental representation [66], the adjoint [83, 97, 108, 109, 110], or both [67, 68, 69, 70, 104, 105, 106], are among the possibilities. In spite of the fact that these models possess vacua leading to confining strings with $N$-ality, the different field contents and Higgs potentials make it necessary to work on a case by case basis to determine the precise vortex profiles and the behavior of the string tension. For example, a model motivated by supersymmetry and based on three complex adjoint fields was analyzed in Ref. [97]. Although the group action on the vacua manifold is not transitive in this case, the physical properties in the different sectors can be related by means of appropriate mappings between them. Moreover, a numerical analysis of the vortex solutions showed a string tension closely approximated by a Casimir law. An important question is how to build a bridge between this type of approach and center-vortex scenarios. Recently, in Ref. [56], the effective description of an ensemble of two-dimensional percolating worldsurfaces with attached monopole worldlines in 4d was related to a YMH effective model. In the effective description, the dual gauge field represents the Goldstone modes in a condensate of one-dimensional defects, which generate the worldsurfaces, while a set of adjoint Higgs fields reproduce the monopole degrees of freedom. The field content in Ref. [56] was chosen so as to implement the monopole fusion rules; in particular, models with an adjoint flavor index naturally encompass all possibilities. In this case, the phenomenological parameters can be chosen so as to obtain a transitive group action and drive $SU(N) \to Z(N)$ SSB. Transitivity of the vacua manifold automatically renders the

different choices (labeled by points in $SU(N)/Z(N)$) physically equivalent. Then, among the alternatives, a detailed analysis of this type of model is of special interest. In this thesis, despite the large number of fields, we will show that the system acquires a collective behavior where the classical vortex solutions are well accommodated by a small ($N$ and $k$-independent) number of profiles. Moreover, we shall obtain a region in parameter space where the exact asymptotic Casimir law holds. In this regime, most of the field profiles become frozen at their vacuum value while the nontrivial ones obey the Nielsen-Olesen equations, thus reproducing the chromoelectric field measured in the lattice (see Secs. 4.2 and 4.3). In Sec. 4.4, we will show the result of numerical simulations in other regions. In this respect, it is interesting to note that, at asymptotic distances, the linear $k$-scaling, expected to occur in the large $N$ limit, was reproduced by including monopole variables [111].

## 4.1 Effective description of 4d percolating center vortices

Here, we review the ensembles of oriented and nonoriented center vortices in four dimensions as proposed in [56]. In that study, instead of deriving the effective description of center-vortex ensembles with negative tension and positive stiffness, the discussion was initiated from the natural Goldstone modes defined on the lattice (see also Sec. 2.1.2). The missing steps are expected to be implemented by deriving diffusion loop equations including the effect of stiffness. The lattice description of an Abelian ensemble of worldsurfaces coupled to an external Kalb–Ramond field in the form

$$\int d\sigma_1 d\sigma_2 \, B_{\mu\nu}(X(\sigma_1,\sigma_2))\Sigma^{\mu\nu}(X(\sigma_1,\sigma_2)) \quad , \quad \Sigma^{\mu\nu} = \frac{\partial X^\mu}{\partial\sigma_1}\frac{\partial X^\nu}{\partial\sigma_2} - \frac{\partial X^\nu}{\partial\sigma_1}\frac{\partial X^\mu}{\partial\sigma_2} \, , \qquad (4.1)$$

where $X^\mu(\sigma_1,\sigma_2)$ is a parametrization of the worldsurface, was obtained in [55]. This was done in terms of a complex-valued string field $V(C)$, where $C$ is a closed loop formed by a set of lattice links. The associated action is

$$S_V = -\sum_C \sum_{p\in\eta(C)} \left[\bar{V}(C+p)U_p V(C) + \bar{V}(C-p)\bar{U}_p V(C)\right] + \sum_C m^2 \bar{V}(C)V(C) \, . \qquad (4.2)$$

$\eta(C)$ is the set of plaquettes that share at least one common link with $C$, while $C+p$ is the path that follows $C$ until the initial site of the common link, then detours through the other three links of $p$, and continues along the remaining part of $C$. In addition, the coupling (4.1) originates the plaquette field $U_p = e^{ia^2 B_{\mu\nu}(p)}$. Then, the following polar

decomposition was considered

$$V(C) = w(C) \prod_{l \in C} V_l \quad , \quad V_l \in U(1) \; , \tag{4.3}$$

with a phase factor that has a "local" character, as it was written in terms of the holonomy along $C$ of gauge field link-variables $V_l$. Finally, when a condensate is formed ($m^2 < 0$), it was argued that the modulus is practically frozen[1], so that $w(C) \approx w > 0$. By using this fact in equation (4.2), the only links whose contribution do not cancel are those belonging to $p$:

$$\bar{V}(C+p) U_p V(C) = w^2 \prod_{l \in C+p} \prod_{l' \in C} \bar{V}_l U_p V_{l'} = w^2 U_p \prod_{l \in p} \bar{V}_l \; . \tag{4.4}$$

Thus,

$$S^{(4)}_{\rm latt}(\alpha_p) = \tilde{\beta} \sum_p {\rm Re} \; \left[ \mathbb{I} - \bar{U}_p \prod_{l \in p} V_l \right] \; . \tag{4.5}$$

where the sum is over all plaquettes $p$ and a constant was added such that the action vanishes for a trivial plaquette. Then, the description of a loop condensate, where loops are expected to percolate, is much simpler than that associated with a general phase. The string field parameter gives place to simpler gauge field Goldstone variables $V_\mu = e^{i\Lambda_\mu(l)}$, governed by a Wilson action with frustration $U_p$. This was the starting input used in [56]. An external Kalb–Ramond field that generates the center elements when the simplest center-vortex worldsurface link $\mathcal{C}_{\rm e}$ is obtained by replacing $B_{\mu\nu} \to \frac{2\pi k}{N} s_{\mu\nu}$, where $k$ is the $N$-ality of the quark representation D and

$$s_{\mu\nu} = \int_{S(C_e)} d^2\tilde{\sigma}_{\mu\nu} \delta^{(4)}(x - X(\sigma_1, \sigma_2)) \; , \tag{4.6}$$

$$d^2\tilde{\sigma}_{\mu\nu} = \frac{1}{2} \epsilon_{\mu\nu\alpha\beta} \left( \frac{\partial X^\alpha}{\partial \sigma_1} \frac{\partial X^\beta}{\partial \sigma_2} - \frac{\partial X^\beta}{\partial \sigma_1} \frac{\partial X^\alpha}{\partial \sigma_2} \right) d\sigma_1 d\sigma_2 \tag{4.7}$$

is localized on $S(\mathcal{C}_{\rm e})$. In the lattice, this localized source corresponds to a frustration $U_p = e^{i\alpha_p}$, where $\alpha_p = -2\pi k/N$ if $p$ intersects $S(\mathcal{C}_{\rm e})$ and it is trivial otherwise. Similarly to the 3d case, it is possible to check a posteriori that the lattice expansion involves an average of center elements over closed worldsurfaces (see 2.1.2). This is a consequence of the properties of $U(1)$ group integrals. This also applies to the non-Abelian extension $V_\mu \in SU(N)$, governed by

$$S^{\rm latt}_{\rm V}(\alpha_{\mu\nu}) = \tilde{\beta} \sum_{\mathbf{x}, \mu < \nu} {\rm Re \; tr} \left[ I - \bar{U}_{\mu\nu} V_\mu(x) V_\nu(x+\hat{\mu}) V^\dagger_\mu(x+\hat{\nu}) V^\dagger_\nu(x) \right] \; ,$$

[1] Similarly to the 3d case, this phase should be stabilized by a quartic interaction.

where plaquettes are denoted as usual. The closed surfaces are generated because $N \otimes \bar{N}$ contain a singlet. Interestingly, the $SU(N)$ version has additional configurations where $N$ open worldsurfaces meet at a loop formed by a set of links. This is due to the presence of a singlet in the product of $N$ link variables. Therefore, the associated normalized partition function

$$\frac{Z_{\rm v}^{\rm latt}[\alpha_{\mu\nu}]}{Z_{\rm v}^{\rm latt}[0]} \quad , \quad Z_{\rm v}^{\rm latt}[\alpha_{\mu\nu}] = \int [\mathcal{D}V_\mu]\, e^{-S_{\rm V}^{\rm latt}(\alpha_{\mu\nu})} \tag{4.8}$$

is an average of the center elements generated when a Wilson loop in representation D is linked by an ensemble of oriented center-vortex worldsurfaces with matching rules.

### 4.1.1 Including nonoriented center vortices in 4d

Although thin oriented or nonoriented center vortices contribute with the same center-element to the Wilson loop, they are distinct gauge field configurations, with different Yang–Mills action densities. It is then important to underline that the ensemble measure could depend on the monopole component. In order to attach center vortices to monopoles, dual adjoint holonomies defined on a "gas" of monopole loops and fused worldlines were included. In this case, because of the integration properties in the group there are additional relevant configurations like those of Figure 4.1a,b. The use of adjoint holonomies is in line with the fact that monopoles carry weights of the adjoint representation (the difference of fundamental weights), see [56, 61].

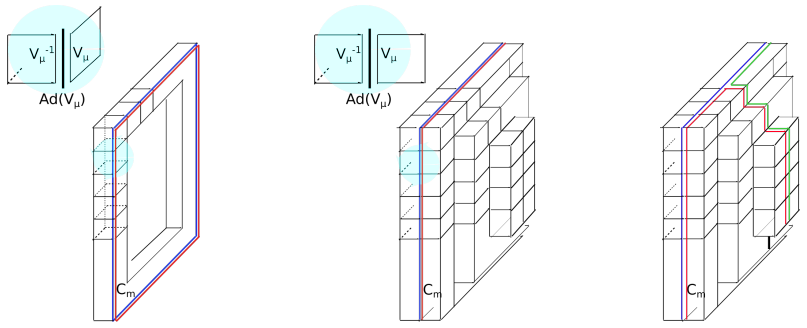


(**a**) (**b**) (**c**)

Figure 4.1: Non−oriented center vortices containing monopole worldlines. We show a configuration that contributes to the lowest order in $\tilde{\beta}$ (**a**), and one that becomes more important as $\tilde{\beta}$ is increased (**b**). A nonoriented center vortex with three matched monopole worldlines is shown in (**c**).

Then, partial contributions with $n$-loops were generated by

$$Z^{\text{latt}}_{\text{mix}}[\alpha_{\mu\nu}]\big|_{\text{p}} \propto \int [\mathcal{D}V_\mu]\, e^{-S^{\text{latt}}_{\text{V}}(\alpha_{\mu\nu})}\, \mathcal{W}^{(1)}_{\text{Ad}} \ldots \mathcal{W}^{(n)}_{\text{Ad}}$$
$$\mathcal{W}^{(k)}_{\text{Ad}} = \frac{1}{N^2-1}\,\text{tr}\Big(\prod_{(x,\mu)\in\mathcal{C}^{\text{latt}}_k} \text{Ad}\big(V_\mu(x)\big)\Big)\,, \tag{4.9}$$

where $\text{Ad}(\cdot)$ stands for the adjoint representation.

In addition to the matching rules of $N$ worldsurfaces, which in the continuum occur as $N$ different fundamental magnetic weights add up to zero, monopole worldlines carrying different adjoint weights (roots) can also be fused. For example, when $N \geq 3$, three worldlines carrying different roots that add up to zero can be created at a point. For this reason, we also considered partial contributions to the ensemble like

$$Z^{\text{latt}}_{\text{mix}}[\alpha_{\mu\nu}]\big|_{\text{p}} \propto \int [\mathcal{D}V_\mu]\, e^{-S^{\text{latt}}_{\text{V}}(\alpha_{\mu\nu})}\, D^{\text{latt}}_3\,, \tag{4.10}$$

where $D^{\text{latt}}_3$ is formed by combining three adjoint holonomies $\text{Ad}(\Gamma^{\text{latt}}_j)$ (see Figure 4.1c). Other natural rules involve the matching of four worldlines. Then, weighting the monopole holonomies with the simplest geometrical properties (tension and stiffness), the lattice mixed ensemble of oriented and nonoriented center vortices with matching rules can be pictorially represented as

$$Z^{\text{latt}}_{\text{mix}}[\alpha_{\mu\nu}] = \int [\mathcal{D}V_\mu]\, e^{-S^{\text{latt}}_{\text{V}}(\alpha_{\mu\nu})} \times \ldots \tag{4.11}$$

where the dots represent possible combinations of holonomies as illustrated in Figure 4.2.

Then, noting that $e^{i2\pi k/N} = e^{-i\,2\pi\,\beta\cdot w_{\text{e}}}$, where $\beta$ is a fundamental magnetic weight and $w_{\text{e}}$ is a weight of the quark representation D, the naive continuum limit, $V_\mu(x) = e^{ia\Lambda_\mu(x)}$, $\Lambda_\mu \in \mathfrak{su}(N)$, led to

$$Z_{\text{mix}}[s_{\mu\nu}] = \int [\mathcal{D}\Lambda_\mu]\, e^{-\int d^4x\, \frac{1}{4\tilde{g}^2}\,(F_{\mu\nu}(\Lambda) - 2\pi s_{\mu\nu}\beta_{\text{e}}\cdot T)^2} \times \ldots \tag{4.12}$$

The dots represent all possible monopole configurations to be attached to center-vortex worldsurfaces (see Figure 4.3).

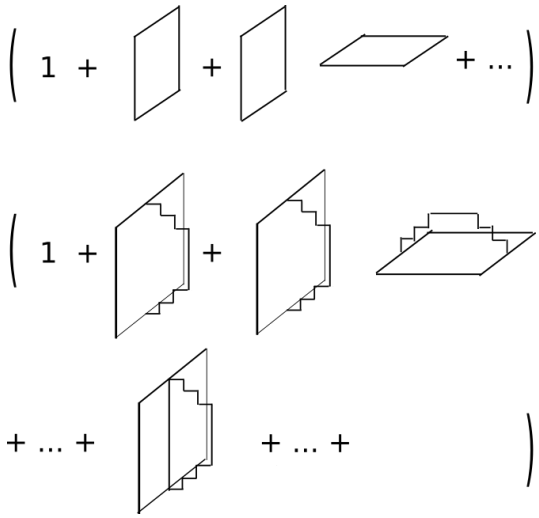


Figure 4.2: Natural combinations of holonomies that can be used to model the mixed ensemble of oriented and nonoriented center vortices. Each contribution is weighted with tension and stiffness.

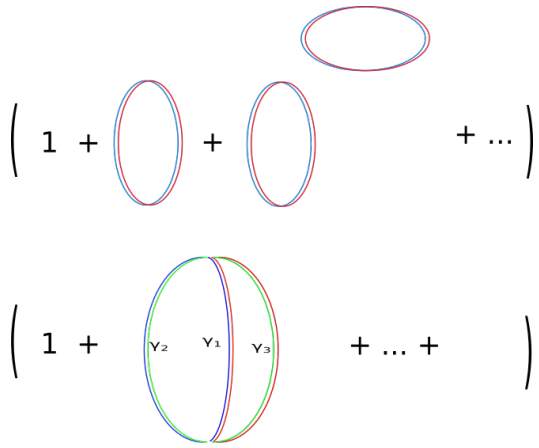


Figure 4.3: Continuum limit of the monopole sector. The worldline contributions are obtained from the solution to a Fokker–Planck diffusion equation.

Next, in Ref. [56], the effective description of the monopole sector was obtained. For example, a diluted ensemble of a given species of monopoles (first line in Figure 4.3), with tension $\mu$ and stiffness $\frac{1}{\kappa}$, was generated by

$$e^{\int_0^\infty \frac{dL}{L} \int d^4x\, du\, \mathrm{tr}\, Q(x,u,x,u,L)} \,, \tag{4.13}$$

where $Q$ is given by Eq. (D.1) and D corresponds to the adjoint representation. In the small-stiffness approximation, the non-Abelian diffusion equation for $Q$ is solved by Eq. (D.12), with

$$O = -\frac{\pi}{12\kappa} \left(\partial_\mu - i\,\mathrm{Ad}\big(\Lambda_\mu\big)\right)^2 + \mu I_{\mathscr{D}_{\mathrm{Ad}}} \,, \tag{4.14}$$

Therefore, the factor in Eq. (4.13) was approximated by

$$e^{-\mathrm{Tr}\,\ln O} = \int [\mathcal{D}\zeta][\mathcal{D}\zeta^\dagger]\, e^{-\int d^4x \left((D_\mu \zeta^\dagger, D_\mu \zeta) + \tilde{m}^2(\zeta^\dagger,\zeta)\right)}$$
$$m^2 = (12/\pi)\,\mu\kappa \quad , \quad D_\mu(\Lambda)\,\zeta = \partial_\mu \zeta - i\,[\Lambda_\mu, \zeta]\,, \tag{4.15}$$

where $\zeta$ is an emergent complex adjoint field. The Killing form $\langle\,,\rangle$ is defined in the Lie algebra as

$$\langle X, Y\rangle = \mathrm{Tr}(\mathrm{Ad}(X)\,\mathrm{Ad}(Y))\,. \tag{4.16}$$

In the continuum, the path-integral of $\mathrm{Ad}(\Gamma[\Lambda])$ over shapes and lengths led to the Green's function for the operator $O$, so that fusion rules like the one in Eq. (4.10) (see the second line in Figure 4.3) became effective Feynman diagrams. Indeed, to differentiate the monopole lines that can be fused, the monopole loop ensemble was extended to include different species. At the end, a set of real adjoint fields $\psi_I \in \mathfrak{su}(N)$ emerged ($I$ is a flavor index). This, together with the non-Abelian Goldstone modes (gauge fields), led to a class of effective Yang–Mills–Higgs (YMH) models,

$$Z_{\mathrm{mix}}[s_{\mu\nu}] = \int [\mathcal{D}\Lambda_\mu][\mathcal{D}\psi]\, e^{-\int d^4x \left[\frac{1}{4g^2}(F_{\mu\nu}(\Lambda)-J_{\mu\nu})^2 + \frac{1}{2}(D_\mu\psi_I, D_\mu\psi_I) + V_{\mathrm{H}}(\psi)\right]}\,. \tag{4.17}$$

$$J_{\mu\nu} = 2\pi\beta_{\mathrm{e}}\cdot T s_{\mu\nu} \quad , \quad s_{\mu\nu} = \int_{S(\mathcal{C})} d^2\tilde{\sigma}_{\mu\nu}\delta^{(4)}(x - w(s,\tau))\,. \tag{4.18}$$

$\beta_{\mathrm{e}}$ is a magnetic weight associated with the quark representation, and $s_{\mu\nu}$ is concentrated on any surface $S(\mathcal{C})$, parametrized by $w(s,\tau)$, whose border is $\mathcal{C}$. The vertex couplings weight the abundance of each fusion type. Percolating monopole worldlines (positive stiffness and negative tension) favor a spontaneous symmetry breaking phase that can easily correspond to $\mathrm{SU}(N) \to Z(N)$ SSB. This pattern has been extensively studied in the literature (see [66, 67, 68, 69, 70, 71, 83, 97, 112] and references therein).

## 4.2 The effective YMH model

A wide class of $SU(N)$ Yang-Mills-Higgs models can be given by the general action ($\psi_I \in \mathfrak{su}(N)$)

$$S = \int d^4x \left(\frac{1}{4}\langle F_{\mu\nu}, F_{\mu\nu}\rangle + \frac{1}{2}\langle D_\mu\psi_I, D_\mu\psi_I\rangle + V_{\mathrm{H}}(\psi)\right)\,, \tag{4.19a}$$

$$F_{\mu\nu} = \frac{i}{g}\,[D_\mu, D_\nu] \quad , \quad D_\mu = \partial_\mu - ig[\Lambda_\mu,\ ] = \partial_\mu + g\Lambda_\mu \wedge\ . \tag{4.19b}$$

Here, we defined

$$X \wedge Y = -i[X, Y]\,, \tag{4.20}$$

and disregarded the external source, as we will be interested in infinitely long vortices. Under a gauge transformation $U \in SU(N)$, we have

$$\Lambda_\mu \to U\Lambda_\mu U^{-1} + \frac{i}{g} U\partial_\mu U^{-1} \quad , \quad \psi_I \to U\psi_I U^{-1} \, . \tag{4.21a}$$

In the flavor-symmetric effective model [83], the flavor index takes values in the $\mathfrak{su}(N)$ Lie algebra, that is, the number of flavors $I = 1, \ldots, N^2 - 1$ matches the dimension of $\mathfrak{su}(N)$. In this case, we shall denote the adjoint flavors as $\psi_A \in \mathfrak{su}(N)$. With this matching, if the manifold of vacuum configurations were given by

$$\Lambda_\mu = \frac{i}{g} S\partial_\mu S^{-1} \quad , \quad \psi_A = vST_AS^{-1} \, , \tag{4.22a}$$

then $N$-ality would be naturally implemented via the spontaneous symmetry breaking pattern $SU(N) \to Z(N)$. Here, $T_A$ is an $\mathfrak{su}(N)$ Lie algebra basis. Indeed, in this case, the only transformation that leaves a Higgs field vacuum configuration invariant is $U \in Z(N)$. The quartic potential

$$\langle \psi_A \wedge \psi_B - v f_{ABC}\psi_C \rangle^2 \, , \tag{4.23}$$

were $f_{ABC}$ are the antisymmetric structure constants, would lead to these vacua. However, this potential would also lead to a degenerate trivial vacuum $\psi_A = 0$. Then, by expanding this expression and introducing independent coefficients for each term, a natural potential,

$$V_{\mathrm{H}}(\psi) = c + \frac{\mu^2}{2}\langle \psi_A, \psi_A \rangle + \frac{\kappa}{3} f_{ABC}\langle \psi_A \wedge \psi_B, \psi_C \rangle + \frac{\lambda}{4}\langle \psi_A \wedge \psi_B, \psi_A \wedge \psi_B \rangle \, , \tag{4.24}$$

was proposed in Ref. [83] ($c$ is adjusted such that $V_{Higgs} = 0$ on $\mathcal{M}$). In this manner, a region in parameter space that only leads to nontrivial vacua, characterized by

$$v = -\frac{\kappa}{2\lambda} + \sqrt{\left(\frac{\kappa}{2\lambda}\right)^2 - \frac{\mu^2}{\lambda}} \, , \tag{4.25}$$

was obtained. Throughout this thesis, we shall separate the adjoint indices $A$ into Cartan $q = 1, \ldots, N-1$ and off-diagonal $\alpha$, $\bar{\alpha}$ labels. The elements $T_q$ form a maximal commuting set, while the remaining elements are defined in terms of root vectors $E_{\pm\alpha}$

$$T_\alpha = \frac{E_\alpha + E_{-\alpha}}{\sqrt{2}} \quad , \quad T_{\bar{\alpha}} = \frac{E_\alpha - E_{-\alpha}}{\sqrt{2}i} \, , \tag{4.26}$$

where $\alpha$ is a positive root of $\mathfrak{su}(N)$. For the notation and conventions, see Appendix A.

## 4.3 The vortex ansatz

In order to represent a straight infinite vortex along the z-axis (for a general presentation about topological objects, see Ref. [113]) we consider the ansatz

$$\Lambda_0 = 0 \quad , \quad \Lambda_i = S\mathcal{A}_i S^{-1} + \frac{i}{g} S\partial_i S^{-1} \quad , \quad \psi_A = h_{AB} S T_A S^{-1} \quad , \quad S = e^{i\varphi\beta\cdot T} \; . \tag{4.27}$$

Since there is cylindrical symmetry, the profiles $h_{AB}$ can be taken as functions of $\rho$ alone, with $(\rho,\, \varphi,\, z)$ being cylindrical coordinates. Clearly, they must obey

$$h_{AB}(\rho \to \infty) = v\delta_{AB} \tag{4.28}$$

so that their contribution to the energy per unit length is also finite. The vortex charge is represented by $\beta = 2N\omega$, where $\omega$ is a weight of $\mathfrak{su}(N)$ and is closely connected with the $N$-ality $k$. For example, when $\omega$ is a weight of the fundamental representation, $\omega = \omega_1, \omega_2, ...\omega_N$, then the vortex has $k = 1$, while if it is a root $\alpha$, then the $N$-ality is that of the adjoint representation ($k = 0$). A general $N$-ality can be reproduced by taking $\omega$ as the highest weight of the $k$-antisymmetric representation

$$\omega = \Lambda_k = \sum_{i=1}^{k} \omega_i \; . \tag{4.29}$$

Regarding the Higgs fields $\psi_A$ in Eq. (4.27), the number of profile functions $h_{AB}$ scales with $N^4$. However, in the next section, we shall see that the vortex solutions display a collective behavior with a fixed reduced number of field profiles. A closer look at the local basis $n_A = ST_AS^{-1}$,

$$n_q = T_q \; , \tag{4.30a}$$

$$n_\alpha = \cos(\alpha\cdot\beta\,\varphi)\, T_\alpha - \sin(\alpha\cdot\beta\,\varphi)\, T_{\overline{\alpha}} \; , \tag{4.30b}$$

$$n_{\overline{\alpha}} = \cos(\alpha\cdot\beta\,\varphi)\, T_\alpha + \sin(\alpha\cdot\beta\,\varphi)\, T_{\overline{\alpha}} \; , \tag{4.30c}$$

reveals that, whenever $\alpha\cdot\beta \neq 0$, the elements $n_\alpha$ are ill-defined along the vortex line. On the other hand, the elements $n_q$ and $n_\alpha$ with $\alpha\cdot\beta = 0$ have no defects. This leads to a natural splitting between $\psi_q$ and $\psi_\alpha, \psi_{\bar{\alpha}}$. In terms of the Cartan-Weyl sectors, the anstaz has the simpler structure:

$$\psi_\alpha = h_\alpha S T_\alpha S^{-1} \quad , \quad \psi_{\bar{\alpha}} = h_\alpha S T_{\bar{\alpha}} S^{-1} \quad , \quad \psi_q = h_{qp} S T_p S^{-1} \; , \tag{4.31}$$

and the regularity condition

$$h_\alpha(\rho \to 0) = 0 \quad \text{if} \quad \alpha \cdot \beta \neq 0 \, . \tag{4.32}$$

Regarding the gauge sector, notice that $S$ is ill-defined along the $z$-axis, while $\Lambda_i$ must be smooth. Furthermore, $\Lambda_i$ should be a pure gauge when $\rho \to \infty$, so that the magnetic energy per unit length stored in the vortex is finite. Both issues can be resolved if we consider

$$\mathcal{A}_i = (a-1)\partial_i\varphi \, \beta \cdot T \, , \tag{4.33}$$

with the boundary and regularity conditions

$$a(\rho \to \infty) = 1 \quad , \quad a(\rho \to 0) = 0 \, . \tag{4.34}$$

Indeed, for antisymmetric weights, this choice closes the equations of motion.

So far, the equations of motion read

$$\frac{1}{\rho}\frac{\partial a}{\partial \rho} - \frac{\partial^2 a}{\partial \rho^2} = g^2 h_\alpha^2 (1-a)\,(\beta\cdot\gamma)\,(\gamma \cdot T) \ , \tag{4.35a}$$

$$\nabla^2 h_{qp} = \mu^2 h_{qp} + h_\gamma^2 \kappa \gamma_q \gamma_p + \lambda h_\gamma^2 h_{ql}\gamma_l\gamma_p \ , \tag{4.35b}$$

$$\begin{aligned} \nabla^2 h_\alpha = {} & (1-a)^2 \left(\alpha\cdot\beta/\rho\right)^2 h_\alpha + \mu^2 h_\alpha \\ & + 2\kappa h_\alpha \alpha_q h_{qp} \alpha_p + \kappa N_{\alpha,\gamma}^2 h_\gamma h_{\alpha+\gamma} + \lambda h_\alpha^3 \alpha^2 \\ & + \lambda h_\gamma^2 h_\alpha N_{\alpha,\gamma}^2 + \lambda h_\alpha \alpha_q h_{qp} h_{pl} \alpha_l \ . \end{aligned} \tag{4.35c}$$

In Eq. (4.35), $\gamma$ is summed over all the roots except in Eq. (4.35c) where $\gamma \neq -\alpha$ and there is no summation over the repeated positive root $\alpha$. When $\gamma < 0$, $h_\gamma = h_{-\gamma}$ is understood. Although smaller, the number of profiles in Eq. (4.35) still scales with $N^2$. In what follows, we shall further reduce their number by carefully studying the equations of motion. We shall initially address the simpler $k = 1$ case and then we will extend the analysis to $k > 1$.

### 4.3.1 Case k=1

In Ref. [83], a reduced ansatz was constructed for $SU(2)$ and $SU(3)$, and it was numerically explored in Ref. [114]. Note that for $N \leq 3$ there is no variety in the possible string tensions as vortices with $k$ and $-k$ have the same tension, and for $N = 3$ the $N$-ality $k = 2$ is equivalent to $k = -1$. In this subsection we shall extend the $k = 1$ case for an arbitrary $N$, while the $k > 1$ case will be worked out in the next subsection. In view of Eqs. (4.30) and (4.35c), it is natural to propose a collective behavior that only depends

on the product $\alpha \cdot \beta$,

$$h_\alpha = h_{\overline{\alpha}} = \begin{cases} h_0, \text{ if } \alpha \cdot \beta = 0 \ , \\ h, \text{ if } \alpha \cdot \beta = 1 \ . \end{cases} \tag{4.36}$$

As a consequence, Eq. (4.35a) turns out to be

$$\frac{1}{\rho}\frac{\partial a}{\partial \rho} - \frac{\partial^2 a}{\partial \rho^2} = g^2 h^2 (1 - a) \ . \tag{4.37}$$

With regard to the Cartan sector, Eq. (4.35b) involves only three matrices: The $\rho$-dependent $\mathbb{H}|_{qp} = h_{qp}$ and the constant ones

$$\mathbb{A}|_{qp} = \sum_{\alpha>0 \ ; \ \alpha\cdot\beta=1} \alpha|_q \alpha|_p \ ; \ \mathbb{A}_0|_{qp} = \sum_{\alpha>0 \ ; \ \alpha\cdot\beta=0} \alpha_0|_q \alpha_0|_p \ , \tag{4.38}$$

which satisfy

$$\mathbb{A} + \mathbb{A}_0 = \frac{1}{2}\mathbb{I} \ , \tag{4.39a}$$

$$\mathbb{A}_0^2 = \frac{N-1}{2N}\,\mathbb{A}_0 \ . \tag{4.39b}$$

Thus, we can use Eq. (4.39a) to eliminate $\mathbb{A}$ and cast Eq. (4.35b) into the form

$$\big[\big(\nabla^2 - \mu^2 - \frac{\lambda}{2}h^2\big)\,\mathbb{I} - \lambda(h_0^2 - h^2)\,\mathbb{A}_0\big]\mathbb{H} = \frac{\kappa}{2}h\mathbb{I} + \kappa(h_0 - h)\mathbb{A}_0 \ . \tag{4.40}$$

As the Laplacian is a scalar operator, the inversion of the matrix operator in the first member will be a power series in $\mathbb{A}_0$. Then, because of Eq. (4.39b), the solution for $\mathbb{H}$ in Eq. (4.40) must be a linear combination of $\mathbb{I}$ and $\mathbb{A}_0$. We can define a pair of projectors, $\mathbb{M}_1 + \mathbb{M}_2 = \mathbb{I}$, $\mathbb{M}_i\mathbb{M}_j = \delta_{ij}\mathbb{I}$, by taking

$$\mathbb{M}_2 = \frac{2N}{N-1}\,\mathbb{A}_0 \ , \tag{4.41}$$

and write

$$\mathbb{H} = h_1\mathbb{M}_1 + h_2\mathbb{M}_2 \ . \tag{4.42}$$

In this manner, if these profiles satisfy

$$\nabla^2 h_1 = \mu^2 h_1 + (\kappa + \lambda h_1)h^2 \ , \tag{4.43a}$$

$$\nabla^2 h_2 = \mu^2 h_2 + \frac{h^2 + (N-1)h_0^2}{N}(\kappa + \lambda h_2) \ , \tag{4.43b}$$

then the equations in the Cartan sector close. Now, to simplify those for $h$ and $h_0$, we note that according to our conventions the coefficients $N_{\alpha,\gamma}$ are given by (see Sec. 5.5 in

Table 4.1

| Profile types | Number of terms |
|---|---|
| $(h_\alpha,\ h_\gamma,\ h_{\alpha+\gamma}) = (h, h, h_0)$ | $N-2$ |
| $(h_\alpha,\ h_\gamma,\ h_{\alpha+\gamma}) = (h, h_0, h)$ | $N-2$ |
| $(h_\alpha,\ h_\gamma,\ h_{\alpha+\gamma}) = (h_0, h_0, h_0)$ | $2(N-3)$ |
| $(h_\alpha,\ h_\gamma,\ h_{\alpha+\gamma}) = (h_0, h, h)$ | $2$ |

Ref. [94])

$$N_{\alpha,\gamma}^2 = \frac{1}{2}\alpha\cdot\alpha = \frac{1}{2N}\ , \tag{4.44}$$

when $\alpha+\gamma$ is a root, and they are zero otherwise. Thus, in order to perform the summation over $\gamma$ in Eq. (4.35c), we have to count the number of terms for each profile combination. For a fixed $\alpha$, the multiplicities are summarized in Table 4.1. Combining these ingredients, the remaining Higgs equations can be simplified to

$$\begin{aligned}
\nabla^2 h_0 &= \mu^2 h_0 + \frac{h_0}{N}(2\kappa h_2 + \lambda h_2^2 + \lambda h_0^2) \qquad (4.45a)\\
&\quad + \frac{(\kappa+\lambda h_0)}{N}(h^2 + (N-3)h_0^2)\ ,\\
\nabla^2 h &= \mu^2 h + \frac{(1-a)^2}{\rho^2}h + \frac{\lambda}{2}h^3\\
&\quad + \frac{(N-2)}{2N}hh_0(2\kappa+\lambda h_0) + \frac{(2\kappa+\lambda h_1)}{2(N-1)}hh_1 \qquad (4.45b)\\
&\quad + \frac{(N-2)}{2N(N-1)}(2\kappa+\lambda h_2)hh_2\ .
\end{aligned}$$

They must be solved with the Higgs profiles approaching the vacuum value $v$ when $\rho\to\infty$, so as to comply with Eq. (4.28), while $h(\rho)$ must also obey the regularity condition (4.32).

### 4.3.2 Case $k > 1$

To solve the case $k>1$, we consider a general $\beta = 2N\Lambda^k$ in Eq. (4.27). The reasoning to be followed is very similar to the previous one. The main difference is that we have to split the positive roots with $\alpha\cdot\beta = 0$ into two categories:

$$\tilde{\alpha}_0 = \omega_{i\le k} - \omega_{j\le k}\ , \tag{4.46a}$$

$$\alpha_0 = \omega_{i>k} - \omega_{j>k}\ . \tag{4.46b}$$

The point is that $\alpha_0$ and $\tilde{\alpha}_0$ have a slightly different behavior. For example, there are $k(k-1)$ roots of type $\tilde{\alpha}_0$ and $(N-k)(N-k-1)$ roots of type $\alpha_0$, which generates a difference when counting the terms in (4.35c). Note that for $k=1$ there are no roots of

type $\tilde{\alpha}_0$. The roots associated with a rotating $n_\alpha$ are given by

$$\alpha = \omega_{i\leq k} - \omega_{j>k} \ . \tag{4.47}$$

Thus, we are led to introduce three profiles in the $\alpha$-sector,

$$h_\alpha = \begin{cases} \tilde{h}_0, \ \text{if } \alpha = \tilde{\alpha}_0 \\ h_0, \ \text{if } \alpha = \alpha_0 \\ h, \ \text{if } \alpha \cdot \beta = 1 \ . \end{cases} \tag{4.48}$$

In any case, the equation for $a$ remains that in (4.37). This time, in order to solve the matrix part of Eq. (4.35b) we use three matrices $\mathbb{I}$, $\tilde{\mathbb{A}}_0$ and $\mathbb{A}_0$ instead of two. Following a similar reasoning, we can introduce three projectors, $\mathbb{M}_1 + \mathbb{M}_2 + \mathbb{M}_3 = \mathbb{I}$, determined by

$$\mathbb{M}_2 = \frac{2N}{N-k}\mathbb{A}_0 \quad , \quad \mathbb{M}_3 = \frac{2N}{k}\tilde{\mathbb{A}}_0 \ . \tag{4.49}$$

In terms of them, the solution for $\mathbb{H}$ is

$$\mathbb{H} = h_1\mathbb{M}_1 + h_2\mathbb{M}_2 + h_3\mathbb{M}_3 \tag{4.50}$$

where $h_1$ satisfies Eq. (4.43a), while $h_2$ and $h_3$ are determined by

$$\nabla^2 h_2 = \mu^2 h_2 + \left(\frac{kh^2 + (N-k)h_0^2}{N}\right)(\kappa + \lambda h_2) \ , \tag{4.51a}$$

$$\nabla^2 h_3 = \mu^2 h_3 + \left(\frac{(N-k)h^2 + k\tilde{h}_0^2}{N}\right)(\kappa + \lambda h_3) \ . \tag{4.51b}$$

Here, we begin to see how the center symmetry is made explicit by the ansatz. When the $Z(N)$ charge is changed from $k$ to $N-k$, the equations for $h_2$ and $h_3$ get interchanged, provided that $h_0$ and $\tilde{h}_0$ are also interchanged, which will be justified in the following discussion.

For a fixed $\alpha$, the mutliplicity of terms in Eq. (4.35c) with a given profile combination $(h_\alpha,\ h_\gamma,\ h_{\alpha+\gamma})$ are displayed in table 4.2. In addition, in expressions such as the energy, where a sum over $\alpha$ is required, the above numbers should be multiplied by $k(N-k)$ if $n_\alpha$ rotates, by $\frac{k(k-1)}{2}$ if the root is of type $\tilde{\alpha}_0$, and by $\frac{(N-k)(N-k-1)}{2}$ if it is of type $\alpha_0$. With

Table 4.2

| Profile types | # terms | Profile types | # terms |
|---|---|---|---|
| $(h, h, \tilde{h}_0)$ | $(k-1)$ | $(\tilde{h}_0, h, h)$ | $2(N-k)$ |
| $(h, h, h_0)$ | $(N-k-1)$ | $(\tilde{h}_0, \tilde{h}_0, \tilde{h}_0)$ | $2(k-2)$ |
| $(h, \tilde{h}_0, h)$ | $(k-1)$ | $(h_0, h, h)$ | $2k$ |
| $(h, h_0, h)$ | $(N-k-1)$ | $(h_0, h_0, h_0)$ | $2(N-k-2)$ |

this information at hand, the equations for $h$, $h_0$ and $\tilde{h}_0$ become

$$\nabla^2 h_0 = \mu^2 h_0 + \frac{h_0}{N}(2\kappa h_2 + \lambda h_2^2 + \lambda h_0^2) + \frac{(\kappa + \lambda h_0)}{N}(kh^2 + (N-k-2)h_0^2) \,, \tag{4.52a}$$

$$\nabla^2 \tilde{h}_0 = \mu^2 \tilde{h}_0 + \frac{\tilde{h}_0}{N}(2\kappa h_3 + \lambda h_3^2 + \lambda \tilde{h}_0^2) + \frac{(\kappa + \lambda \tilde{h}_0)}{N}((N-k)h^2 + (k-2)\tilde{h}_0^2) \,, \tag{4.52b}$$

$$\begin{aligned} \nabla^2 h = \mu^2 h + \frac{(1-a)^2}{\rho^2} h + \frac{\lambda}{2} h^3 + \frac{h h_1}{2k(N-k)}(2\kappa + \lambda h_1) \\ + \frac{N-k-1}{2N(N-k)}(2\kappa + \lambda h_2) h h_2 + \frac{k-1}{2Nk}(\kappa + \lambda h_3) h h_3 \\ + \frac{N-k-1}{2N}(2\kappa + \lambda h_0) h h_0 + \frac{k-1}{2N}(2\kappa + \lambda \tilde{h}_0) h \tilde{h}_0 \,. \end{aligned} \tag{4.52c}$$

with boundary conditions similar to those for $k = 1$, where $h$ is the only profile with a regularity condition along the vortex line. As anticipated, under $k \to N - k$ we have

$$h_2 \leftrightarrow h_3 \quad , \quad h_0 \leftrightarrow \tilde{h}_0 \,. \tag{4.53}$$

Indeed, due to these properties, the center symmetry is made explicit: the energy of a vortex with charge $k$ and an antivortex with charge $N - k$ are the same. Incidentally, it is easy to see that the differences $\Delta h = h_0 - h_2$ and $\Delta \tilde{h} = \tilde{h}_0 - h_3$ are governed by

$$(\nabla^2 - \mu^2)\Delta h = \frac{\lambda h^2 + \lambda(N-k-1)h_0^2 - \kappa h_0}{N} \Delta h \,, \tag{4.54a}$$

$$(\nabla^2 - \mu^2)\Delta \tilde{h} = \frac{\lambda h^2 + \lambda(k-1)\tilde{h}_0^2 - \kappa \tilde{h}_0}{N} \Delta \tilde{h} \,. \tag{4.54b}$$

for which $h_0 = h_2$ and $\tilde{h}_0 = h_3$ are solutions. This obviously holds for $k = 1$ and leads to a welcomed additional reduction in the number of profiles.

Replacing the ansatz in the energy functional for the action (4.19), we find

$$\begin{aligned} E &= \int d^3x \, \frac{k(N-k)}{\rho^2} \left( \frac{|\nabla a|^2}{g^2} + h^2(1-a)^2 \right) \\ &+ \frac{1}{2}|\nabla h_1|^2 + \frac{1}{2}\mu^2 h_1^2 + \frac{(N-k)^2-1}{2}(|\nabla h_2|^2 + \mu^2 h_2^2) \\ &+ \frac{k^2-1}{2}(|\nabla h_3|^2 + \mu^2 h_3^2) + k(N-k)(|\nabla h|^2 + \mu^2 h^2) \\ &+ \lambda \frac{k(N-k)}{4} h^4 + C_1 h^2 + C_2 \, , \end{aligned} \tag{4.55}$$

where $C_1$ and $C_2$ are given by

$$\begin{aligned} C_1 &= \frac{h_1}{2}(2\kappa + \lambda h_1) + \frac{k(N-k)^2 - k}{2N}(2\kappa + \lambda h_2) h_2 \\ &+ \frac{(N-k)(k^2-1)}{2N}(2\kappa + \lambda h_3) h_3 \, , \\ C_2 &= \frac{(N-k)^3 + k - N}{N} \left( \kappa \frac{h_2^3}{3} + \lambda \frac{h_2^4}{4} \right) + \kappa \frac{k^3 - k}{3N} h_3^3 \\ &\lambda \frac{k^3 - k}{4N} h_3^4 - (d^2-1) \left( \frac{\mu^2 v^2}{2} + \frac{\kappa v^3}{3} + \frac{\lambda v^4}{4} \right) \, . \end{aligned}$$

A particularly interesting region in parameter space is $\mu^2 = 0$. In this case, except for $a$ and $h$, the profiles are frozen at the vacuum value $v$. This is possible because only $a$ and $h$ satisfy regularity conditions at $\rho = 0$. Moreover, on the vortex ansatz, the nontrivial Higgs profiles $a$ and $h$ get Abelianized in the sense that they satisfy the usual Nielsen-Olesen (NO) equations. This is interesting because the YM chromoelectric field distribution obtained from the lattice is precisely that of the NO vortex-string [9]. The crucial difference is that in our case $N$-ality is automatically implemented due to the underlying non-Abelian structure. Furthermore, at $\mu^2 = 0$, a direct calculation shows that the collective behavior gives rise to an exact Casimir scaling of the energy per unit vortex length (string tension)

$$\sigma_k = k(N-k)\, \sigma_{\rm NO} \, . \tag{4.56}$$

Indeed, apart from a factor $(N+1)^{-1}$, the factor $k(N-k)$ is precisely the quadratic Casimir of the k-antisymmetric representation. In other words, an exact Casimir law

$$\sigma_k = \frac{C_2(A_k)}{C_2(F)}\, \sigma_1 \tag{4.57}$$

is analytically verified at $\mu^2 = 0$.

## 4.4 Numerical solutions

In principle, the numerical exploration of the model parameter space $(g, \mu^2, \kappa, \lambda)$ is a hard task since it is four-dimensional. Fortunately, we can reduce it to two dimensions by a simple rescaling, defining the dimensionless quantities

$$\bar{x}_i = -\frac{\kappa}{g} x_i \ , \ \bar{g} = 1 \ , \ \bar{\mu} = -\frac{g}{\kappa}\mu \ , \ \bar{\kappa} = -1 \, , \, \bar{\lambda} = \frac{\lambda}{g^2} \ ,$$

which implies the energy per unit lengh rescaled as

$$\sigma(g, \mu^2, \kappa, \lambda) = -\frac{\kappa}{g^3}\, \sigma(1, \bar{\mu^2}, -1, \bar{\lambda}) \ . \tag{4.58}$$

Then, for a given $N$-ality $k$, the ratio $\frac{\sigma_k}{\sigma_1}$ can only depend on $\bar{\mu}^2$, $\bar{\lambda}$. Furthermore, when computing the string tension ratios, we observed that they essentially depend on the combination $\bar{\mu}^2\bar{\lambda}$, so we will also fix $\bar{\lambda} = 1$ when evaluating this ratio. It is important to underline that the reduction from four parameters to one applies only to $\frac{\sigma_k}{\sigma_1}$ while other observables may display a more complex behavior. For example, another important quantity we can always fit is the fundamental string tension $\sigma_1$. For every $\bar{\mu}^2$ and $\bar{\lambda}$, including $\bar{\lambda} \neq 1$, we can evaluate the rescaled string tension and then set the proper $\kappa$ and $g$ in Eq. (4.58) to obtain the well-established value $\sigma_1 = (440 \ \text{Mev})^2$. With regard to the numerical procedure, we initially discretized the coupled equations for $a$, $h$, $h_1$, $h_2$ and $h_3$. For this aim, we used finite differences with a range $\bar{\rho} \in [0.001, 10]$ partitioned into 150 points. Then, we randomly swept over the domain updating each site using the relaxation method until the desired degree of convergence was met. All the simulations were implemented in MATHEMATICA. We defined an error function as the modulus of the deviations summed over the various equations and integrated over the domain, using it to establish a numerical convergence criterion.

In Fig. 4.4, we plot $a(\rho)$ and $h(\rho)$ for various values of $\mu^2$, all of them with $g = \lambda = -\kappa = 1$. Note that there are only small changes in the whole range considered. Since this seems to be true for other values of $g$, $\kappa$ and $\lambda$, we expect these profiles to be well approximated by those of the Nielsen-Olesen vortex. On the other hand, Fig. 4.5 shows that the profile $h_1$ is more influenced by changes in $\mu^2$. A similar behavior was also observed for $h_2$ and $h_3$. In Fig. 4.6, we plot the quantity

$$\Delta_C(k) = 1 - \frac{N-1}{k(N-k)}\frac{\sigma_k}{\sigma_1} \ , \tag{4.59}$$

for $N = 8$ and various values of $k$. It measures deviations between the Casimir law. At $\bar{\mu}^2 = 0$, this function passes by zero, a point where we showed an exact Casimir scaling. The simulations did not converge well for $\bar{\mu}^2 < -\frac{12}{9\bar{\lambda}}$. It is interesting to note that the Casimir law is only slightly deviated from in the whole region we were able to explore. In

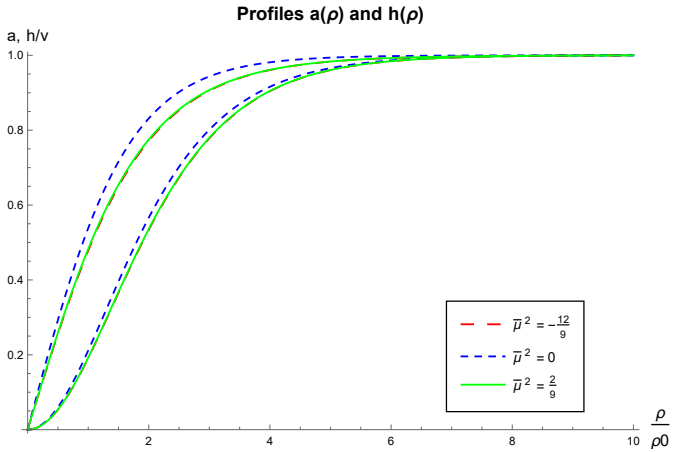


Figure 4.4: Profiles $a(\rho)$ and $h(\rho)$ for various $\bar{\mu}^2$. The profile $a$ is that with a linear behavior around $\rho = 0$.

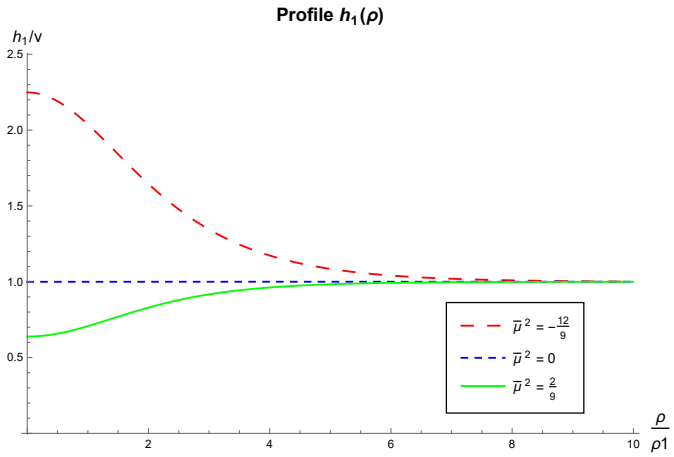


Figure 4.5: Profile $h_1(\rho)$ for various $\bar{\mu}^2$.

addition, as $\Delta_C(k)$ is positive, the scaling law of the model is slightly below the Casimir law. Recalling that the Sine law lies above the Casimir, it is not a surprise that in the whole range the model shows larger deviations when compared with the Sine law (cf. Fig. 4.7), via the relative difference

$$\Delta_S(k) = 1 - \frac{\sin\left(\frac{\pi}{N}\right)}{\sin\left(\frac{k\pi}{N}\right)} \frac{\sigma_k}{\sigma_1} \,. \tag{4.60}$$

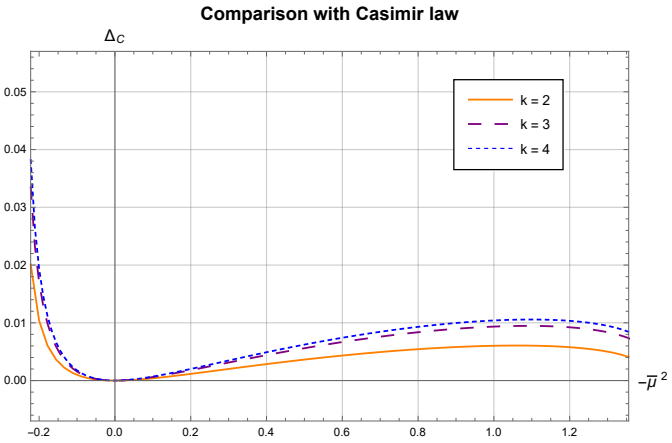


Figure 4.6: Plot of $\Delta_C(k)$ with $N = 8$. Notice the region depicted is that where the SSB takes place, including positive $\bar{\mu}^2$.

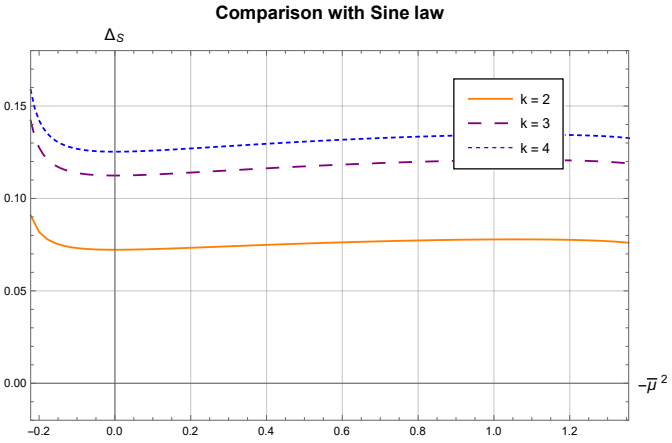


Figure 4.7: Plot of $\Delta_S(k)$ with $N = 8$. The deviations are much larger in the whole region explored.

# Chapter 5

# Stability of the Casimir law in 4d

In the previous chapter, we studied the adjoint flavor-symmetric model defined by Eqs. (4.19) and (4.24). Due to the nontrivial first homotopy group of the associated vacua manifold $\mathcal{M} = \frac{SU(N)}{Z(N)}$, $\Pi_1(\mathcal{M}) = Z(N)$, the vortex solutions to the static field equations are topologically stable. Among the possible configurations are those containing just one infinite straight string, characterized by the general ansatz in Eq. (4.27). Considering $\mathcal{A}_i = (a/g)\partial_i\varphi\beta \cdot T$, we obtained vortex solutions for the $k$-A and $k$-Symmetric ($k$-S) representations. When $\mu^2 = 0$, the solution for the fields with no regularity conditions at $\rho = 0$ is frozen everywhere at the vacuum value:

$$\psi_q = vT_q \quad , \quad \psi_\alpha = vT_\alpha \quad \text{when} \quad \alpha \cdot \beta = 0 \, . \tag{5.1}$$

This led to the following asymptotic exact behavior of the string tension for the $k$-A representation

$$\frac{\sigma(k\text{-A})}{\sigma(\text{F})} = \frac{k(N-k)}{N-1} = \frac{C_2(k\text{-A})}{C_2(\text{F})} \, , \tag{5.2}$$

This agrees with the large distance behavior of the Wilson loop [6]. It is trivial to extend the discussion to the $k$-S irrep [117]. In this case, the model is equivalent to a Ginzburg-Landau theory with winding number $k$. Then, at the BPS point $\lambda = g^2$ of the Abelianized $\mu^2 = 0$ model, we have

$$\frac{\sigma(k\text{-S})}{\sigma(\text{F})} = k > \frac{k(N-k)}{N-1} = \frac{\sigma(k\text{-A})}{\sigma(\text{F})} \, , \tag{5.3}$$

for $k > 1$. Then, when a $k$-S string is long enough, it is energetically favorable to create valence gluon excitations around the quark sources to produce a $k$-A string. However, in order to establish the asymptotic Casimir scaling law one must show that $\sigma(k\text{-A})$ is the lowest tension among all the irreps with $N$-ality $k$. In that case, $k$-A strings would be settled as the stable confining states. This is one of the properties we will be able to address exactly in this chapter. For this aim, we need an analysis of the field equations

for any representation D(·) of $SU(N)$. We will show that there is a point in parameter space where the complicated set of second order equations,

$$D_j F_{ij} = g D_i \psi_A \wedge \psi_A \ , \tag{5.4a}$$

$$D_i D_i \psi_A = \frac{\delta V_H}{\delta \psi_A} \ , \tag{5.4b}$$

can be reduced to a set of first order BPS equations. In flavor-symmetric models, this reduction was shown in Refs. [104, 115, 116] when the Higgs fields are in the fundamental representation, and in Ref. [114], only for $SU(2)$, when the Higgs fields are in the adjoint. Here, using $\mathcal{A}_i$ along a general Cartan direction, we shall be able to accomodate a vortex for a general D(·). These objects are characterized by the magnetic weight $\beta = 2N\lambda^D$, with $\lambda^D$ being the highest weight of the representation D(·). For the various definitions and properties, see Appendix B.

## 5.1 BPS equations

In the Nielsen-Olesen model governed by the action ($D_\mu = \partial_\mu - ig\Lambda_\mu$, $\phi \in \mathbb{C}$)

$$S_{\text{Abe}} = \int d^4x \Big( -\frac{1}{4} F_{\mu\nu} F_{\mu\nu} + \frac{1}{2} D_\mu \phi D_\mu \phi - \frac{\lambda}{8} (\phi\phi^* - v^2)^2 \Big) \ , \tag{5.5}$$

when $\lambda < g^2$, a single vortex with higher winding number $n$ is energetically more favorable than $n$ separated vortices with winding number 1. When $\lambda > g^2$, the situation is reversed. For a recent discussion about the fitting of lattice data with the Nielsen-Olesen model, see Refs. [9, 10, 11, 12] and references therein.

At $\lambda = g^2$, also known as the BPS point, the vortices do not interact, as the energy of any configuration with winding number $n$ is given by

$$E = g v^2 \int d^3x \, B_3 = 2\pi v^2 n \ . \tag{5.6}$$

In this Abelian setting, the equations of motion at the BPS point can be reduced to be first order

$$D_+ \phi = 0 \ , \ B_3 = \frac{g}{2} (v^2 - \phi\phi^*) \ , \ B_1 = B_2 = 0 \ , \tag{5.7}$$

where $D_\pm = D_1 \pm i D_2$. For a detailed discussion on this topic, see Ref. [113]. In the non Abelian context, this type of BPS point is known to occur in flavor-symmetric $SU(N) \to Z(N)$ models constructed in terms of $N$ Higgs fields in the fundamental representation [104, 115, 118]. In this section, we will show that there is a set of BPS equations that provide solutions to the flavor-symmetric $SU(N) \to Z(N)$ model formed by $N^2 - 1$ adjoint Higgs fields, at $\mu^2 = 0$ and $\lambda = g^2$ (cf. Eqs. (4.19), (4.24), (5.4)). Moreover, we will show

that these equations can be closed with an ansatz that accommodates center vortices carrying the weights of any $SU(N)$ group representation.

Initially, for every pair $\psi_\alpha, \psi_{\bar{\alpha}}$, with $\alpha > 0$, we define

$$\zeta_\alpha = \frac{\psi_\alpha + i\psi_{\bar{\alpha}}}{\sqrt{2}} \,, \tag{5.8}$$

which is in the complexified $\mathfrak{su}(N)$ Lie algebra ($\alpha$ is a positive root). We shall consider configurations for an infinite static vortex. Because of translation symmetry along the $x^3$-direction, we require

$$B_1 = B_2 = 0 \quad , \quad D_3\psi_A = 0 \,. \tag{5.9}$$

Next, motivated by the BPS equations in Refs. [104, 115, 119] involving Higgs fields transforming in the fundamental and adjoint representations, for the field-dependence transverse to the string we propose the first-order equations

$$D_+\zeta_\alpha = 0 \quad \Leftrightarrow \quad D_-\zeta_\alpha^\dagger = 0 \quad , \quad D_1\psi_q = D_2\psi_q = 0 \,, \tag{5.10a}$$

$$B_3 = g\sum_{\alpha>0}\left(v\alpha|_q\psi_q - [\zeta_\alpha, \zeta_\alpha^\dagger]\right) \,. \tag{5.10b}$$

In terms of the original fields, we can also write

$$D_\pm\psi_\alpha = \mp iD_\pm\psi_{\bar{\alpha}} \,, \tag{5.11}$$

$$B_3 = g\sum_{\alpha>0}\left(v\alpha|_q\psi_q - \psi_\alpha \wedge \psi_{\bar{\alpha}}\right) \,. \tag{5.12}$$

### 5.1.1 The ansatz

Regarding the ansatz, we shall use Eqs. (4.27) and (4.31), with $\mathcal{A}_i$ being a general field in the Cartan subalgebra $\mathfrak{C}$, not necessarily proportional to $\beta \cdot T$,

$$\mathcal{A}_i = \sum_{l=1}^{N-1} \frac{a_l - d_l}{g} \partial_i\varphi\beta^{l-\mathrm{A}} \cdot T \,, \tag{5.13}$$

where $\beta^{(l)} = 2N\lambda^{l-\mathrm{A}}$ and $\lambda^{l-\mathrm{A}}$, $l = 1, \ldots, N-1$ are the antisymmetric (fundamental) weights, which provide a basis $\beta^{(l)} \cdot T$ for $\mathfrak{C}$. The Dynkin numbers $d_l$ are the positive integer coefficients obtained when expressing $\beta$ as a linear combination of $\beta^{l-\mathrm{A}}$. The profiles $a_l$ must obey the boundary conditions

$$a_l(0) = 0 \quad , \quad a_l(\infty) = d_l \,. \tag{5.14}$$

The first guarantees the a finite action density and a well-defined strength field along the vortex core while the second ensures that the gauge field is a pure gauge, cf. (4.27),

$$\Lambda_i \to \frac{\partial_i \varphi}{g} \beta \cdot T \,, \quad \text{when } \rho \to \infty \,. \tag{5.15}$$

From this ansatz, it also follows that $D_i \psi_q = \partial_i \psi_q$ and, from Eqs. (5.9), (5.10a), that the fields $\psi_q$ must be homogeneous. We shall take $\psi_q \equiv v T_q$. Also notice that Eq. (5.10a) leads to

$$D_+ \left[\zeta_\alpha, \zeta_{\alpha'}\right] = \left[D_+ \zeta_\alpha, \zeta_{\alpha'}\right] + \left[\zeta_\alpha, D_+ \zeta_{\alpha'}\right] = 0 \,, \tag{5.16}$$

if both $\alpha$ and $\alpha'$ are positive roots. This suggests that $[\zeta_\alpha, \zeta_{\alpha'}]$ is proportional to another $\zeta_{\alpha''}$. In addition, the boundary conditions imply

$$\left[\zeta_\alpha, \zeta_{\alpha'}\right] \to v^2 \mathcal{N}_{\alpha,\alpha'} \left[E_\alpha, E_{\alpha'}\right] = v^2 \mathcal{N}_{\alpha,\alpha'} E_{\alpha+\alpha'}; \,, \quad \text{when } \rho \to \infty \,. \tag{5.17}$$

Then, it is natural to assume

$$\left[\zeta_\alpha, \zeta_{\alpha'}\right] = v \mathcal{N}_{\alpha,\alpha'} \zeta_{\alpha+\alpha'} \,. \tag{5.18}$$

Regarding this proposal, it is important to check if it is consistent with the regularity conditions at $\rho = 0$. Fortunately, when both $\alpha, \alpha'$ are positive roots, these equations are always consistent.

If $\alpha \cdot \beta \neq 0$, because of the ansatz (4.31) and Eq. (4.30), we must impose $\zeta_\alpha(\rho \to 0) = 0$. These conditions are compatible as the highest weight is always a positive integer linear combination of fundamental weights (see App. B). In addition, the inner product between a fundamental weight and a positive root is positive. Therefore, if $\beta \cdot \alpha \neq 0$ or $\beta \cdot \alpha' \neq 0$, then $\beta \cdot (\alpha + \alpha') \neq 0$. In this case, to avoid the defect in Eq. (4.30), $\zeta_{\alpha+\alpha'}$ will be zero at $\rho = 0$, in accordance with the regularity condition on at least one of the factors in the left-hand side of Eq. (5.18). On the other hand, when both $\beta \cdot \alpha = 0$ and $\beta \cdot \alpha' = 0$, the associated basis elements do not rotate so $\psi_\alpha$, $\psi_{\bar{\alpha}}$, $\psi_{\alpha'}$, $\psi_{\bar{\alpha}'}$ are not fixed at the origin. In this case, just like $\psi_q$, it holds that $D_i \psi_\alpha = \partial_i \psi_\alpha$. For this reason, when $\beta \cdot \alpha = 0$ we will assume $\psi_\alpha = v T_\alpha$, $\psi_{\bar{\alpha}} = v T_{\bar{\alpha}}$. Consequently, Eq. (5.18) also holds in this case, as it simply follows from the commutation relations between $E_\alpha$ and $E_{\alpha'}$. Moreover, it is not difficult to check that this solves the equations for $\psi_\alpha$ when $T_\alpha$ and $T_{\bar{\alpha}}$ do not rotate.

### 5.1.2 Reduced scalar BPS equations

Notice that

$$\begin{aligned} D_+(\Lambda)\zeta_\alpha &= SD_+(\mathcal{A})(h_\alpha E_\alpha)S^{-1} = \Big(\partial_+ h_\alpha - i\partial_+\varphi h_\alpha \sum_{l=1}^{N-1}(a_l - d_l)\alpha\cdot\beta^{l-\mathrm{A}}\Big)SE_\alpha S^{-1} \,, \\ B^3 &= \sum_{l=1}^{N-1}\frac{1}{g\rho}\frac{\partial a_l}{\partial\rho}\beta^{l-\mathrm{A}}\cdot T = g\sum_{\alpha>0} v^2\alpha\cdot T - \psi_\alpha\wedge\psi_{\bar\alpha} = g\sum_{\alpha>0}(v^2 - h_\alpha^2)S\alpha\cdot TS^{-1} \,. \end{aligned} \tag{5.19}$$

These two relations imply the BPS equations for the the gauge and Higgs profiles

$$\partial_+ \ln h_\alpha = i\partial_+\varphi\sum_{l=1}^{N-1}(a_l - d_l)\alpha\cdot\beta^{l-\mathrm{A}} \,, \tag{5.20a}$$

$$\frac{1}{\rho}\frac{\partial a_l}{\partial\rho} = g^2\sum_{\alpha>0}(v^2 - h_\alpha^2)\alpha\cdot\alpha^{(l)} \,. \tag{5.20b}$$

Here, we used the well-known property involving the fundamental weights and the simple roots $\alpha^{(p)} = \omega_p - \omega_{p+1}$:

$$\alpha^{(p)}\cdot\beta^{l-\mathrm{A}} = \delta^{pq} \,. \tag{5.21}$$

We have already discussed the property $\zeta_\alpha\wedge\zeta_{\alpha'} = v\zeta_{\alpha+\alpha'}$. Naturally, this leads to $h_\alpha h_{\alpha'} = vh_{\alpha+\alpha'}$, which is consistent with Eq. (5.20a). Furthermore, as a general root can be written as a positive sum of simple roots with unit coefficients, the profiles $h_{\alpha^{(p)}}$ associated with simple roots, which satisfy

$$\partial_+ \ln h_{\alpha^{(p)}} = i\partial_+\varphi(a_p - d_p) \,, \tag{5.22}$$

can be used to generate all the others.

## 5.2 Making contact with the $SU(N)\to Z(N)$ model

### 5.2.1 The gauge-field equations

From Eqs. (5.9), (5.10b), recalling that

$$B_i = \frac{1}{2}\varepsilon_{ijk}F_{jk} \quad , \quad F_{ij} = \varepsilon_{ijk}B_k \,, \tag{5.23}$$

we can imply

$$D_jF_{ij} = \varepsilon_{ijk}D_jB_k = -g\varepsilon_{ij3}D_j(\psi_\alpha\wedge\psi_{\bar\alpha}) \,. \tag{5.24}$$

If we take $i = 1$ and use the BPS equation for $\psi_\alpha$, $\psi_{\bar{\alpha}}$, we get

$$\begin{aligned} D_j F_{1j} &= -gD_2(\psi_\alpha \wedge \psi_{\bar{\alpha}}) = -gD_2\psi_\alpha \wedge \psi_{\bar{\alpha}} - g\psi_\alpha \wedge D_2\psi_{\bar{\alpha}} \\ &= \frac{ig}{2}\left(D_+\psi_\alpha \wedge \psi_{\bar{\alpha}} - D_-\psi_\alpha \wedge \psi_{\bar{\alpha}} + \psi_\alpha \wedge D_+\psi_{\bar{\alpha}} - \psi_\alpha \wedge D_-\psi_{\bar{\alpha}}\right) \\ &= \frac{ig}{2}\left(-iD_+\psi_{\bar{\alpha}} \wedge \psi_{\bar{\alpha}} - iD_-\psi_{\bar{\alpha}} \wedge \psi_{\bar{\alpha}} + i\psi_\alpha \wedge D_+\psi_\alpha + i\psi_\alpha \wedge D_-\psi_\alpha\right) \\ &= -g\left(\psi_\alpha \wedge \frac{D_+ + D_-}{2}\psi_\alpha + \psi_{\bar{\alpha}} \wedge \frac{D_+ + D_-}{2}\psi_{\bar{\alpha}}\right) = gD_1\psi_A \wedge \psi_A \,. \end{aligned} \tag{5.25}$$

This is nothing but the component $i = 1$ of Eq. (5.4a). A similar calculation can be done for $i = 2$, while $i = 3$ is trivially satisfied.

### 5.2.2 Cartan Higgs-sector

Now, to make contact with the solutions to the Higgs-field equations (5.4b), we have to look for a Higgs potential $V_{\mathrm{H}}$ that is compatible with the BPS equations. In particular, Eqs. (5.9), (5.10a) imply $D_i D^i \psi_q = 0$, so that $V_{\mathrm{H}}$ must imply

$$\frac{\delta V_H}{\delta \psi_q} = 0 \tag{5.26}$$

on the ansatz given in Eqs. (4.27), (4.31) and (5.13), which closes the BPS equations. In what follows, we will see that this happens when it is given by Eq. (4.24) with $\mu^2 = 0$ and $\lambda = g^2$. In this case,

$$\frac{\delta V_H}{\delta \psi_A} = \lambda \psi_B \wedge (\psi_A \wedge \psi_B - v f_{ABC}\psi_C) \,, \tag{5.27}$$

where $v = -\frac{\kappa}{\lambda}$. Indeed, applying the same ansatz, we get

$$\begin{aligned} \frac{\delta V_H}{\delta \psi_q} &= \lambda \sum_{\alpha>0} \psi_\alpha \wedge (\psi_q \wedge \psi_\alpha - v f_{q\alpha\bar{\alpha}}\psi_{\bar{\alpha}}) + \psi_{\bar{\alpha}} \wedge (\psi_q \wedge \psi_{\bar{\alpha}} - v f_{q\bar{\alpha}\alpha}\psi_\alpha) \\ &= \lambda v \sum_{\alpha>0} \left(h_\alpha S T_\alpha S^{-1}\right) \wedge \left(\alpha|_q h_\alpha S T_{\bar{\alpha}} S^{-1} - \alpha|_q h_\alpha S T_{\bar{\alpha}} S^{-1}\right) = 0 \,. \end{aligned} \tag{5.28}$$

### 5.2.3 Off-diagonal Higgs-sector

Let us now analyze the equations for fields labelled by roots. The BPS equations lead to

$$D^2\zeta_\alpha = D_-D_+\zeta_\alpha - g[B_3, \zeta_\alpha] = g^2 \sum_{\alpha'>0} \left[[\zeta_{\alpha'}, \zeta^\dagger_{\alpha'}] - v^2\alpha' \cdot T, \zeta_\alpha\right] \,. \tag{5.29}$$

The sum over $\alpha'$ involves all positive roots, including $\alpha$. On the other hand, according to the equations of the model, we have

$$D^2\zeta_\alpha = F_\alpha \quad , \quad F_\alpha = \frac{1}{\sqrt{2}}\left(\frac{\delta V}{\delta \psi_\alpha} + i\frac{\delta V}{\delta \psi_{\bar{\alpha}}}\right) . \tag{5.30}$$

In view of Eq. (5.27), $F_\alpha$ receives contributions from the index types $B = q, \alpha, \bar{\alpha}, \gamma, \bar{\gamma}$ where $\gamma > 0$ is a root different from $\alpha$. The partial contribution originated from the Cartan labels $B = q$ is given by

$$F_\alpha^{(B=q)} = \frac{\lambda}{\sqrt{2}}\psi_q \wedge (\psi_\alpha \wedge \psi_q - v f_{\alpha q\bar{\alpha}}\psi_{\bar{\alpha}} + i\psi_{\bar{\alpha}} \wedge \psi_q - iv f_{\bar{\alpha}q\alpha}\psi_\alpha) . \tag{5.31}$$

Using the ansatz equations (4.27), (4.31), and also $\psi_q = vT_q$, we have

$$\psi_\alpha \wedge \psi_q = v f_{\alpha q\bar{\alpha}}\psi_{\bar{\alpha}} , \tag{5.32a}$$

$$\psi_{\bar{\alpha}} \wedge \psi_q = v f_{\bar{\alpha}q\alpha}\psi_\alpha , \tag{5.32b}$$

which imply $F_\alpha^{(B=q)} = 0$. Next, there is a contribution originated from $B = \alpha, \bar{\alpha}$

$$\begin{aligned} F_\alpha^{(B=\alpha,\bar{\alpha})} &= \frac{\lambda}{\sqrt{2}}\left(\psi_{\bar{\alpha}} \wedge (\psi_\alpha \wedge \psi_{\bar{\alpha}} - v f_{\alpha\bar{\alpha}q}\psi_q) + i\psi_\alpha \wedge (\psi_{\bar{\alpha}} \wedge \psi_\alpha - v f_{\bar{\alpha}\alpha q}\psi_q)\right) \\ &= \lambda\frac{\psi_{\bar{\alpha}} - i\psi_\alpha}{\sqrt{2}} \wedge (\psi_\alpha \wedge \psi_{\bar{\alpha}} - v f_{\alpha\bar{\alpha}q}\psi_q) \\ &= \lambda\left[[\zeta_\alpha, \zeta_\alpha^\dagger] - v\alpha\cdot\psi, \zeta_\alpha\right] , \end{aligned} \tag{5.33}$$

where we used the property

$$\psi_\alpha \wedge \psi_{\bar{\alpha}} = \left[\zeta_\alpha, \zeta_\alpha^\dagger\right] . \tag{5.34}$$

Finally, we evaluate $F_\alpha^{(B=\gamma,\bar{\gamma})} = P_\alpha + Q_\alpha$, where $P_\alpha$ ($Q_\alpha$) is the part without (with) explicit dependence on the structure constants. They are given by a sum over positive roots $\gamma \neq \alpha$

$$P_\alpha = \lambda\sum_{\gamma\neq\alpha}\left(\psi_\gamma \wedge (\zeta_\alpha \wedge \psi_\gamma) + \psi_{\bar{\gamma}} \wedge (\zeta_\alpha \wedge \psi_{\bar{\gamma}})\right) \tag{5.35a}$$

$$Q_\alpha = \frac{\lambda v}{\sqrt{2}}\sum_{\gamma\neq\alpha}\left(f_{\alpha\gamma\bar{\delta}}\psi_\gamma \wedge \psi_{\bar{\delta}} - f_{\alpha\bar{\gamma}\delta}\psi_{\bar{\gamma}} \wedge \psi_\delta - if_{\bar{\alpha}\gamma\delta}\psi_\gamma \wedge \psi_\delta - if_{\bar{\alpha}\bar{\gamma}\bar{\delta}}\psi_{\bar{\gamma}} \wedge \psi_{\bar{\delta}}\right) . \tag{5.35b}$$

Using Eq. (5.18), we arrive at

$$P_\alpha = \lambda\sum_{\gamma\neq\alpha}\left(\zeta_\gamma \wedge (\zeta_\alpha \wedge \zeta_\gamma^\dagger) + \zeta_\gamma^\dagger \wedge (\zeta_\alpha \wedge \zeta_\gamma)\right) = \lambda\sum_{\gamma\neq\alpha}\left(\left[[\zeta_\gamma, \zeta_\gamma^\dagger], \zeta_\alpha\right] - 2v\mathcal{N}_{\alpha,\gamma}[\zeta_\gamma^\dagger, \zeta_{\alpha+\gamma}]\right) . \tag{5.36}$$

On the other hand, by using Eqs. (A.10) and (5.8) it is possible to cast $Q_\alpha$ in the form

$$Q_\alpha \;=\; \lambda v \sum_{\gamma\neq\alpha} \left(\mathcal{N}_{\alpha,\gamma}[\zeta^\dagger_\gamma, \zeta_{\alpha+\gamma}] + \mathcal{N}_{\alpha,-\gamma}[\zeta_\gamma, \zeta_{\alpha-\gamma}]\right) \tag{5.37}$$

Let us analyze the term with label $\alpha-\gamma$. Because $\gamma$ is a positive root, $\alpha-\gamma$ is not necessarily positive, so we cannot use Eq. (5.18) right away. Instead, we shall split this term into two contributions: $\gamma=\gamma^+$ ($\gamma=\gamma^-$) such that $\alpha-\gamma^+$ ($\alpha-\gamma^-$) is a positive (negative) root. In the second case

$$\lambda v\mathcal{N}_{\alpha,-\gamma^-}[\zeta_{\gamma^-}, \zeta_{\alpha-\gamma^-}] = \lambda v\mathcal{N}_{\alpha,-\sigma-\alpha}[\zeta_{\sigma+\alpha}, \zeta_{-\sigma}] = \lambda v\mathcal{N}_{\alpha,\sigma}\left[\zeta^\dagger_\sigma, \zeta_{\sigma+\alpha}\right] \;, \tag{5.38}$$

where $\sigma$ is a positive root that, when summed with $\alpha$, yields another positive root. This is precisely the condition on $\gamma$ in the first term of Eq. (5.37). Therefore,

$$Q_\alpha = \lambda v \sum_{\gamma\neq\alpha} 2\mathcal{N}_{\alpha,\gamma}[\zeta^\dagger_\gamma, \zeta_{\alpha+\gamma}] + \lambda v \sum_{\gamma^+} \mathcal{N}_{\alpha,-\gamma^+}[\zeta_{\gamma^+}, \zeta_{\alpha-\gamma^+}] \;, \tag{5.39}$$

which together with the result for $P_\alpha$ yields

$$F^{(B=\gamma,\bar\gamma)}_\alpha \;=\; \lambda \sum_{\gamma\neq\alpha} \left[[\zeta_\gamma, \zeta^\dagger_\gamma], \zeta_\alpha\right] + \lambda v \sum_{\gamma^+} \mathcal{N}_{\alpha,-\gamma^+}[\zeta_{\gamma^+}, \zeta_{\alpha-\gamma^+}] \;. \tag{5.40}$$

By the definition of $\gamma^+$, $\alpha-\gamma^+$ is positive so we can use Eq. (5.18) once again to write

$$\begin{aligned} F^{(B=\gamma,\bar\gamma)}_\alpha = &\quad \lambda \sum_{\gamma\neq\alpha} \left[[\zeta_\gamma, \zeta^\dagger_\gamma], \zeta_\alpha\right] + \lambda v^2 \sum_{\gamma^+} \mathcal{N}_{\alpha,-\gamma^+}\mathcal{N}_{\gamma^+,\alpha-\gamma^+}\zeta_\alpha \\ = &\quad \lambda \sum_{\gamma\neq\alpha} \left[[\zeta_\gamma, \zeta^\dagger_\gamma], \zeta_\alpha\right] - \lambda v^2 \sum_{\gamma^+} \mathcal{N}^2_{\alpha,-\gamma^+}\zeta_\alpha \;. \end{aligned} \tag{5.41}$$

To evaluate the sum over $\gamma^+$, we need to count how many roots are consistent with the $\alpha-\gamma^+>0$ condition. For this objective, we can use that $\alpha=\omega_I-\omega_J$ for some $I<J$. Then, there are two cases

$$\begin{aligned} \gamma^+ &= \omega_I-\omega_l \;, I<l<J \Rightarrow J-I-1 \quad \text{possibilities,} \\ \gamma^+ &= \omega_l-\omega_J \;, I<l<J \Rightarrow J-I-1 \quad \text{possibilities.} \end{aligned}$$

Moreover, since $\mathcal{N}^2_{\alpha,-\gamma^+}=\frac{1}{2N}$ in both of these cases, we have

$$\sum_{\gamma^+} \mathcal{N}^2_{\alpha,-\gamma^+} = \frac{J-I-1}{N} \;. \tag{5.42}$$

The sum of the $\mathcal{N}^2$-factors in Eq. (5.41) can be rewritten as a sum of $(\alpha\cdot\gamma)$-factors:

$$\sum_{\gamma\neq\alpha}\alpha\cdot\gamma=\frac{N+J-I-3}{2N}-\frac{N-J+I-1}{2N}=\sum_{\gamma^+}\mathcal{N}^2_{\alpha,-\gamma^+}\ , \tag{5.43}$$

where we used a similar counting to determine how many positive roots $\gamma$ different from $\alpha$ have $\alpha\cdot\gamma=\pm\frac{1}{2N}$. In addition, using the ansatz,

$$\alpha\cdot\gamma\zeta_\alpha=[\gamma\cdot T,\zeta_\alpha]\ , \tag{5.44}$$

so that

$$F_\alpha^{(B=\gamma,\bar\gamma)}=\lambda\sum_{\gamma\neq\alpha}\left[[\zeta_\gamma,\zeta_\gamma^\dagger]-v^2\gamma\cdot T,\zeta_\alpha\right]\ . \tag{5.45}$$

Finally, joining this result with the previous ones, namely $F_\alpha^{(B=q)}=0$ and Eq. (5.33), we get

$$D^2\zeta_\alpha=\lambda\big[[\zeta_\alpha,\zeta_\alpha^\dagger]-v^2\alpha\cdot T,\zeta_\alpha\big]+\lambda\sum_{\gamma\neq\alpha}\left[[\zeta_\gamma^\dagger,\zeta_\gamma]-v^2\gamma\cdot T,\zeta_\alpha\right]=\lambda\sum_{\alpha'>0}\left[v^2\alpha'\cdot T-[\zeta_{\alpha'},\zeta_{\alpha'}^\dagger],\zeta_\alpha\right]\ , \tag{5.46}$$

which equals Eq. (5.29) for $\lambda=g^2$.

## 5.3 String tension for quarks in representation D

In the previous sections, for each quark representation, we showed that at $\mu^2=0$, $\lambda=g^2$ the proposed vortex ansatz that closes the BPS equations provide a static vortex solution for the $SU(N)\to Z(N)$ YMH model defined in Eq. (4.19). From Eqs. (5.8)-(5.10), the associated energy per unit-length is

$$\epsilon\ =\ \int d^2x\left(\frac{1}{2}\langle B_3,B_3\rangle+\sum_{\alpha>0}\langle D_i\zeta_\alpha^\dagger,D_i\zeta_\alpha\rangle+V_{\rm H}(\psi)\right)\ , \tag{5.47}$$

where $d^2x$ integrates over the transverse directions to the infinite string. Using Derrick's theorem in two dimensions, we can equate the potential energy of the Higgs field to that of the gauge field, thus obtaining

$$\begin{aligned}\epsilon\ &=\ \int d^2x\,\langle B_3,B_3\rangle-\langle\zeta_\alpha^\dagger,D^2\zeta_\alpha\rangle\\ &=\ \int d^2x\,\langle B_3,B_3\rangle-\langle\zeta_\alpha^\dagger,D_-D_+\zeta_\alpha\rangle+g\langle\zeta_\alpha^\dagger,[B_3,\zeta_\alpha]\rangle=\int d^2x\,\langle B^3,B^3+g[\zeta_\alpha,\zeta_\alpha^\dagger]\rangle\\ &=\ \int d^2x\,gv^2\langle B^3,2\delta\cdot T\rangle=gv^2\oint\langle\Lambda_i,2\delta\cdot T\rangle\,dx_i\ ,\end{aligned} \tag{5.48}$$

where $\delta$ is the sum of all positive roots and the last integral must be taken along a cicle with infinite radius. Recalling Eq. (5.15), this implies that

$$\epsilon = 2\pi g v^2 \beta \cdot 2\delta \ . \tag{5.49}$$

at the BPS point. In particular, note that the $k$-A string tension scales with the quadratic Casimir, as $\beta \cdot 2\delta = \frac{N}{N+1} C_2(k\text{-A})$ in this case. This is the result we obtained in Ref. [117]. The new important physical consequence that we will derive from Eq. (5.49) is that for a general representation D$(\cdot)$ with $N$-ality $k$, the asymptotic string tension satisfies

$$\frac{\sigma(\mathrm{D})}{\sigma(\mathrm{F})} = \frac{C_2(k\text{-A})}{C_2(\mathrm{F})} \ , \tag{5.50}$$

which is one of the possible behaviors observed in lattice simulations.

In what follows, we shall see that the smallest $\beta \cdot 2\delta$ factor is given by the $k$-A weight. To prove this result, some Young Tableaux technology, useful to study the properties of the irreducible representations, is required. In this discussion, we shall closely follow the ideas in Ref. [41]. A Young Tableau consists of a number of boxes organized according to the following rules:

1. The maximum allowed number of boxes on a given column is $N-1$.

2. The number of boxes in a given column ($n_i$) should be lower or equal than the number in any column to the left. That is, $i > j \to n_i \leq n_j$.

3. The number of boxes in a given row ($m_i$) should be lower or equal than the number in any row above. That is, $i > j \to m_i \leq m_j$.

Every diagram drawn according to these rules corresponds to an irreducible representation of $SU(N)$. Many related properties can be easily identified in this language [41]. The $N-$ality of a representation is simply given by the number of boxes of the Young Tableau, modulo $N$. The Dynkin indices $d_k$ of the highest weight $\lambda^D$ satisfy [41][1]

$$\lambda^D = \sum_{l=1}^{N-1} d_l \lambda^{l\text{-A}} \quad , \quad d_i = m_i - m_{i+1} \ . \tag{5.51}$$

In general, when a box is moved from an upper to a lower row, an irrep. with more antisymmetries is obtained. For example, the Young tableau for the $k$-A ($k$-S) irrep. has one column (row) with $k$ boxes, as shown in Fig. 5.1. For an irrep. with $N$-ality $k$, that is, a Young tableau with a total number of boxes of the form $k + nN$, the scaling factor

[1] When $i = N-1$, we take $m_N = 0$.

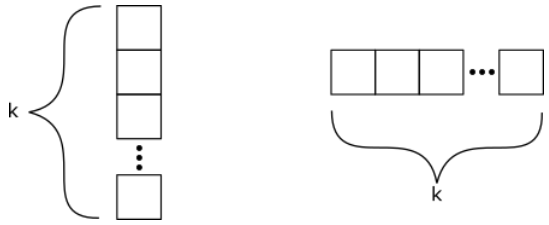


Figure 5.1: Young tableaux for the $k$-A (left) and $k$-S (right) representations.

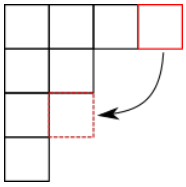

Figure 5.2: An example of transformation on a tableau that decreases the scaling factor $\beta \cdot 2\delta$.

can be written as

$$\beta \cdot 2\delta \;\; = \;\; \frac{N}{N+1} \sum_{l=1}^{N-1} d_l \, l(N-l) = N(k+nN) - \frac{2N}{N+1} \sum_{l=1}^{N-1} m_l \, l \; . \tag{5.52}$$

Then, if a pair of irreps. D and D$'$ with magnetic weights $\beta$ and $\beta'$, respectively, have the same $N$-ality $k$, we obtain

$$\Delta\beta \cdot 2\delta = \beta' \cdot 2\delta - \beta \cdot 2\delta = N^2 \Delta n - \frac{2N}{N+1} \sum_{l=1}^{N-1} \Delta m_l \, l \; , \tag{5.53}$$

$\Delta m_l = m'_l - m_l$, $\Delta n = n' - n$, where the primed variables refer to D$'$. Let us initially consider a pair of Young tableaux with the same number of boxes. If a box is moved from an upper row $I$ to a lower row $J$ (see, for example, Fig. 5.2), we have $I < J$ and $\Delta m_J = -\Delta m_I = 1$; consequently, $\Delta\beta \cdot 2\delta = \frac{2N}{N+1}(I-J) < 0$. This means that, for a given number of boxes $k+nN$, the tableau with smallest $\beta \cdot 2\delta$ is that in which the boxes are as lowered as possible. Among these tableaux, we need to compare those having different $n$ but the same $N$-ality. As an initial example, let us begin by comparing the pair shown in Fig. 5.3 and assume that the column of the first one is not completely full, i.e. $k \leq N-2$.

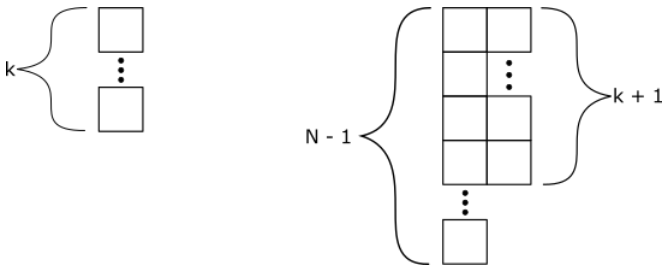


Figure 5.3: Fully antisymmetric Young tableau with $k$ (left) and $N+k$ (right) boxes.

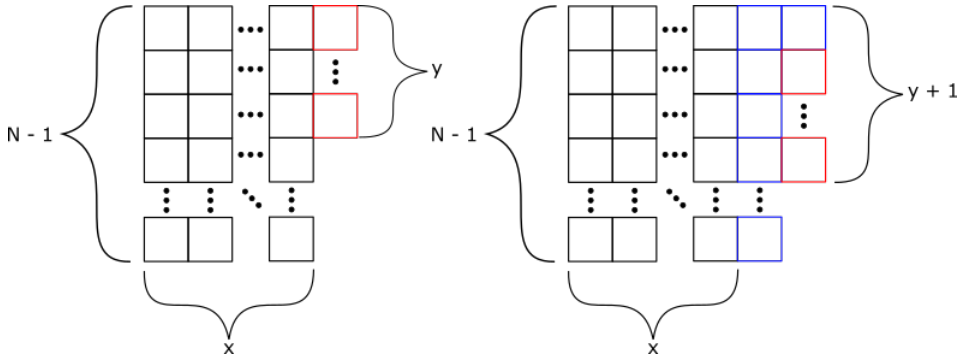


Figure 5.4: Fully antisymmetric Young tableau with $k+nN$ (left) and $k+(n+1)N$ (right) boxes. There are $y$ boxes (in red) in the partly full column in the first tableau and $N$ boxes (in blue) were added in the second one (colors online).

In this case, we see that

$$\Delta m_i = \begin{cases} 2, \text{ if } i = k, \\ 1, \text{ otherwise.} \end{cases} \tag{5.54}$$

Also, $\Delta n = 1$ because we are comparing $k$ with $k + N$ boxes, in which case

$$\Delta\beta \cdot 2\delta \;\; = \;\; N^2\Delta n - \frac{2N}{N+1}\sum_{l=1}^{N-1}\Delta m_l\, l = \frac{2N}{N+1}(N-k) > 0\,. \tag{5.55}$$

This means the scaling factor increases when we go from $k$ to $N + k$ boxes. This can be readily extended to the general case depicted in Fig. 5.4. Because $\beta \cdot 2\delta$ depends only on the difference of the number of boxes, the $x$ full columns in both diagrams can be disregarded for our purposes. The values of $x$ and $y$ are such that $y+x(N-1) = k+nN$. In fact, the analysis of the relevant part of these two tableaux is completely analogous to that of Fig. 5.3, which leads to the same result of Eq. (5.55) but with $y$ instead of $k$. Since $1 \leq y \leq N-1$, the net difference continues to be positive. In summary, the smallest scaling factor within a given $N$-ality $k$ corresponds to the single column tableau on the left side of Fig. 5.3, namely, the one corresponding to the $k$-A representation.

Now, to complete the analysis of the asymptotic scaling, we need to recall how the Wilson loop is assessed in the effective model, as this is the observable used in the lattice to compute string tensions. Indeed, as discussed in Chapters 1 and 4, where we reviewed the ideas of Ref. [56], this model emerges as an effective description of center-element averages, which depend on the linking number between center vortices and the Wilson loop $\mathcal{C}$. The Wilson loop average is given by Eq. (4.17), which contains the frustration source $J_{\mu\nu}$. As usual, the confining state in the presence of a static quark-antiquark pair is obtained from a rectangular Wilson loop with one side along the Euclidean time with length $T \to \infty$. In the energy functional, $J_{\mu\nu}$ gives place to unobservable Dirac strings with endpoints at the (physical) quark and antiquark locations. Solutions of the form (4.27), with modified regularity conditions so as to cancel the Dirac strings, can be

obtained. They correspond to smooth finite strings, which in the limit of large quark-antiquark separations make contact with the BPS solutions we studied here. However, at asymptotic distances, most of these solutions are in fact local minima or metastable states. Other finite energy solutions where the Dirac strings are also canceled may involve dynamical adjoint monopoles (valence gluons) created around the sources [120]. As the adjoint representation has trivial $N$-ality, the favored asymptotic confining string will be the one with the lowest energy among those with the same $N$-ality ($k$) of D($\cdot$). From the previous discussion, this corresponds to the $k$-A string, which settles the asymptotic Casimir scaling in Eq. (5.50).

## 5.4 Tetraquark configurations

In Monte Carlo simulations, when studying an observable that creates static sources during a large time interval $T$, the leading behavior is dominated by the lowest energy state that can be created. Then, in the effective model, this state must be compared with the lowest energy configuration compatible with the conditions imposed by the sources. For example, it is clear that the lattice simulation of the Wilson loop in the $k$-A irrep. must be compared with a straight string (with cylindrical symmetry), running from the quark to the antiquark. This will be the global minimum, as the introduction of dynamical monopoles or wiggles will certainly increase the energy. Indeed, at asymptotic distances, where the effective model is expected to be valid, this will make contact with the translationally symmetric BPS $k$-A string solution.

Now, at $\mu^2 = 0$, the nontrivial profiles for translationally symmetric configurations with any number of $k$-A strings, given by the ansatz in Eq. (4.27), were shown to obey Nielsen-Olesen equations [117]. At the critical coupling, this implies that they do not interact. However, this is not necessarily related with the behavior of fluxes in Yang-Mills observables. For example, to analyze a situation with a pair of sources and sinks (see Fig. 5.5a), an observable that creates a tetraquark must be considered. Again, the lattice result has to be compared with the global minimization of the effective energy functional in the presence of the static probes, without any further restrictions on the fields. On the other hand, the multivortex critical solutions do not contemplate the minimization with respect to translationally nonsymmetric configurations. That is, when the sources and sinks are far apart from each other, the noninteracting translationally invariant configuration could be a metastable state associated with a local minimum. Then, let us take a closer look to the case of $SU(3)$ with fundamental quarks. As pointed out in Refs. [121, 122, 123], the flux distribution strongly depends on the distance between the quark-antiquark pairs. For $R_1 > \sqrt{3}R_2$ (with asymptotic values for both $R_1$ and $R_2$), the energy distribution is given by a double Y-shaped configuration, as depicted in Fig. 5.5b. This behavior was

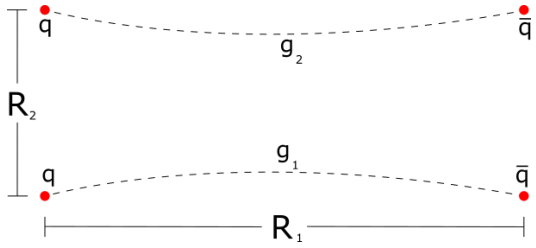


(a) A pair of sources and sinks

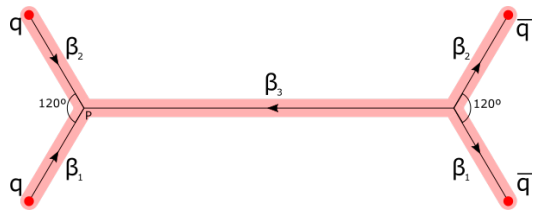


(b) Double Y-shaped configuration in $SU(3)$

Figure 5.5: $qq\bar{q}\bar{q}$ probes: a) The stable flux configuration includes the energy minimization over all possible guiding-centers $g_1$, $g_2$. b) For $R_1 > \sqrt{3}R_2$, the coalescence of $g_1$, $g_2$ is favored, as the sum of fundamental $\mathfrak{su}(3)$ weights $\beta_1, \beta_2$ is an antifundamental weight $-\beta_3$ ($N$-ality).

computed in the lattice, by considering the tetraquark observable [121]

$$W_{4q}[A_\mu] = \frac{1}{12}\epsilon^{abc}\epsilon^{def}\epsilon^{a'b'c'}\epsilon^{d'e'f'}\Gamma_1|^{aa'}\Gamma_2|^{bb'}\Gamma_G|^{cf}\Gamma_3|^{d'd}\Gamma_4|^{e'e}\Gamma_{G'}|^{f'c'} \ , \tag{5.56}$$

where $A_\mu$ is the fundamental field of pure Yang-Mills theory and the different holonomies $\Gamma$ are evaluated along the paths $\gamma_1, \ldots, \gamma_4$, $\gamma_G$, $\gamma_{G'}$ (see Fig. 5.6).

In the center-vortex ensemble picture, the tetraquark observable is related with the average of

$$W_{4q} = \prod_{i=1}^{4} z^{\sum_w L(\gamma_i^c, w)} z^{\sum_w 2L(\gamma_5^c, w)} \tag{5.57}$$

over closed worldsurfaces $w$, as this is the contribution to the tetraquark variable $W_{4q}$ when evaluated on thin center-vortices. Here, $z = e^{i2\pi/3}$ is a center element, and the closed paths $\gamma_1^c, \gamma_2^c$ (resp. $\gamma_3^c, \gamma_4^c$) are the composition of $\gamma_1, \gamma_2$ (resp. $\gamma_3, \gamma_4$) with the adjacent dotted line $\gamma_L$ (resp. $\gamma_R$). In addition, the closed path $\gamma_5^c$ is given by the composition of $\gamma_G, \gamma_L, \gamma_{G'}$ and $\gamma_R$. $L(\gamma_k^c, w)$ is the linking number between $w$ and the closed paths $\gamma_k^c$, while the factor 2 is because $\gamma_5^c$ has opposite orientation compared with $\gamma_1^c, \ldots, \gamma_4^c$, and $z^{-1} = z^2$. Then, the only difference here is the choice of external source to be considered

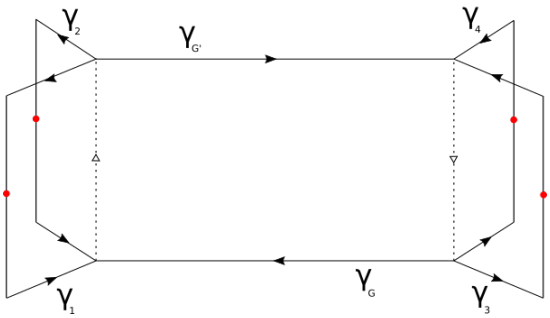


Figure 5.6: Representation of the tetraquark observable $W_{4q}$. The dashed lines represent optional holonomies that can be included without changing this variable.

in Eq. (4.17). Due to Eq. (5.57), a possibility is given by

$$J_{\mu\nu} = 2\pi \sum_{k=1}^{5} \beta(\gamma_k^c) \cdot T s_{\mu\nu}^k \tag{5.58}$$

where $s_{\mu\nu}^k$ is localized on a surface $S(\gamma_k^c)$ whose border is $\gamma_k^c$ and

$$\beta(\gamma_1^c) = \beta(\gamma_3^c) = \beta_1 \quad , \quad \beta(\gamma_2^c) = \beta(\gamma_4^c) = \beta_2 \quad , \quad \beta(\gamma_5^c) = \beta_3 = -\beta_1 - \beta_2 \ , \tag{5.59}$$

where $\beta_k = 2N\omega_k$, and $\omega_1$, $\omega_2$, $\omega_3$ are the three (ordered) weights of the fundamental representation of $SU(3)$. Indeed, in the lattice, this introduces a frustration factor in the Wilson action

$$e^{-i\alpha_{\mu\nu}} \quad , \quad \alpha_{\mu\nu} = \alpha_{\mu\nu}^1 + \cdots + \alpha_{\mu\nu}^1 - \alpha_{\mu\nu}^5 \quad , \quad \alpha_{\mu\nu}^k = \begin{cases} 2\pi\beta(\gamma_k^c)\cdot T & \text{if } \langle\mu\nu\rangle \text{ intersects } S(\gamma_k^c) \\ 0 & \text{otherwise,} \end{cases}$$

defined on the lattice plaquettes $\langle\mu\nu\rangle$. In the expansion of the Wilson action, the nontrivial contribution is originated from plaquettes distributed on closed worldsurfaces $w$. When $\gamma_k^c$ links $w$, then $S(\gamma_k^c)$ is intersected. This gives a factor $e^{i2\pi\beta_1\cdot T} = e^{i2\pi\beta_2\cdot T} = zI$ or $e^{-i2\pi\beta_3\cdot T} = e^{i2\pi(\beta_1+\beta_2)\cdot T} = z^2 I$, thus reproducing Eq. (5.57). It is also interesting to note that the weight choice in Eq. (5.59) is related with the Petrov-Diakonov representation of $W_{4q}$ (see App. C). Similarly to the case of a single Wilson loop, at fixed $t$ the external source in Eq. (5.58) will give rise to unobservable Dirac lines, which can be chosen as entering the lower (upper) antiquark and leaving the lower (upper) quark with $\beta_1$

($\beta_2$). In this case, in order for the energy to be finite, a configuration based on a phase $S = e^{i(\beta_1\chi_1 + i\beta_2\chi_2)\cdot T}$ is required, where $\chi_1$ ($\chi_2$) is multivalued when going around a closed path designed to cancel the Dirac string of type $\beta_1$ ($\beta_2$). This leaves the effect of a pair of guiding centers $g_1$, $g_2$ (Fig. 5.5a) where the fields must be in a false vacuum, so that the energy will be mainly concentrated around them. It is clear that for $R_1 > \sqrt{3}R_2$ (with asymptotic $R_1$, $R_2$), the energy minimization, which includes the variation of $g_1$ and $g_2$, will favor a Y-shaped global minimum as shown in Fig. 5.5b. This is due to the fact that, in the common part, the sum of fundamental magnetic weights $\beta_1$ and $\beta_2$ will combine to $-\beta_3$, which implies the same energy cost of a single fundamental string. In other words, the observed Y-shaped configuration is nothing but the reflection of $N$-ality stated in the language of weights.

# Chapter 6

# Center-Vortex Sectors in Continuum YM Theory

After Singer's theorem [64], it became clear that the usual Faddeev-Popov procedure to quantize non-Abelian Yang-Mills theories must be somehow modified in the non-perturbative regime. Because of a topological obstruction, there is no condition $g(A) = 0$ that can globally fix the gauge on the whole configuration space $\{A_\mu\}$. Hence, when such condition is imposed, the path integral still contains redundant degrees of freedom (d.o.f) associated with gauge fields obeying $g(A) = 0$ and related by nontrivial gauge transformations. Such spurious configurations are typically called Gribov copies. The usual way to deal with this obstruction was implemented in the Landau gauge by V. N. Gribov in his seminal work [124], see also Ref. [125]. In his proposal, a path-integral restricted to a subset of $\{A_\mu\}$ was implemented so as to eliminate infinitesimal copies. As a consequence, the perturbative gauge propagator is destabilized, giving place to one with complex poles, while the ghost propagator is enhanced. Later on, many other developments were achieved. In the Landau gauge, D. Zwanziger was able to construct a local and renormalizable action [126] which was afterwards refined by the inclusion of dimension two condensates [127, 128]. Beyond this gauge, it is worth mentioning important progress in the maximal Abelian gauge [129, 130, 131] and the linear covariant gauges [132, 133, 134], see also Ref. [135]. Finally, we refer to a Becchi-Rouet-Stora-Tyutin (BRST) invariant formulation of the path integral restriction, with a local and renormalizable action, that was implemented as a gauge independent recipe [136, 137, 138].

In Ref. [61], a different procedure to deal with Singer's obstruction was introduced, by splitting the configuration space into domains $\vartheta_\alpha \subset \{A_\mu\}$ where local sections are well-defined. Of course, Singer's theorem does not pose any problem to define regions with a local section having no Gribov copies. The important point is that, in order for these

regions to serve as a basis to implement the new proposal, they must form a partition

$$\{A_\mu\} = \cup_\alpha \vartheta_\alpha \quad , \quad \vartheta_\alpha \cap \vartheta_\beta = \emptyset \ \text{ if } \ \alpha \neq \beta \ . \tag{6.1}$$

In that case, we would have ($S_{\rm YM} = \frac{1}{4g^2}\int d^4x\, F_{\mu\nu}^2$)

$$Z_{\rm YM} = \sum_\alpha Z_{(\alpha)} \quad , \quad \langle O\rangle_{\rm YM} = \sum_\alpha \frac{Z_{(\alpha)}}{Z_{\rm YM}} \langle O\rangle_{(\alpha)} \tag{6.2}$$

$$Z_{(\alpha)} = \int_{\vartheta_\alpha} [DA_\mu]\, e^{-S_{\rm YM}[A]} \quad , \quad \langle O\rangle_{(\alpha)} = \frac{1}{Z_{(\alpha)}} \int_{\vartheta_\alpha} [DA_\mu]\, e^{-S_{\rm YM}[A]} O[A] \ , \tag{6.3}$$

and the usual Fadeev-Popov procedure could be separately implemented on each domain $\vartheta_\alpha$. In Ref. [61], motivated by lattice procedures used to detect center vortices by looking at the lowest eigenfuntions of the adjoint covariant Laplacian [17, 18], a partition of $\{A_\mu\}$ was generated in the continuum. For this purpose, a gauge invariant auxiliary action $S_{\rm aux}[A,\psi]$ for a tuple $\psi = (\psi_1, \ldots, \psi_{N_{\rm f}})$ of auxiliary adjoint scalar fields $\psi_I$, $I = 1, \ldots, N_{\rm f}$, was considered. Then, the gauge field $A_\mu$ was correlated with the solution $\psi = \psi(A)$ to the set of classical equations of motion

$$\frac{\delta S_{\rm aux}}{\delta \psi_I} = 0 \quad , \quad \psi_I \in \mathfrak{su}(N) \quad , \quad I = 1, \ldots, N_{\rm f} \ , \tag{6.4}$$

with appropriate boundary and regularity conditions. Since the auxiliary action is gauge invariant, when an orbit of $A_\mu$ is followed, an orbit in the auxiliary space $\{\psi\}$ is described, with components

$$\psi_I(A^U) = U \psi_I(A)\, U^{-1} \quad , \quad A_\mu^U = U A_\mu U^{-1} + iU\partial_\mu U^{-1} \ . \tag{6.5}$$

Next, a polar decomposition of the tuple $\psi$ was introduced. [1]

$$\psi_1 = S q_1 S^{-1}, \ \ldots \ , \psi_{N_{\rm f}} = S q_{N_{\rm f}} S^{-1} \ , \tag{6.6}$$

based on a concept of "pure modulus" condition for a tuple $q = (q_1, \ldots, q_{N_{\rm f}})$:

$$f(q) = 0 \quad , \quad f \in \mathfrak{su}(N) \ . \tag{6.7}$$

After this initial stage, we would have auxiliary variables $q(A)$ and $S(A)$ such that, when moving along the orbit of $A_\mu$, $q(A)$ stays invariant while the phase describes an orbit $S(A^U) = US(A)$. The point is that even for smooth finite-action configurations $A_\mu$, $S(A)$ will generally contain defects, which cannot be removed by means of the regular

[1] In general, a relation between tuples of the form given in Eq. (6.6) shall be simply denoted by $\psi = q^S$.

$U$-mappings associated with gauge transformations. That is, it is not possible to define a "unitary" gauge $S(A) = I$ on $\{A\}$. What can be done is to define regions $\mathscr{V}(S_0) \subset \{A_\mu\}$ formed by gauge fields that can be gauge-transformed to $S(A^U) = S_0$, where $U$ is regular and $S_0$ is a reference (class representative), characterized by a given distribution of defects. In other words, the gauge can be fixed with the $\mathscr{V}(S_0)$-dependent condition:

$$f_{S_0}(A) = 0 \quad , \quad A_\mu \in \mathscr{V}(S_0) \quad , \quad f_{S_0}(A) = f(S_0^{-1}\psi_1(A)\, S_0,\ \ldots\ , S_0^{-1}\psi_{N_{\rm f}}(A)\, S_0)\ . \tag{6.8}$$

As this is a local condition in the configuration space $\{A\}$, it is possibile to have no copies in this setting, while staying in line with Singer's theorem. Note also that any pair of different class representatives $S_0$, $S_0'$ are such that $S_0' \neq US_0$ (for regular $U$) so that a gauge field $A_\mu$ cannot be in different regions. Then, as all the gauge fields belong to some region, the above procedure gives a partition of $\{A_\mu\}$: $\vartheta_\alpha \to \mathscr{V}(S_0)$. The labels correspond to oriented and nonoriented center vortices with nonabelian degrees of freedom (d.o.f.), where the nonoriented component is generated by monopoles (in 4d) or instantons (in 3d). Therefore, the YM field averages in Eq. (6.2) involve an ensemble integration over topological defects (sector labels) with a weight $Z_{(S_0)}/Z_{\rm YM}$ that is in principle calculable. Indeed, the all-orders perturbative renormalizability of the vortex-free sector was shown in Ref. [62]. The calculation of each sector, followed by the ensemble integration, is expected to give rise to the confining behavior in the nonperturbative regime. Of course, this program tends to be prohibitively hard in the continuum. Nonetheless, understanding some of their facets could shed light on how to organize an approximation scheme on each sector. For example, in the calculation of quadratic fluctuations around a straight thin center-vortex, different self-adjoint extensions are possible [139]. Which one to use should be determined from first principles and on physical grounds. This could also provide a guide to compute the different sectors in the lattice. The gauge-fixing method is based on many underlying assumptions. In this part of the thesis, we aim at discussing them at the classical level, paying special attention to sectors that include center vortices. The purpose is to improve the understanding of the consistency of this procedure.

## 6.1 Yang-Mills (global) gauge-fixings

In this section, we provide a brief discussion of some of the gauge-fixings commonly used along the history of continuum and lattice nonabelian gauge theories. These gauges are global, in the sense that a unique condition is imposed on the whole configuration space. This discussion will be useful to compare them with our local procedure and show, in the next section, how their problems and limitations could be avoided.

In the continuum, globally defined gauge-fixing conditions,

$$f(A) = 0 \quad , \quad A_\mu \in \{A_\mu\} \, , \tag{6.9}$$

were extensively studied. For example, the Landau gauge corresponds to $f(A) = \partial_\mu A_\mu$. Of course, due to Singer's (no-go) theorem [64], it is impossible to find a continuous condition on the whole configuration space $\{A_\mu\}$ such that $f(A^U) = 0 \Rightarrow U = \mathbb{I}$. Then, in this framework, to continue working with the traditional methods, which are based on a single global $f(A)$, the path-integral was restricted to a subset of $\{A_\mu\}$. This is known as the first Gribov region, where infinitesimal copies are eliminated, although it generally contains finite copies. This region can also be defined as the smallest connected set, containing the trivial configuration $A_\mu = 0$, such that the (gauge-dependent) Fadeev-Popov (FP) operator is positive definite [124]. In the infrared regime, it is believed that the YM path-integral in Landau gauge is dominated by the Gribov horizon [140, 141], which is formed by configurations such that the corresponding FP operator has zero modes. These operators were studied in the continuum and in the lattice for the Coulomb and Landau gauges [142, 143, 144]. For example, in the Landau gauge, where the FP operator is given by

$$M^{ab}_{\text{Landau}} = -\partial_\mu D^{ab}_\mu \delta^{(4)}(x - y) \, , \tag{6.10}$$

it was shown that smooth center vortices and instantons belong to the Gribov horizon [22, 145, 146].

In the lattice, center vortices and their properties have been extensively studied in the confining regime. In this case, although a gauge-fixing is not necessary to compute observables, it is relevant for the purpose of identifying the dominant configurations in the infrared regime. This was initially done within the Maximal Center Gauge (MCG) [15, 16, 20], which brings each link element as close as possible to a center element. Given an initial field configuration $U_\mu(x) \in SU(N)$ (link-variables), the gauge is defined by the following maximization over gauge transformations $g(x)$

$$\max_g \sum_{x,\mu} \left( \text{tr} \, \text{Ad}\big(U^g_\mu(x)\big) \right) \quad , \quad \text{Ad}\big(U^g_\mu(x)\big) = R^{\text{T}}(x) \, \text{Ad}\big(U_\mu(x)\big) R(x + \mu) \, , \tag{6.11}$$

where $R = \text{Ad}\big(g\big)$ ($\text{Ad}(\cdot)$ denotes the adjoint representation of $SU(N)$)). In Ref. [20], this gauge was extended to the continuum by means of the requirement

$$\min_\Sigma \min_g \int d^D x \, \left( \text{tr} \, (A^g - a_\Sigma)^2 \right) \, , \tag{6.12}$$

where $a_\Sigma$ is the gauge field for a thin vortex localized on $\partial\Sigma$, a closed surface. For local extrema, a condition can be obtained by first considering the minimization with respect

to $G = e^{i\theta}$, with infinitesimal $\theta$, and fixed $\Sigma$:

$$[\partial_\mu + a^\Sigma_\mu, A_\mu] - \partial_\mu a^\Sigma_\mu = 0 \; . \tag{6.13}$$

If this step were free from Gribov copies, we would have a unique gauge field $A_\Sigma$ that satisfies Eq. (6.13), and the continuum Maximal Center Gauge would be completed by determining the best $\Sigma$:

$$\min_\Sigma \int d^D x \, \mathrm{tr}(A[a_\Sigma] - a_\Sigma)^2 \; . \tag{6.14}$$

On a conceptual level, this is an interesting procedure aimed at bringing $A_\mu$ as close as possible to a thin center vortex field $a_\Sigma|_\mu$. However, as pointed out in Ref. [20], this route would require further improvements. This is due to the large mismatch between a smooth $A_\mu$ and a thin center-vortex field $a_\Sigma|_\mu$ at points that are close to any $\partial\Sigma$, where the difference $A - a_\Sigma$ is divergent. Thus, the condition (6.12) is always achieved for $a_\Sigma = 0$, for vortex-like smooth configurations $A_\mu$. Among the possibilities to avoid this problem, a smoothed $a_\Sigma$ or the replacement $\mathrm{tr}(\cdot) \to s(\mathrm{tr}(\cdot))$ in Eq. (6.12), with $s(t)$ a monotonically increasing function, was considered in Ref. [20]. An issue pointed in that work is that, to avoid the divergence at $\partial\Sigma$, $s(t)$ cannot diverge as $t \to \infty$. However, this property would not penalize large deviations between $A_\mu$ and $a_\Sigma|_\mu$ in other regions. In addition, for certain functions like $s(t) = -\tanh(R^4 t^2)$, it was noted that the optimal $\partial\Sigma$ does not coincide with the guiding-center of a smooth center-vortex $A_\mu$, even for the simplest example.

Another important class of gauges in the lattice consider a set of eigenvectors $\phi^{(j)}$ corresponding to the lowest eigenvalues of the discretized covariant adjoint Laplacian,

$$\Delta^{ab}_{xy}(U)\phi^{(j)}_b(y) = \mu_j \phi^{(j)}_a(x) \; . \tag{6.15}$$

The gauge can then be fixed by imposing different conditions on the "lowest" eigenfunctions, i.e., the ones associated with the lowest eigenvalues. For instance, in the Laplacian Center Gauge (LCG) [17], the gauge is achieved by the composition of a pair of $SU(N)$ gauge transformations on the link variables. The first one is such that the lowest eigenfunction $\phi^{(1)}$ is oriented along the Cartan subalgebra. Then, a transformation is performed to make the color components of the second lowest eigenfunction $\phi^{(2)}$ satisfy some conventional conditions, while keeping $\phi^{(1)}$ fixed. The possibility of replacing the pair of Laplacian eigenfunctions by other adjoint fields in the continuum was first pointed out in Ref. [147], although a specific realization for these fields was not presented. In addition, the use of the above mentioned global gauge-fixing condition on these fields would lead to singular gauge-fixed fields, due to the large topological phases associated with center vortices. In the lattice, we would also like to mention the Direct Laplacian Center Gauge (DLCG), introduced in Ref. [18] to address the above mentioned mismatch

between smooth and thin configurations in the MCG. For $SU(2)$, instead of using the function $s(t)$, the smoothing of the MCG was done by promoting $R(x) \in SO(3)$ to a new degree of freedom $M(x)$, given by a $3\times 3$ real matrix, and then performing the constrained maximization

$$\max_M \sum_{x,\mu} \mathrm{tr}\, \big(M^{\mathrm{T}}(x)\, \mathrm{Ad}\big(U_\mu(x)\big) M(x+\mu)\big) \quad , \quad \frac{1}{\mathcal{V}} \sum_x M^{\mathrm{T}}(x) M(x) = I_{3\times 3}\ , \tag{6.16}$$

with $\mathcal{V}$ the lattice volume. Then, it was shown that the solution can be written in terms of the three lowest eigenfunctions of Eq. (6.15), $M_{ab}(x) = \phi_b^{(a)}(x)$. In the next step, an $SO(3)$-field was extracted from $M(x)$ through a polar decomposition. This field was then mapped to $SU(2)$ and the link-variables were gauge transformed to satisfy the adjoint version of the lattice Laplacian Landau Gauge (LLG) introduced in Ref. [148]. Finally, the DLCG was achieved by relaxing these link-variables to the closest configuration that satisfies the MCG. In Ref. [18], it was argued that the DLCG is preferable to the LLG since it avoids the presence of small scale fluctuations in the P-vortex surfaces of projected configurations.

## 6.2 The local gauge-fixing in continuum YM theory

In the lattice, the use of global gauge-fixing conditions, in the various center gauges discussed in Sec. 6.1, is always possible because there is no concept of singular ill-defined phase field $S(x)$, when $x$ represents the discrete lattice sites. On the other hand, in the continuum, any attempt of defining a global condition, in a procedure that detects nonabelian large topological phases $S(x)$, $x \in \mathbb{R}^4$, would lead to singular gauge-fixed fields. For example, this occurs in the global gauge of Ref. [149]. In that case, among the natural large phases there are those corresponding to monopoles. Then, a gauge-fixing based on a global orientation of the auxiliary fields, where $S(x)$ is removed, leads to gauge fields $A_\mu$ containing singularities (Dirac strings). A similar situation would occur in gauge fixings in the continuum based on a set of adjoint auxiliary fields $\psi_I \in \mathfrak{su}(N)$, $I = 1, \ldots, N_{\mathrm{f}}$. This time, the topological phases $S(x) \in SU(N)$ will certainly include center-vortex defects. In addition, monopole-like phases will generally be attached to a pair of (physical) center-vortex defects.[2] Again, there will be an obstruction to implement a global $\psi_I$ orientation, for every $A_\mu \in \{A_\mu\}$. By enforcing such a condition, ill-defined gauge fixed fields $A_\mu^{\mathrm{gf}}$ would be produced. On the other hand, in the continuum, it is precisely the clear distinction between regular and singular $SU(N)$-mappings that enables

[2] These configurations are known as nonoriented center vortices (see Ref. [20]).

the introduction of the equivalence relation

$$S(x) \sim S'(x) \qquad \text{if } \exists \text{ regular } U(x) \ / \qquad S'(x) = U(x)S(x) \ , \tag{6.17}$$

Such distinction and equivalence relation have no meaning for fields defined on the lattice. In the continuum, it enables us to think of generating, a priori, a catalog of different equivalence classes $[S_0]$, where $S_0(x)$ is a class representative. For example, in gauges based on adjoint auxiliary fields, a possible reference would be $S_0 = e^{i\chi\beta\cdot T}$, where $\chi$ is a multivalued harmonic function and $\beta$ is a fundamental magnetic weight, such that $S_0$ changes by a center element when going around a closed surface $\partial\Sigma$. Of course, there is also a center-vortex free sector that can be labeled by $S_0 \equiv I$. Other phases represent center-vortices that are nonoriented in the Lie algebra (see Refs. [20, 56]). Here, we will not discuss the general classification of sectors. Instead, we shall analyze some examples. However, it is important to underline that, as noted in Ref. [56], multiplying a label $S_0$ by a regular mapping on the right generally leads to a physically inequivalent label. The identification of these nonabelian degrees of freedom is an important property in the continuum which has no clear counterpart in the lattice. Using a mechanism that maps $A_\mu$ to $S$ in a gauge covariant way, we can look for the previously defined reference label $S_0$ that is equivalent to $S$. Then, instead of a global condition on $\{A_\mu\}$, we can require the gauge-fixed $A_\mu^{\text{gf}}$ to be mapped into $S_0$, which is attained by a regular gauge transformation.

The simplest known example where local gauge-fixings are used is in the context of the Abelian Higgs Model [150]. In the unitary gauge, the phase of the Higgs field is required to be trivial. However, this condition cannot be applied to the Nielsen-Olesen vortex. For a straight infinite vortex, the best we can do is to fix the gauge field as $\phi = h\, e^{i\varphi}$, where $\varphi$ is the polar angle ($\partial^2\varphi = 0$). This is one of the motivations that led to the gauge-fixing proposal for pure YM theories in Ref. [61]. There, the construction of $S$ was done by introducing a set of adjoint auxiliary fields that minimize an auxiliary action

$$S_{\text{aux}} = \int d^4x \left(\langle D_\mu\psi_I, D_\mu\psi_I\rangle + V_{\text{aux}}\right) \qquad , \qquad D_\mu\psi = \partial_\mu\psi_I - i\left[A_\mu, \psi_I\right] . \tag{6.18}$$

The consideration of $\psi(A) = (\psi_1, \ldots, \psi_{N_{\text{f}}})$, solution to this minimization problem (cf. Eq. (6.4)), has the advantage that, unlike the lowest eigenfunctions of the covariant Laplacian, it is a a well-posed problem in the continuum. Of course, at the quantum level, these fields were introduced by means of an identity, keeping the pure Yang-Mills dynamics unchanged. Regarding the field content and auxiliary potential, they were chosen such that the components $\psi_I$ of the classical solution $\psi(A)$ enable a simple concept of "modulus" tuple and the extraction of a phase. For this aim, $S_{\text{aux}}$ was proposed to display $SU(N) \to Z(N)$ SSB, which requires $N_{\text{f}} \geq N$ (see also Sec. 6.3). Among the

many possible flavors of auxiliary fields, the choice $N_{\rm f} = N^2 - 1$ was preferred, as a simple auxiliary action and procedure to extract the phase $S$ can be given for general $SU(N)$. Then, $V_{\rm aux}$ can be chosen such that it is minimized by the nontrivial solutions to

$$-i[\psi_I, \psi_J] = v\, f_{IJK}\, \psi_K \ , \tag{6.19}$$

namely, $\psi_I = vST_IS^{-1}$, where $T_I$, $I = 1, \ldots, N^2 - 1$ is the usual Lie basis. In regions where $A_\mu$ is close to a pure gauge, the solution will be close to a rotated frame. This "dynamical tendency" can be thought of as playing a similar role to the normalization and orthogonality property of the Laplacian eigenvector fields in the DLCG (cf. Eq. (6.16)). The polar decomposition of a tuple $\psi$ (cf. Eqs. (6.6) and (6.7)) was done by defining a modulus tuple $q$ as the rotated $\psi$ that minimizes the average square distance

$$\sum_I \langle q_I - vT_I \rangle^2 \ . \tag{6.20}$$

This implies that $q_I$ is "aligned" with the Lie basis $T_I$ on average,

$$\sum_I [q_I, T_I] = 0 \ . \tag{6.21}$$

Then, this procedure allows for the construction of $S(A)$ (the phase of $\psi(A)$) and the identification of the sector $\mathscr{V}(S_0)$ where $A_\mu$ is. Finally, the gauge can be fixed by the sector-dependent condition

$$f_{S_0}(\psi) = [S_0^{-1}\psi_I(A)S_0, T_I] = 0 \ , \tag{6.22}$$

see Eq. (6.8). This procedure, proposed in Ref. [61], has many points of contact with Laplacian center gauges used in the lattice. As discussed in Sec. 6.1, the possibility of using adjoint fields other than the Laplacian eigenfunctions in the continuum was first pointed out in Ref. [147]. In our procedure we gave a realization of the auxiliary fields through a set of classical equations of motion while, instead of a pair, we considered various adjoint flavors. This field content simplified the extraction of a covariant phase out of $\psi$. Indeed, our concept of polar decomposition generalizes to $SU(N)$ the usual decomposition of the $3 \times 3$ real matrix, formed with the three lowest eigenvectors, used in the lattice adjoint LLG in $SU(2)$. In addition, as already explained, by considering local gauge-fixing conditions on $\mathscr{V}(S_0) \subset \{A_\mu\}$ , we were able to avoid singular gauge-fixed fields.

On the other hand, for oriented center vortices, our procedure differes from the continuum global MCG, as it is not based on comparing $A_\mu$ with the singular configurations $a_\Sigma$. The closed manifold $\partial\Sigma$ is not obtained after a best fit to $a|_\Sigma$, but by reading the

defects in $S(A)$. It is also very different from the traditional global gauge-fixings. For instance, in the Landau gauge, the Gribov copies associated with smooth center vortex or instanton configurations (cf. Eq. (6.10)) are related with zero mode solutions to a Schrödinger-like equation. It should be emphasized that the FP operator for this type of global gauges is completely different from the FP operator $J_{S_0}$ in any local sector $\mathscr{V}(S_0)$, which is related with the algebraic condition in Eq. (6.22). Therefore, there is no a priori reason to expect $J_{S_0}$ to contain zero modes. In order to address the possibility of copies, the analysis must be completely reformulated. Instead of considering a general $A_\mu \in \{A_\mu\}$, it should be separately done for $A_\mu \in \mathscr{V}(S_0)$, for every possible label $S_0$. As an initial step, to see if we are on a good direction, we will address some examples based on the simplest smooth center vortices. In particular, in Sec. 6.4, we will show that the associated guiding-centers are correctly detected in the nonabelian mapping $S(A)$, that the gauge-fixed field is regular, and that no copies will arise in this case.

## 6.3 Investigating the new procedure

In the local procedure, if the solution to Eq. (6.4) is unique (after imposing regularity and boundary conditions), in a first step we may associate each field in $\{A_\mu\}$ with the auxiliary tuple $\psi(A)$ that minimizes the auxiliary action $S_{\text{aux}}[A, \psi]$. For this mapping to be useful to fix the gauge, a necessary condition is that different gauge fields of the same orbit are associated with different $\psi(A)$. If $\psi(A)$ is left invariant by nontrivial transformations $\psi_I(A) \to U\psi_I(A)U^{-1}$, $U \in SU(N)$, then no matter what the second step is, the final prcedure will have gauge copies. If this is successful, in a second step, given a tuple $\psi(A)$, we would like to fix the gauge by imposing a condition that is satisfied by only one $\psi(A)$ as we move on the orbit of $A_\mu$. Again, because of Singer's theorem, it is impossible to find a global and continuous gauge-fixing condition. However, the idea is to implement a different gauge-fixing condition on each sector of a partition of $\{A_\mu\}$. In summary, for the gauge fixing to be well-defined, we need:

1. Appropriate regularity and boundary conditions on the auxiliary fields so as to have a unique solution $\psi(A)$ to Eq. (6.4).

2. The auxilary-field content and the auxiliary action must be such that $\psi(A)$ is injective on any gauge orbit. This means,

$$\psi(A^U) = \psi(A) \Rightarrow U \in Z(N) \,, \tag{6.23}$$

   where $Z(N)$ is the center group of $SU(N)$. This is just the requirement that the fields transform homogeneously under the gauge group in a LCG formulated in the continuum [147].

3. A univocally defined polar decomposition of $\psi(A)$. In this case, besides inducing the partition $\mathscr{V}(S_0)$, a local condition on $\mathscr{V}(S_0)$ with no copies,

$$f_{S_0}(\psi(A)) = 0 \quad \text{and} \quad f_{S_0}(\psi(A^U)) = 0 \Rightarrow U = \mathbb{I} \,, \tag{6.24}$$

would be implemented in terms of the "pure modulus" concept discussed in Eqs. (6.7), (6.8) whose solution[3] is given by $\psi = q^{S_0}$ .

If these requirements are fulfilled, we would have an $S_0$-dependent gauge-fixing condition, without copies on each local sector $\mathscr{V}(S_0)$ of the partition of $\{A_\mu\}$. As in other gauge-fixing procedures, the main idea is not to arrive at a closed expression for the gauge-fixed field $A_\mu^{\text{g.f.}}$. This could only be done for some specific cases. In fact, the objective is to properly quantize YM theory. Here, we shall briefly comment about the above requirements, relating them with the quantization procedure introduced in Ref. [61]. A detailed analysis will be developed in the next sections.

Regarding item 1, the natural regularity condition is to consider continuous single-valued auxiliary fields. In addition, as the gauge fields $A_\mu$ with finite YM action are asymptotically pure gauge, the natural boundary condition is that $\psi$ is covariantly constant at infinity,

$$D_\mu \psi \to 0 \quad \text{when} \quad |x| \to \infty \,. \tag{6.25}$$

This is consistent with the equations of motion if $\psi(x) \to \bar{\psi}(x) \in \mathcal{M}$ in this limit, where $\mathcal{M}$ is the vacua manifold of $S_{\text{aux}}$. In Ref. [61], starting from the pure YM partition function,

$$Z_{\text{YM}} = \int [DA_\mu]\, e^{-S_{\text{YM}}[A]} \,, \tag{6.26}$$

or the YM correlations, we introduced auxiliary fields satisfying Eq. (6.4) by means of an identity

$$1 = \int [D\psi] \det \left( \frac{\delta^2 S_{\text{aux}}}{\delta\psi_I \delta\psi_J} \right) \delta \left( \frac{\delta S_{\text{aux}}}{\delta\psi_I} \right) \,, \tag{6.27}$$

in the integrand of the $A_\mu$ path-integration. Given $A_\mu$, to correctly implement this identity, the argument of the $\delta$-functional must have a unique zero, and the quadratic operator in the determinant must be positive definite. This is nothing but the uniqueness requirement, which is met by the regularity and boundary conditions discussed above. In addition, the positivity of the quadratic form is related to solutions $\psi(A)$ with minimum auxiliary action.

[3] In general, a relation between tuples of the form given in Eq. (6.6) shall be simply denoted by $\psi = q^S$.

Now, the manifold $\mathcal{M}$ must be nontrivial, that is, $S_{\text{aux}}$ must be constructed with an appropriate spontaneous symmetry breaking (SSB) pattern. If not, $\psi(A)$ could easily take values close to zero in a spacetime region, and the condition (6.23) in item 2 would be violated. In other words, we need $\psi(A)$ to be nontrivial almost everywhere to be able to extract information from it. Indeed, injectivity will be favored if points $\bar{\psi}$ in $\mathcal{M}$ satisfy (6.23), which corresponds to require an auxiliary action with an $SU(N) \to Z(N)$ Spontaneous Symmetry Breaking (SSB) pattern. For this to happen, a minimum value of $N_{\text{f}} = N$ flavors is needed (see Sec. 6.3). In this case, $\mathcal{M} = SU(N)/Z(N) = \text{Ad}(SU(N))$, where $\text{Ad}(\cdot)$ stands for the adjoint representation, and $SU(N)$ acts transitively on this manifold. Then, for a univocally defined polar decomposition (item 3), the asymptotic boundary condition would be

$$\psi(x) \to \bar{\psi}(x) = u^{\bar{S}} \quad \text{when} \quad |x| \to \infty \,, \tag{6.28}$$

where $u$ is the pure modulus tuple in $\mathcal{M}$ and $\bar{S} = \bar{S}(x)$ is only defined at infinity by

$$A_\mu \to \bar{S}\partial_\mu \bar{S}^{-1} \quad \text{when} \quad |x| \to \infty \,. \tag{6.29}$$

Next, to represent the YM quantities in terms of a partition in the local sectors $\mathscr{V}(S_0)$, we introduced a second identity in the integrand of Eq. (6.27)

$$1 = \sum_{S_0} 1_{S_0} \quad , \quad 1_{S_0} = \int [DU]\, \delta(f_S(\psi)) \det(J(\psi)) \quad , \quad S = US_0 \,, \tag{6.30}$$

where $J(q)$ is the Fadeev-Popov operator associated to the condition (6.24). According to item 3, the characteristic function $1_{S_0}$ is nontrivial on fields of the form $\psi = q^S$, $f(q) = 0$. As $\psi$ is single-valued, when we get close to the defects of $S_0$, the fields accompanying Lie algebra components rotated by $S_0$ must tend to zero. When restricted to $\mathscr{V}(S_0)$, in order for the left-hand side of $1_{S_0}$ in Eq. (6.30) to be one, there should be a unique $U$ that solves $f_S(\psi) = 0$. This is expected to be addressed by the consideration of the $SU(N) \to Z(N)$ SSB pattern and a good definition of polar decomposition with a univocally defined phase (and modulus).

Let us analyze some possibilities for the auxiliary action $S_{\text{aux}}$ in Eq. (6.18), initially focusing on the $SU(2)$ case. As $\text{Ad}(SU(2)) = SO(3)$, the group action on an adjoint scalar field can be pictured as an orthogonal rotation of a three-component vector. Then, noting that any vector is left invariant by an $SO(2)$ subgroup of rotations, we clearly see that it is not possible to produce $SU(2) \to Z(2)$ SSB with a single scalar field. The situation is different if we consider two adjoint scalar fields

$$S_{\text{aux}} = \int d^4x \left( \langle D_\mu \psi_1, D_\mu \psi_1 \rangle + \langle D_\mu \psi_2, D_\mu \psi_2 \rangle + V(\psi_1, \psi_2) \right) \,. \tag{6.31}$$

In this case, if the two vectors are linearly independent, it is clear that there will be no set of continuous transformations that leave them invariant. However, the potential must be chosen carefully. Asymptotically, the scalar fields should tend to $\mathcal{M}$. It is therefore important that we choose $V$ so as the field components of the tuples in $\mathcal{M}$ are linearly independent vectors. If we choose

$$V(\psi_1, \psi_2) = \lambda_1(\langle\psi_1, \psi_1\rangle - v^2)^2 + \lambda_2(\langle\psi_2, \psi_2\rangle - v^2)^2 \,, \tag{6.32}$$

pathological configurations satisfying $\psi_1 = \psi_2$, with $\langle\psi_1, \psi_1\rangle = v$, will belong to $\mathcal{M}$. They are left invariant by rotations with axis $\psi_1$. This can be fixed by adding the term $\langle\psi_1, \psi_2\rangle^2$ (see Ref. [151]). Then, $\mathcal{M}$ will consist of two orthogonal vectors which are only invariant by $Z(2) \subset SU(2)$ discrete transformations. Had we added $\langle[\psi_1, \psi_2], [\psi_1, \psi_2]\rangle$ instead, the pathology would persist. For general $SU(N)$, among the interesting possibilities is the color-flavor symmetric action containing $N^2 - 1$ $SU(N)$ adjoint scalar fields $\psi_A \in \mathfrak{su}(N)$, $A = 1, \ldots, N^2 - 1$, and auxiliary potential $V_{\text{aux}}$ given by $V_{\text{H}}$ in Eq. (4.24). This was adopted in Ref. [61]. Then, the tuple $\psi(A)$ would be obtained by solving the equations

$$D^2\psi_A = \mu^2\psi_A + \kappa f^{ABC}\psi_B \wedge \psi_C + \lambda\psi_B \wedge (\psi_A \wedge \psi_B) \,. \tag{6.33}$$

As argued in Ref. [83], this potential admits $SU(N) \to Z(N)$ SSB, and is thus a good auxiliary action candidate. Indeed, $V_{\text{aux}}$ is minimized by tuples which are rotated Lie basis, satisfying Eq. (6.19), with $v$ given by Eq. (4.25). It is important to underline that although $S_{\text{aux}}$ and $S_{\text{H}}$, given in Eq. (4.19), are similar from a mathematical point of view, the physical contexts are completely different. In Section 4.2, the action governs the infrared physics in an effective manner. There, the gauge field $\Lambda_\mu$ and the Higgs fields are emergent quantities, representing percolating center-vortices and monopoles, respectively. In the present chapter, $A_\mu$ is the fundamental gauge field that describes the strong interactions, while the auxiliary adjoint fields have no physical meaning. They just provide a means to fix the gauge.

## 6.4 Properties of the Yang-Mills sectors

In this section, we provide explicit examples of gauge field configurations belonging to nontrivial sectors labeled by center vortices. Then, we show that the procedure allows us to identify more general sectors labeled by nonabelian d.o.f.. These are not related to ambiguities, but are in fact physically inequivalent possibilities located at the same center-vortex guiding centers.

### 6.4.1 Some sectors labeled by a guiding center

Let us start with some general remarks about thick center-vortex configurations of the form

$$A_\mu = g a(x) \partial_\mu \chi \beta \cdot T \quad , \quad \beta \cdot T \equiv \beta|_q T_q \ , \tag{6.34}$$

where $\chi$ is a multivalued angle when we go around some closed surface $\Omega$ (guiding center), the elements $T_q$ $(q = 1, \ldots, N-1)$ are Cartan generators of $\mathfrak{su}(N)$, and $a(x)$ is a scalar profile that goes to 1 at infinity. In principle, this profile could be any smooth function. However, regularity conditions must be imposed on $a(x)$ to prevent singularities in $A_\mu$ and the associated $F_{\mu\nu}$. First of all, $a(x) = 0$ at $\Omega$, otherwise $A_\mu$ would not be well-defined there. Next, we evaluate

$$F_{\mu\nu} = (\partial_\mu a \partial_\nu \chi - \partial_\nu a \partial_\mu \chi) \beta \cdot T + a(x) \left[\partial_\mu, \partial_\nu\right] \chi \beta \cdot T \ . \tag{6.35}$$

We have $\left[\partial_\mu, \partial_\nu\right] \chi = 0$ everywhere except at $\Omega$, where $a(x) = 0$, so that we can disregard this term. When probing the behavior of $a(x)$ at points very close to $\Omega$, we can take $\chi = \varphi$, the angle of polar coordinates, with the $z - t$ plane taken as the tangent plane passing throught the nearest point $x_0 \in \Omega$. Consequently

$$\frac{1}{4}\langle F_{\mu\nu}, F^{\mu\nu} \rangle = \frac{1}{2} \beta \cdot \beta \left( \partial_\mu a \partial^\mu a \partial_\nu \chi \partial^\nu \chi - (\partial_\mu a \partial^\mu \chi)^2 \right) = \frac{1}{2\rho^2} \beta \cdot \beta \left( \partial_\mu a \partial^\mu a - (\hat{\varphi} \cdot \nabla a)^2 \right) \ . \tag{6.36}$$

If we expand $a(x) = a^{(1)}(\varphi, z, t)\rho + a^{(2)}(\varphi, z, t)\rho^2 + ...$, we must impose $a^{(1)}(\varphi, z, t) = 0$ or, otherwise, the action would be infinite due to the divergence of $\langle F_{\mu\nu}, F^{\mu\nu} \rangle$ near $x_0$. In other words, on very general grounds, both $a(x)$ as well as its derivative in the local $\rho$ direction should vanish at every point of $\Omega$. In particular, this excludes thin-vortex configurations, as they are associated to an infinite Yang-Mills action density. Thus, within our framework, typical calculations of the partial contribution $Z_{(S_0)}$ to the Yang-Mills ensemble will consist of path-integrals with regularity conditions at the center-vortex guiding-centers. This problem is similar to the computation of a Casimir energy, but with conditions imposed on surfaces with higher codimension $d = 2$. In ref. [152], the dynamical Casimir effect associated to a moving Dirichlet point was discussed for $d = 1, 2, 3$. The case $d \geq 2$ was found more subtle to deal with, as it is necessary to renormalize the coupling to obtain a finite effective action for the particle. Codimension $d = 2$ is particularly interesting as the coupling acquires dependence on an arbitrary mass scale $\mu$. In this case, it was found that the effective action contains a term proportional to $\dot{u}^2$, $u$ being an unitary tangent vector to the particle's trajectory. If we interpret the nontrivial trajectory of the particle as a curved vortex-like object, this term would be associated to stiffness. It would be interesting to generalize this calculation to gauge theories, This could allow to make contact with the observed properties of center vortices

in the lattice, which display stiffness and tension terms [49, 56, 153]. It is also worth noting that investigations regarding quantum corrections to the effective action of a thin center-vortex were carried out in Ref. [139]. In particular, the one-loop correction to the thin vortex energy was shown to vanish for integer fluxes, for a particular choice of self-adjoint extension of the operator accompanying the fluctuations. The physical determination we are proposing here is different, so that the partial contribution of a center-vortex sector should be reexamined.

### 6.4.2 Antisymmetric center vortices with charge $k$

If there is a regular transformation $U \in SU(N)$ such that

$$[S_0^{-1}U^{-1}\psi_A\, U S_0, u_A] = 0\ , \forall x\ , \tag{6.37}$$

where $u_A = vT_A$, then $A_\mu \in \mathcal{V}(S_0)$. To proceed, we can consider sectors labeled by $S_0 = e^{i\chi\beta\cdot T}$, where $\beta$ is a magnetic weight of the $k$-antisymmetric representation. By defnition, a pair of phases associated with different guiding centers $\Omega$ and $\Omega'$ belong to different sectors. Accordingly, the respective solutions $\psi_A$ and $\psi'_A$ will be different, as the regularity conditions to solve the equations of motion will occur at different locations. Now, let us analyze configurations with cylindrical symmetry

$$A_\mu = a(\rho)\partial_\mu\varphi\, \beta\cdot T\ . \tag{6.38}$$

The profile $a(\rho)$ satisfies the regularity and boundary conditions $a(\rho = 0) = 0$ and $a(\rho \to \infty) = 1$, respectively. The second condition implies that these are in fact thick center-vortices with $Z(N)$ charge $k$, as they contribute an elementary center element to the $k-$th power, for large enough Wilson Loops that link them. In particular, if we consider as $a(\rho)$ the profile computed in Section 4.3, we already know the auxiliary tuple $\psi(A)$, which is given by Eq. (4.31) and the profiles computed in that section. Although they have the same guiding-centers ($\rho = 0$), center vortices corresponding to different antisymmetric weights belong to different sectors. This is because the set of roots $\{\alpha_r\}$ that satisfy $\alpha\cdot\beta \neq 0$ changes with the $N$-ality $k$. To see this, consider, without loss of generality, that $k > k'$. Then, denoting $\beta = \beta^k$, $\beta' = \beta^{k'}$, we have

$$\beta\cdot\alpha_{k'p} = -1 \quad , \quad \beta'\cdot\alpha_{k'p} = 0 \quad , \quad \text{for } p \leq k\ , \tag{6.39}$$

$$\beta\cdot\alpha_{k'q} = 0 \quad , \quad \beta'\cdot\alpha_{k'q} = 1 \quad , \quad \text{for } q > k'\ . \tag{6.40}$$

On the one hand, this implies that the auxiliary field-profiles are different, as they satisfy different regularity conditions. Moreover, taking $U = \mathbb{I}$, we have

$$[{S'_0}^{-1}\psi_A S'_0, u_A] = 2iv \sum_\alpha h_\alpha \sin(\alpha \cdot (\beta - \beta')\,\varphi)\,\alpha|_q T_q \,. \tag{6.41}$$

When approaching $\rho = 0$, the regularity conditions yield

$$[{S'_0}^{-1}\psi_A S'_0, u_A] \approx -2iv \sum_{\alpha\cdot\beta=0} h_\alpha(0) \sin(\alpha \cdot \beta'\,\varphi)\,\alpha|_q T_q \,. \tag{6.42}$$

As we know that $h_\alpha(0) \neq 0$ for $\alpha\cdot\beta = 0$, and that there are roots satisfying (6.40), this can only be nullified for every $\varphi$ when $\beta = \beta'$. This implies that the gauge field characterized by $\beta$ belongs to $\mathcal{V}(S_0)$, with $S_0 = e^{i\varphi\beta\cdot T}$, and already satisfies the gauge condition. This also applies to more general profiles $a(\rho)$, not necessarily those obtained in Section 4.3, as the general auxiliary ansatz, with symmetric profiles $h_{AB}$ closes the equations of motion, and leads to

$$[{S_0}^{-1}\psi_A S_0, u_A] = v\, h_{AB}[T_B, T_A] = 0 \,. \tag{6.43}$$

Sectors characterized by different antisymmetric weights, represent physically inequivalent center-vortex configurations that have the same guiding-centers.

### 6.4.3 Nonabelian degrees of freedom

In nonabelian models with spontaneous symmetry breaking, vortices can have an internal orientational moduli [66, 67, 68]. In our case, although we are dealing with a pure gauge theory, a similar situation occurs when defining the different sectors. As discussed in Ref. [56], the multiplication of a general defect $S_0$ by a regular phase $\tilde{U}(x) \in SU(N)$ on the right could yield a physically inequivalent label. For $S_0 = e^{i\varphi\beta\cdot T}$, the new configuration is given by

$$A_\mu = a\, iS\partial_\mu S^{-1} = S\mathcal{A}_\mu S^{-1} + iS\partial_\mu S^{-1} \quad , \quad \mathcal{A}_\mu = (1-a) iS^{-1}\partial_\mu S \tag{6.44}$$

$$S = \tilde{U} e^{i\varphi\beta\cdot T}\tilde{U}^{-1} \,, \tag{6.45}$$

while the associated solution can be written in the form $\psi_A = S\bar{\psi}_A S^{-1}$, where $\tilde{U}$ and $\bar{\psi}_A$ are single-valued and regular. Using

$$S^{-1}\partial_\mu S = \tilde{U} e^{-i\varphi\beta\cdot T}\tilde{U}^{-1}\partial_\mu \tilde{U} e^{i\varphi\beta\cdot T}\tilde{U}^{-1} + i\partial_\mu\varphi \tilde{U}\beta\cdot T\tilde{U}^{-1} + \tilde{U}\partial_\mu\tilde{U}^{-1}, \tag{6.46}$$

$$S^{-1}(D_\mu(A)D^\mu(A)\psi_A)S \;=\; \Box\bar{\psi}_A + 2\mathcal{A}_\mu \wedge \partial_\mu\bar{\psi}_A + \partial_\mu\mathcal{A}_\mu \wedge \bar{\psi}_A + \mathcal{A}_\mu \wedge (\mathcal{A}_\mu \wedge \bar{\psi}_A) \;, \tag{6.47}$$

and the regularity conditions of $\bar{\psi}_A$ and $a(x)$ to expand $\bar{\psi}_A = \bar{\psi}_A^{(0)} + \bar{\psi}_A^{(1)}\rho + ...$, $a(x) = a^{(1)}\rho + a^{(2)}\rho^2 + ...$, we see that the term of order $\rho^{-2}$ in Eq. (6.47) is

$$\frac{\partial^2\bar{\psi}_A^{(0)}}{\partial\varphi^2} - 2\tilde{X} \wedge \frac{\partial\bar{\psi}_A^{(0)}}{\partial\varphi} + \tilde{X} \wedge (\tilde{X} \wedge \bar{\psi}_A^{(0)}) \quad , \quad \tilde{X} = \tilde{U}\beta \cdot T\tilde{U}^{-1} \;. \tag{6.48}$$

Since $\bar{\psi}_A$ is single-valued and regular, the zeroth order term $\bar{\psi}_A^{(0)}$ in the $\rho$-expansion cannot depend on $\varphi$. In addition, since the force $\frac{\delta S_{\rm aux}}{\delta\psi_A}$ has no term of order $\rho^{-2}$, at the guiding center it must be verified

$$\tilde{X} \wedge (\tilde{X} \wedge \bar{\psi}_A^{(0)}) = 0 \;. \tag{6.49}$$

Taking the scalar product with $\bar{\psi}_A^{(0)}$ and using the positivity of the metric, we get,

$$\tilde{X} \wedge \bar{\psi}_A^{(0)} = 0 \;, \tag{6.50}$$

which implies $\tilde{U}$-dependent regularity conditions on the components of $\bar{\psi}_A$ that do not commute with $\tilde{X}$. In this way, even when considering a $k = 1$ fundamental center-vortex with a given guiding-center, we showed that there are gauge field configurations that belong to a continuum of physically inequivalent sectors of the Yang-Mills theory. These are genuine nonabelian degrees of freedom that must be integrated in the YM ensemble.

## 6.5 Infinitesimal injectivity of $\psi(A)$

In this section we shall see that injectivity is related to the positivity of the operator introduced in the identity of Eq. (6.27), and to the absence of nontrivial gauge transformations that leave invariant the auxiliary fields. Then, we show that the functional is injective for typical configurations of the vortex-free sector. A particular example in the one-vortex sector is also provided.

### 6.5.1 Conditions for injectivity

The equations of motion originated from the auxiliary action $\Sigma = \delta S/\delta\psi$ is a functional of $\psi$ and $A_\mu$, $S = S(\psi, A_\mu)$, and it is invariant under an infinitesimal gauge transformation, i.e. $\delta\Sigma = \delta_A\Sigma + \delta_\psi\Sigma = 0$, with

$$\delta_A \equiv \int \delta A_\mu^a \frac{\delta}{\delta A_\mu^a} \quad , \quad \delta_\psi \equiv \int \delta\psi_I^a \frac{\delta}{\delta\psi_I^a} \;. \tag{6.51}$$

Thus, by acting with a variation $\delta_\psi$ on $S$, we should get the corresponding solution to another gauge field on the same orbit, $A^U_\mu$. Then, we should study if

$$\delta_A \frac{\delta S}{\delta \psi^a_I(x)} = -\delta_\psi \frac{\delta S}{\delta \psi^a_I(x)} = -\int dy \frac{\delta^2 S}{\delta \psi^a_I(x)\psi^b_J(y)} f^{bmn}\xi^m(y)\psi^n_J(y) = 0 \tag{6.52}$$

has nontrivial solutions. We may multiply this equation by $f^{am'n'}\xi^{m'}(x)\psi^{n'}_I(x)$ and integrate over $x$ to arrive at

$$\int dx\, dy\, \frac{\delta^2 S}{\delta \psi^a_I(x)\psi^b_J(y)} v^a_I(x)v^b_J(y) = 0\ , \quad , \quad v^a_I(x) = f^{amn}\xi^m(x)\psi^n_I(x) = (\xi(x)\wedge\psi_I(x))|_a\ . \tag{6.53}$$

Since $\psi^a_I$ is a minimum of $S$, all the eigenvalues of $\frac{\delta^2 S}{\delta\psi^a_I(x)\psi^b_J(y)}$ must be positive, as was already required for the identity in Eq. (6.27) to be well-defined. Therefore, nontrivial solutions for (6.53) are given by

$$v^a_I = \delta\psi^a_I = 0\ . \tag{6.54}$$

We see that the lack of injectivity is associated to the existence of nontrivial gauge transformations that leave $\psi_I$ invariant. By using the definitions $\Psi \equiv \psi^B_A$, $X \equiv \xi^A M^A$, $M^A|_{BC} \equiv if^{ABC}$, we can rewrite condition (6.54) for our choice of auxiliary action (Eq. (4.24)) as

$$\Psi X = 0\ . \tag{6.55}$$

For nontrivial gauge transformations, the solutions to Eq. (6.55) are related to the existence of zero-modes for $\Psi$. Therefore, we conclude that a lack of infinitesimal injectivity would be associated to configurations that satisfy $\det\Psi = 0$.

### 6.5.2 Vortex-free sector

For the vortex-free sector, in the limit of large $v$, we expect that $\Psi = v\mathbb{I} + \epsilon$, where $\epsilon$ is a small matrix. Defining $b(\epsilon) = \det(v\mathbb{I} + \epsilon)$, we must show that $b(\epsilon) \neq 0$ for small $\epsilon$. By expanding it, we may write

$$b(\epsilon) \approx b(0) + \frac{\partial g}{\partial \epsilon^a}\epsilon^a\ . \tag{6.56}$$

Since $b(0) = \det v\mathbb{I} = v^{N^2-1}$ is a finite (and large) value, we may conclude that the only solution to Eq. (6.55) in this regime is $X = 0$. Hence, on the vortex-free sector, injectivity is ensured.

### 6.5.3 Sectors with center-vortices

The argument of the vortex-free sector cannot be extended to sectors labeled by vortices, as $\Psi$ will necessarily be far from the identity near their guiding-centers. We may, however, consider a particular example for $SU(2)$. The simplest case is the sector labeled by an antisymmetric vortex with charge k=1.Then, as $\beta = \sqrt{2}$, we have $S_0 = e^{i\varphi\sqrt{2}T_1}$, where $\varphi$ is the angle of cylindrical coordinates. For $SU(2)$, the solution $\psi(A)$, when $A$ is a minimum of the action as well, is known to be [114]

$$\begin{aligned}
\psi_1 &= h_1(\rho)T_1 \ , \\
\psi_{\alpha_1} &= h(\rho)S_0 T_{\alpha_1} S_0^{-1} \ , \\
\psi_{\bar{\alpha_1}} &= h(\rho)S_0 T_{\bar{\alpha_1}} S_0^{-1} \ .
\end{aligned} \tag{6.57}$$

In this case, there is only one root $\alpha_1 = \frac{1}{\sqrt{2}}$, satisfying $\alpha_1 \cdot \beta = 1$, and the following relations hold

$$\begin{aligned}
S_0 T_{\alpha_1} S_0^{-1} &= \cos(\varphi)T_{\alpha_1} - \sin(\varphi)T_{\bar{\alpha_1}} \ , \\
S_0 T_{\bar{\alpha_1}} S_0^{-1} &= \cos(\varphi)T_{\alpha_1} + \sin(\varphi)T_{\bar{\alpha_1}} \ .
\end{aligned} \tag{6.58}$$

This implies the following $\Psi$ matrix:

$$\begin{pmatrix}
h_1(\rho) & 0 & 0 \\
0 & h(\rho)\cos(\varphi) & -h(\rho)\sin(\varphi) \\
0 & h(\rho)\cos(\varphi) & h(\rho)\sin(\varphi)
\end{pmatrix} \ . \tag{6.59}$$

Now, the condition (6.55) implies

$$\begin{pmatrix}
0 & h_1(\rho)\xi_3 & h_1(\rho)\xi_2 \\
-\xi_3 h(\rho)\cos(\varphi) - \xi_2 h(\rho)\sin(\varphi) & \xi_1 h(\rho)\sin(\varphi) & \xi_1 h(\rho)\cos(\varphi) \\
-\xi_3 h(\rho)\cos(\varphi) + \xi_2 h(\rho)\sin(\varphi) & -\xi_1 h(\rho)\sin(\varphi) & \xi_1 h(\rho)\cos(\varphi)
\end{pmatrix} = 0 \ . \tag{6.60}$$

For $\rho \neq 0$, this gives $\xi_1 = \xi_2 = \xi_3 = 0$. The only problematic region is the plane $\rho = 0$, which is a region of null measure in $R^4$. The gauge transformations that would leave $\Psi$ invariant, thus leading to the lack of injectivity, should be different from the identity only in this plane. Such transformations are not continuous, so they can be disregarded. The functional $\psi(A)$ is therefore infinitesimally injective in the one-vortex sector for this particular example.

## 6.6 A polar decomposition without infinitesimal copies

As discussed in Sec. 6.3, the injectivity of $\psi(A)$ does not guarantee that the gauge-fixing is free from copies. We still need to show that, for all sectors $S_0$,

$$f_{S_0}(\psi(A)) = f_{S_0}(\psi(A^U)) = 0 \rightarrow U = \mathbb{I} \, . \tag{6.61}$$

We shall see that this condition is related to the absence of zero modes of the operator introduced in the identity of Eq. (6.30). For instance, to analyze Eq. (6.61) in the vortex-free sector, we must show that if

$$(q_I \wedge T_I)|_\gamma = f^{aI\gamma} q_I^a = 0 \, , \tag{6.62}$$

then there is no gauge transformation with nontrivial parameters $\xi^a$, such that

$$f^{aI\gamma} f^{anm} q_I^n \xi^m = 0 \, . \tag{6.63}$$

Of course these are just necessary conditions that a problematic tuple should satisfy, as $q_I$ should also minimize the auxiliary action ((4.24)). These algebraic conditions (6.62),(6.63) can also be written by using the generators in the adjoint representation:

$$\mathrm{Ad}(T_A)|_{BC} \equiv M_A|_{BC} = i f^{ABC} \, , \tag{6.64}$$

and of the matrix

$$Q|_{Ia} = q_I^a \, . \tag{6.65}$$

Then, equations (6.62) and (6.63) become, respectively,

$$Tr(M_b Q) = 0 \, , \tag{6.66}$$

$$Tr(M_\gamma M_b Q)\, \xi^\gamma = 0 \, . \tag{6.67}$$

We may write these conditions as

$$J^{AB} \xi^B = 0 \quad , \quad J^{AB} \equiv Tr(M^A M^B Q) \, ,$$

and conclude that copies are associated with configurations having $\det J = 0$. In fact, in Ref. [61], the operator $J$ is introduced in the Yang-Mills partition function by means of the Fadeev-Popov procedure (see eq. (6.30)). It is therefore expected that copies are related to zeros of this determinant. Let us start by analyzing the above equations for

$SU(2)$. In this case, $f^{ABC} = \frac{\epsilon^{ABC}}{\sqrt{2}}$, and the matrices $M$ and $X$ thus read

$$M_1 = \begin{pmatrix} 0 & 0 & 0 \\ 0 & 0 & \frac{i}{\sqrt{2}} \\ 0 & -\frac{i}{\sqrt{2}} & 0 \end{pmatrix} \quad , \quad M_2 = \begin{pmatrix} 0 & 0 & -\frac{i}{\sqrt{2}} \\ 0 & 0 & 0 \\ \frac{i}{\sqrt{2}} & 0 & 0 \end{pmatrix} \quad , \quad M_3 = \begin{pmatrix} 0 & \frac{i}{\sqrt{2}} & 0 \\ -\frac{i}{\sqrt{2}} & 0 & 0 \\ 0 & 0 & 0 \end{pmatrix} , \tag{6.68}$$

$$X = \xi^A M^A = \begin{pmatrix} 0 & \frac{i}{\sqrt{2}}\xi_3 & -\frac{i}{\sqrt{2}}\xi_2 \\ -\frac{i}{\sqrt{2}}\xi_3 & 0 & \frac{i}{\sqrt{2}}\xi_1 \\ \frac{i}{\sqrt{2}}\xi_2 & -\frac{i}{\sqrt{2}}\xi_1 & 0 \end{pmatrix} . \tag{6.69}$$

The pure modulus condition (6.66) implies that $Q$ is a symmetric matrix, and thus can be parametrized as

$$Q = \begin{pmatrix} Q_{11} & Q_{12} & Q_{13} \\ Q_{12} & Q_{22} & Q_{23} \\ Q_{13} & Q_{23} & Q_{33} \end{pmatrix} . \tag{6.70}$$

The equation for copies (6.67) then reads

$$J^{ab}\xi^b = 0 \quad , \quad J = \begin{pmatrix} Q_{22}+Q_{33} & -Q_{12} & -Q_{13} \\ -Q_{12} & Q_{11}+Q_{33} & -Q_{23} \\ -Q_{13} & -Q_{23} & Q_{11}+Q_{22} \end{pmatrix} \quad , \quad \xi = \begin{pmatrix} \xi^1 \\ \xi^2 \\ \xi^3 \end{pmatrix} . \tag{6.71}$$

In order for the system (6.71) to have a nontrivial solution, the determinant of $C$ should be 0 (this is a necessary condition). This yields

$$\begin{aligned} \det J =& (Q_{22}+Q_{33})(Q_{11}+Q_{33})(Q_{11}+Q_{22}) - 2Q_{12}Q_{23}Q_{13} - Q_{12}^2(Q_{11}+Q_{22}) - Q_{23}^2(Q_{22}+Q_{33}) \\ & - Q_{13}^2(Q_{11}+Q_{33}) = 0 . \end{aligned} \tag{6.72}$$

### 6.6.1 Study of copies in the vortex-free sector

In the vortex-free sector, for the general group $SU(N)$, the gauge-fixed functional $q_I(A)$ satisfies

$$q_I(A) \wedge u_I = 0 , \tag{6.73}$$

$$q_I(A) \to vT_I \, , x \to \infty . \tag{6.74}$$

If there is a copy, then there exists a gauge transformation $U(x)$ such that

$$q_I^U(A) \wedge u_I = 0 \,, \tag{6.75}$$

$$U(x) \to \mathbb{I}, x \to \infty \,. \tag{6.76}$$

For infinitesimal transformations, equation (6.76) reads

$$f^{aI\gamma} f^{anm} q_I^n \xi^m = 0 \,. \tag{6.77}$$

In the vortex-free sector, the boundary condition of Eq. (6.74) will imply (on the limit of large v) that the fields Q are close to $v\,\mathbb{I}$ everywhere, i.e. $q_I^a = \delta_I^a + \epsilon_I^a$. Eq. (6.77) thus becomes

$$\xi^\gamma + f^{aI\gamma} f^{anm} \xi^n \epsilon_I^m = 0 \,, \tag{6.78}$$

$$\xi^m (\delta^{m\gamma} + f^{aI\gamma} f^{anm} \epsilon_I^n) = 0 \,. \tag{6.79}$$

This yields a system of $N^2 - 1$ linear equations in the variables $\xi^a$, with coefficients that will depend on $\epsilon_I^a$, i.e.

$$M(\epsilon)\xi = 0 \,, \tag{6.80}$$

where $M$ is the matrix of coefficients. For this system to have a nontrivial solution, a necessary condition is

$$k(\epsilon) \equiv \det M(\epsilon) = 0 \,. \tag{6.81}$$

Since $k(\epsilon)$ is polynomial on the infinitesimal parameters $\epsilon_I^a$, we may approximate:

$$k(\epsilon) \approx k(0) + \frac{\partial k(\epsilon)}{\partial \epsilon_I^a} \epsilon_I^a \,. \tag{6.82}$$

As $M(0)$ is simply the $(N^2-1) \times (N^2-1)$ identity matrix, we have $k(0) = 1$, a finite value. Therefore, , in the large $v$-limit, there are no Gribov copies for the dominant configurations in the vortex-free sector.

### 6.6.2 Study of copies in a general sector

In a general sector labeled by a defect $S_0$, the functional $\psi_I(A)$ satisfies

$$\frac{\delta S_{\text{aux}}}{\delta \psi_I} = 0 \,. \tag{6.83}$$

For a general $A$ in this sector, $\psi$ will be of the form $\psi_I = US_0 q_I S_0^{-1} U^{-1}$, with $U$ regular. The gauge-fixed $A_\mu$ will be associated to $\zeta_I \equiv S_0 q_I S_0^{-1}$, and should satisfy

$$\zeta_I(A) \wedge \eta_I = 0 \,, \tag{6.84}$$

$$\eta_I \equiv v S_0 T_I S_0^{-1} \,, \tag{6.85}$$

$$\zeta_I(A) \to v S_0 T_I S_0^{-1} \,, x \to \infty \,. \tag{6.86}$$

If there is a copy, then there exists a gauge transformation $U(x)$ such that

$$\zeta_I^U(A) \wedge \eta_I = (US_0 q_I S_0^{-1} U^{-1}) \wedge S_0 T_I S_0^{-1} = 0 \,, \tag{6.87}$$

$$U(x) \to \mathbb{I}, x \to \infty \,. \tag{6.88}$$

We may write condition (6.87) in terms of $q_I$:

$$(S_0^{-1} U S_0 q_I (S_0^{-1} U S_0)^{-1}) \wedge u_I = 0 \,. \tag{6.89}$$

In terms of the matrix $Q$ defined in the previous section, this is

$$R(S_0^{-1} U S_0) Q = Q' \,, \tag{6.90}$$

with $Q, Q'$ being pure modulus matrices. By defining $\tilde{U} \equiv S_0^{-1} U S_0$, we arrive at the conditions that problematic matrices $Q$ should satisfy:

$$R(\tilde{U}) Q = Q' \,, \tag{6.91}$$

$$\tilde{U}(x) \to \mathbb{I} \,, x \to \infty \,. \tag{6.92}$$

An important fact that follows from the definition of $\tilde{U}$ is that if $U$ is infinitesimal, so is $\tilde{U}$. This is so because $S_0 \in SU(N)$, so that it preserves the norm of the vector $\xi$. Specifically,

$$\begin{aligned} U &= \mathbb{I} + \xi^A T^A \to \tilde{U} = \mathbb{I} + (\xi')^A T^A \,, \\ \xi' &= R(S_0)\xi \,. \end{aligned} \tag{6.93}$$

The equation for infinitesimal copies is therefore the same in all sectors. However, in a general sector there is no reason to believe that $q_I$ will be close to $vT_I$ everywhere, since some of its components must go to zero at the guiding centers of the vortices. Gauge transformations with parameters that are non-zero only in these regions surrounding the guiding-centers of the vortices could, in principle, yield copies. However, as $v$ grows, these regions become increasingly small.

An example of configuration that could yield copies is when $A_\mu = a(\rho)\partial_\mu \varphi \beta \cdot T$. As

discussed in (6.57), for $SU(2)$, the solution for $\psi(A)$ is known. It is of the form

$$\psi_I = h_{IJ} S_0 T_I S_0^{-1} \ . \tag{6.94}$$

This implies

$$q_I = h_{IJ} T_J \ . \tag{6.95}$$

The associated $Q-$matrix is symmetric, as required by the gauge fixing. For this to admit infinitesimal copies, eq (6.72) should be satisfied at some finite region. The necessary condition for the existence of copies is (eq. (6.72))

$$2h(h_1 + h)^2 = 0 \ . \tag{6.96}$$

Since the profiles $h_1(\rho)$ and $h(\rho)$ are positive for all $\rho > 0$ (see Ref. [114]), it is easy to see that this condition is only satisfied at $\rho = 0$, which is a region in $R^4$ of null measure. The transformations that lead to copies are not continuous, as they should be nontrivial only in this plane. Then, they should not be considered as associated to gauge transformations. This configuration, therefore, does not admit Gribov copies.

# Chapter 7

# Discussion

Ensembles of percolating center-vortex worldlines and worldsurfaces have been detected in Monte Carlo simulations of $SU(N)$ Yang-Mills theory in 3D and 4D Euclidean spacetime. They are relevant degrees that at asymptotic distances provide a Wilson loop area law with $N$-ality. A complete picture must also relate this law to the formation of a confining flux tube between a quark and antiquark. Such an object, as well as the effect of its transverse quantum fluctuations, have also been observed. This calls for a field model that supports stable smooth topological objects, with the fields localized around a string in real space. Indeed, relying on different field contents and SSB patterns, many models have been explored in the literature. However, this was mainly done independently of the possible underlying ensembles detected in the simulations. In $(3+1)$D, due to Derrick's theorem, besides a vacua manifold for scalars ($\mathcal{M}$) with nontrivial first homotopy group, a gauge field is required to stabilize an infinite[1] stringlike soliton in $\mathbb{R}^3$-real space. In this regard, in a recent work [56], it was satisfying to see that a 4D ensemble of percolating center-vortex worldsurfaces with a sector of correlated monopole worldlines can be generated by a dual gauge field with frustration, and a set of adjoint Higgs fields with $\Pi_1(\mathcal{M}) = Z(N)$.

In this thesis, we analyzed a similar picture in (2+1)D. In 3D spacetime, center vortices generate worldlines, so they became described by (fundamental) scalars with frustration, rather than by a dual gauge field. In addition, a sector of correlated pointlike defects (instantons) led to a discrete set of vacua ($\Pi_0(\mathcal{M}) = Z(N)$). Accordingly, in $(2+1)$D, an infinite (or finite) stringlike soliton in $\mathbb{R}^2$-real space does not require a dynamical gauge field to be stabilized, while the vacua for the scalars must be disconnected.

Initially, we defined a 3D measure to compute averages of center elements that depend on the linking number between a Wilson loop and center-vortex worldlines. Modeling these defects with tension and stiffness, we were able to show that, at large distances, center-vortex loops are effectively described by fundamental Higgs fields. On the one hand, this is related to the fact that elementary center vortices carry fundamental weights,

[1] This can also be extended to a finite object in the presence of appropriate external quark-antiquark sources.

on the other, this type of field is originated when taking into account non-Abelian d.o.f. propagated on the worldlines. The possibility of $N$-line center-vortex matching is natural, as the different weights of the fundamental representation add up to zero. This was included by means of $N$ flavors, which can be arranged as an $N \times N$ complex matrix $\Phi$. All possible combinations of loops and correlated lines were generated by an effective theory with (local) $SU(N)$ magnetic color and (global) $SU(N)$ flavor symmetry. The $N$-line matching is responsible for breaking the local $U(N) = U(1) \times SU(N)$ symmetry, that would be present for loops, to $SU(N)$. If this model were restricted to Abelian-like configurations $\Phi = VI_N$, $V \in \mathbb{C}$, we would make contact with the 't Hooft model, where a $U(1)$ symmetry is spontaneously broken to $Z(N)$, due to presence of a term $V^N + \bar{V}^N$. However, there is no dynamical basis for such a restriction, and at this point our effective description possesses large quantum fluctuations. Next, we incorporated the effect of chains formed by different center-vortex lines interpolated by pointlike defects. For this aim, the variables used to represent chains were carefully written in terms of dual holonomies, in analogy with the ones describing loops and $N$ matched lines. The immersion of all chain combinations into the ensemble led to an additional effective vertex. In a percolating phase, where large center vortices are favored, a discrete set of vacua was then obtained $\Phi = ve^{i\frac{2\pi n}{N}} I_N \, , n = 1, 2, ..., N$, dynamically reducing the $SU(N)$ magnetic color symmetry to the required discrete $Z(N)$. This led to the formation of a stable domain wall sitting on the Wilson loop. Therefore, the center-element average not only displays an asymptotic area law with $N$-ality but it is due to a localized field configuration, which constitutes the interquark confining string. The potential also contains a subleading universal Lüscher term associated with the first corrections to the saddle point: the transverse string fluctuations. The asymptotic string tension for a general antisymmetric representation of $SU(N)$ was then derived by computing the domain wall for a large Wilson loop. The solution is given by a kink that interpolates a pair of different vacua. Furthermore, there is a region in parameter space where the wall is governed by the Cartan sector. In this region, we approximately closed an ansatz to solve the equations of motion and showed that the string tension satisfies the asymptotic Casimir law observed in Monte Carlo simulations of 3D $SU(N)$ Yang-Mills theory.

In 4D spacetime, we studied a dual YMH effective model with $N^2 - 1$ adjoint Higgs fields. In particular, we were able to develop an ansatz for a topologically stable static vortex carrying charge in the $k$-antisymmetric representation. The model has four parameters: the gauge coupling constant $g$, plus the quadratic ($\mu^2$), cubic ($\kappa$), and quartic ($\lambda$) couplings in the Higgs potential. We focused in the region $\mu^2 < \frac{2}{9}\frac{\kappa^2}{\lambda}$, where the $SU(N)_{\text{color}}$ is spontaneously broken to $Z(N)$ and the vacuum manifold is given by $\text{Ad}(SU(N)) = SU(N)/Z(N)$, thus implementing $N$-ality. By using the algebraic structure of the model, especially that concerning the weights and roots of $SU(N)$, we showed that a collective behavior takes place. For $k = 1$, the many adjoint scalar field equations

are closed in terms of the profiles $h$, $h_1$ and $h_2$, while for $k > 1$ only an additional profile $h_3$ is required. Since this is valid for every value of $N$ and $k$, it allows for a simple numerical simulation. Furthermore, when $\mu^2 = 0$, we found an exact Casimir law and nontrivial profiles coinciding with those of the Nielsen-Olesen vortex. This is compatible with the observed string tension and in agreement with the chromoelectric field distribution obtained in the lattice. Finally, upon an appropriate rescaling, the dependence of string tension ratios on the model parameters was reduced from four to two adimensional quantities: $\bar{\mu}^2$ and $\bar{\lambda}$. This made it easier to numerically explore the parameter space by using the relaxation method. We noticed that the scaling law depends in fact on the particular combination $\bar{\mu}^2\bar{\lambda}$ and that it is very stable throughout the parameter space. In particular, taking $N = 8$ as an example, we observed that it deviates by at most 4% from the exact Casimir law at $\bar{\mu}^2 = 0$. Our analysis encourages a thorough exploration of the interplay between ensembles observed in pure Yang-Mills lattice simulations, the associated large distance effective field description, the implied asymptotic properties, and their comparison with Monte Carlo calculations. Some of these connections were successfully verified in the model analyzed here.

In addition, we studied the stability of the Casimir law. As the distance between the quark and antiquark grows, to lower the total energy, the YMH model allows for the formation of dynamical adjoint monopoles localized around the sources (valence gluons). These objects cannot induce transitions that change the $N$-ality of the confining state, so that the asymptotic confining string will be the one with the lowest energy among those with the same $N$-ality. In this thesis, we were able to find a set of BPS equations which provide center string solutions for the 4D YMH effective model. In this manner, we obtained the energy of an infinite string solution to the BPS equations in a general representation of $SU(N)$. We showed that the energy corresponding to the $k$-A representation is the lowest among all the quark representations with $N$-ality $k$. In other words, for widely separated quark/antiquark sources, the stable state is indeed given by the $k$-A string.[2] This together with the fact that the $k$-A string tension was shown to be proportional to the quadratic Casimir, completes the proof that the effective YMH model reproduces an asymptotic Casimir Law.

Finally, we studied the consistency of a recently proposed procedure to fix the gauge on different sectors of the gauge-field configuration space $\{A_\mu\}$. Unlike the usual procedure, based on a unique gauge-fixing condition and a restriction to the first Gribov region (to avoid infinitesimal copies), the proposal is based on the consideration of different local conditions on the infinitely many sectors of a partition of $\{A_\mu\}$. These sectors are labelled by oriented and nonoriented center vortices, and the Yang-Mills path-integral measure includes a sum over partial contributions. This procedure is suited to detect the microscopic features of center vortices in the continuum, which in global gauge-fixing conditions, like

[2]Of course, for the trivial $N$-ality $k = N \pmod N$ this corresponds to the string breaking.

the Landau gauge, are effectively seen signaling the breaking of the perturbative regime at the Gribov horizon [146, 154]. Each partial contribution can be associated to a problem written in a form closer to the usual one. Here, along the way, we clarified the relevance of the regularity conditions to solve the auxiliary field equations and provide a physical determination of center-vortex sectors. In principle, this is different from considering a thin or thick center-vortex background plus quantum fluctuations. Instead, it is based on path integrating over gauge and auxiliary fields with given singular phases and regularity conditions. We provided explicit examples of thick center-vortex configurations belonging to nontrivial sectors. We also discussed the existence of nonabelian degrees of freedom, which are related to physically inequivalent labels with the same guiding centers. Finally, we showed the absence of Gribov copies for typical configurations of the vortex-free sector and for the simplest example in the sector labelled by a center vortex. This points to the idea that a possibility to deal with Singer's obstruction to a global gauge-fixing is to approach Yang-Mills theories as an ensemble of center-vortex degrees.

In a future work, it would be interesting to establish the absence of copies for more general configurations in oriented and nonoriented center-vortex sectors, and for more general values of the gauge-fixing parameters. This, together with the all-orders perturbative renormalizability of these sectors [62], [63], is an important step towards the establishment of the Yang-Mills ensemble in the continuum.

## 7.1 Final thoughts

In this thesis, we mainly studied field models that effectively describe ensembles formed by oriented and nonoriented center vortices in 3d and 4d Euclidean spacetime. These ensembles could capture the confinement properties of $SU(N)$ pure Yang–Mills theory. Different measures to compute center-element averages were discussed. In 3d and 4d, they include percolating oriented center-vortex worldlines and worldsurfaces that generate emergent Goldstone modes, which correspond to compact scalar and gauge fields, respectively. The models also have the natural matching rules of $N$ center vortices, as well as the nonoriented component where center-vortex worldlines (worldsurfaces) are attached to lower-dimensional defects, i.e., instantons (monopole worldlines) in 3d (4d). The effective field content and the SSB pattern of the corresponding models may lead to the formation of a confining center string, represented by a domain wall (vortex) in two-dimensional (three-dimensional) real space. The Lüscher term is originated as usual, from the string-like transverse fluctuations of the flux tube. An asymptotic Casimir law can also be accommodated. This asymptotic behavior was observed in 3d, while in 4d it is among the possibilities.

More recently, the transverse distribution of the 4d YM energy-momentum tensor $T_{\mu\nu}$ and the field profiles have been analyzed at intermediate and nearly asymptotic dis-

tances [9, 10, 11]. In [11], it was numerically shown that the $T_{\mu\nu}$ tensor of the Abelian Nielsen–Olesen (ANO) model cannot fit the $SU(3)$ data at the vortex guiding center for $L = 0.46$ fm (intermediate distance) and $L = 0.92$ fm (near asymptotic distance) at the same time. In fact, in [11], it was shown that the components of the energy-momentum tensor at the origin may not be accommodated for $L = 0.46$ fm. Then, on this basis, an ANO effective model to describe the fundamental string was discarded. However, while it is clear that an effective model for the confining flux tube should work at asymptotic distances, it is not that obvious that the same model could be extrapolated to intermediate distances. By intermediate distances we mean those where the string tension scales with the quadratic Casimir of the quark representation. In particular, this is the region where adjoint quarks are still confined by a linear potential, before the breaking of the adjoint string. On the other hand, in the asymptotic region, gluonic excitations around external quarks in a given irreducible representation $D(\cdot)$ may be created, so as to produce an asymptotic scaling law that only depends on the $N$-ality of $D(\cdot)$. As discussed in this thesis, the effective field descriptions were derived by considering the (weighted) average of center elements over oriented and nonoriented thin center vortices, which is expected to be applicable at asymptotic distances. In other words, we wonder if it is meaningful to discard possible effective models on the basis of the lack of adjustment to lattice data on a wide range that includes the intermediate region, where these models are not expected to fully capture the physics. Additionally, note that the known mechanism to explain intermediate Casimir scaling is based on including center-vortex thickness. In turn, these finite-size effects are not included in the ensemble definition that leads to our effective model. Interestingly, while the lattice data rule out the ANO model at intermediate distances $L = 0.46$ fm, such profiles are still among the possibilities at the nearly asymptotic distance $L = 0.92$ fm. Accordingly, the 4d $SU(N) \to Z(N)$ models we discussed in this review have a point in parameter space where the infinite flux tube profiles Abelianize, while keeping all the required $N$-ality properties. Additionally, the ideas presented in this thesis imply that not only an asymptotic Casimir law should be observed, but also that the transverse confining flux tube profiles for quarks in different representations should be the same, up to the asymptotic scaling law. This is true for both 3d and 4d, with the profiles being of the Sine-Gordon type in 3d. It would be interesting to test these predictions with lattice simulations.

# Appendix A

# Cartan decomposition of $\mathfrak{su}(N)$

Here, we summarize the main properties of the $\mathfrak{su}(N)$ Lie algebra, as well as the conventions used throughout the paper. For a more detailed discussion, see [94]. The construction of the Cartan-Weyl basis is initiated by defining a maximal commutative subspace, whose generators $T_q$ satisfy

$$[T_q, T_p] = 0 \ , \tag{A.1}$$

where $q, p = 1, \ldots, N-1$. The remaining basis elements are the so called root vectors $E_\alpha$, which diagonalize the adjoint action of $T_q$

$$[T_q, E_\alpha] = \alpha|_q E_\alpha \ . \tag{A.2}$$

The eigenvalues $\alpha|_q$ form an $(N-1)$-tuple $\alpha = (\alpha|_1, \alpha|_2, \ldots, \alpha|_{N-1})$ which is referred to as root. Since the dimensions of $\mathfrak{su}(N)$ and the Cartan subalgebra are, respectively, $N^2-1$ and $N-1$, there are $N(N-1)$ root vectors. A well known result is that if $\alpha$ is a root, so is $-\alpha$. Moreover, the associated root vectors are related by

$$E_{-\alpha} = E_\alpha^\dagger \ . \tag{A.3}$$

We are considering the Cartan-Weyl basis $\{T_q, E_\alpha\}$ as orthonormal with respect to the product

$$\langle A, B\rangle = \mathrm{Tr}\big(\mathrm{Ad}(A)\mathrm{Ad}(B)\big) \ , \tag{A.4}$$

where $\mathrm{Ad}(\cdot)$ stands for the adjoint representation. In this case, we have

$$[E_\alpha, E_{-\alpha}] = \sum_{q=1}^{N-1} \alpha_q T_q = \alpha \cdot T \ . \tag{A.5}$$

In order to completely specify the commutation relations of root vectors, we need to address two roots that do not sum up to zero. These relations turn out to be

$$[E_\alpha, E_{\alpha'}] = \mathcal{N}_{\alpha,\alpha'} E_{\alpha+\alpha'} \ , \tag{A.6}$$

where $\alpha' \neq -\alpha$ and $\mathcal{N}_{\alpha,\alpha'}$ vanishes when $\alpha + \alpha'$ is not a root. With the normalization adopted, one can show that

$$\mathcal{N}^2_{\alpha,\alpha'} = \frac{1}{2N} \tag{A.7}$$

whenever it does not vanish. These structure constant also have the property

$$\mathcal{N}_{\alpha',\alpha} = \mathcal{N}_{-\alpha,-\alpha'} = -\mathcal{N}_{\alpha,\alpha'} \ . \tag{A.8}$$

Moreover, if $\alpha, \alpha', \alpha''$ are roots that add up to zero, then

$$\mathcal{N}_{\alpha,\alpha'} = \mathcal{N}_{\alpha'',\alpha} = \mathcal{N}_{\alpha',\alpha''} \ . \tag{A.9}$$

The root vectors $E_\alpha$, which live in the complexified Lie algebra, can be replaced by the hermitian generators $T_\alpha$ and $T_{\bar{\alpha}}$ in Eq. (4.26). When using the latter as basis elements, one must consider only positive roots $\alpha > 0$ to avoid overcounting (for the notion of positiveness, see App. B). In this basis, the following commutation relations hold

$$[T_q, T_\alpha] = i\alpha|_q T_{\bar{\alpha}} \quad , \quad [T_q, T_{\bar{\alpha}}] = -i\alpha|_q T_\alpha \quad , \quad [T_\alpha, T_{\bar{\alpha}}] = i\alpha|_q T_q \ , \tag{A.10}$$

$$[T_\alpha, T_\beta] = \frac{i}{\sqrt{2}}\big(N_{\alpha,\beta} T_{\overline{\alpha+\beta}} + N_{\alpha,-\beta} T_{\overline{\alpha-\beta}}\big) \ , \tag{A.11}$$

$$[T_\alpha, T_{\bar{\beta}}] = -\frac{i}{\sqrt{2}}\big(N_{\alpha,\beta} T_{\alpha+\beta} - N_{\alpha,-\beta} T_{\alpha-\beta}\big) \ , \tag{A.12}$$

$$[T_{\bar{\alpha}}, T_{\bar{\beta}}] = -\frac{i}{\sqrt{2}}\big(N_{\alpha,\beta} T_{\overline{\alpha+\beta}} - N_{\alpha,-\beta} T_{\overline{\alpha-\beta}}\big) \ . \tag{A.13}$$

However, these relations remain true even for negative roots, recalling that the extended hermitian generators are not independent from their positive-root counterparts, and satisfy

$$T_{-\alpha} = T_\alpha \ , \ T_{-\bar{\alpha}} = -T_{\bar{\alpha}} \ . \tag{A.14}$$

# Appendix B

# Weights and representations of $\mathfrak{su}(N)$

A weight of an irreducible representation D of $\mathfrak{su}(N)$ is an $(N-1)$-tuple formed by the eigenvalues of a simultaneous eigenvector of $\mathrm{D}(T_q), q = 1, \ldots, N-1$. Each irreducible representation, or irrep. for short, has its own set of weights. That corresponding to the fundamental representation has $N$ elements $\omega_1, \omega_2, \ldots, \omega_N$ constrained by

$$\omega_1 + \omega_2 + \cdots + \omega_N = 0 \, . \tag{B.1}$$

The weights of the adjoint representation are the roots, as they are eigenvalues for the adjoint action $[T_q, \cdot]$. They can be expressed as the differences

$$\alpha = \omega_i - \omega_j \, , \tag{B.2}$$

for some $i, j = 1, \ldots, N$, which is consistent with the previous counting of $N(N-1)$ roots. Some useful sums are

$$\sum_{i=1}^{N} \omega_i|_q \omega_i|_q = \frac{1}{2N}\delta_{qp} \quad , \quad \sum_{\alpha} \alpha|_q \alpha|_p = \delta_{qp} \, . \tag{B.3a}$$

A weight is said positive if its last nonvanishing component is positive. Consequently, a weight is greater than another if their difference is positive. In particular, given the set of weights of a given irrep., we can always determine the highest. For the fundamental representation, we choose the ordering convention

$$\omega_1 > \omega_2 > \cdots > \omega_N \, . \tag{B.4}$$

Then, a root $\alpha = \omega_i - \omega_j$ is positive if and only if $i < j$.

Among the irreps. with $N$-ality $k$, we have the $k$-Symmetric ($k$-S) and $k$-Antisymmetric ($k$-A), $k = 1, \ldots, N-1$. They are constructed from the totally symmetric and antisymmetric decomposition of $k$ tensor products of the fundamental representation. The

corresponding highest weights are given by[1]

$$\lambda^{k\text{-S}} = k\omega_1 \quad , \quad \lambda^{k\text{-A}} = \sum_{i=1}^{k} \omega_i \ . \tag{B.5}$$

It is important to emphasize that the highest weight of any irrep. can always be written as a nonnegative integer linear combination of the $k$-Antisymmetric weights, which are called fundamental weights (not to be confused with the weights of the fundamental representation). The coefficients are called Dynkin numbers and there is a one-to-one correspondence between irreps. and these combinations.

To end this quick review, the quadratic Casimir operator for a given representation D is

$$C_2(\mathrm{D}) = \sum_{A=1}^{N^2-1} \mathrm{D}(T_A)\mathrm{D}(T_A) \ . \tag{B.6}$$

This operator commutes with every element of $\mathfrak{su}(N)$ and thus it is proportional to the identity matrix. The proportionality constant is known as the quadratic Casimir. For our choice of normalization, the quadratic Casimir for the fundamental, adjoint, $k$-S and $k$-A representations are, respectively,

$$\frac{N^2-1}{2N^2} \quad , \quad 1 \quad , \quad \frac{k(N+k)(N-1)}{2N^2} \quad , \quad \frac{k(N-k)(N+1)}{2N^2} \ . \tag{B.7}$$

Finally, for any irrep. D, the quadratic Casimir can be expressed in the form

$$C_2(\mathrm{D}) = \lambda^D \cdot (\lambda^D + 2\delta)\mathbb{I}_{\mathcal{D}} \ , \tag{B.8}$$

where $\lambda^D$ is the highest weight and $\delta$ is the Weyl vector, given by half the sum of the positive roots.

[1]Notice that $\Lambda^{1\text{-S}} = \Lambda^{1\text{-A}} = \omega_1$.

# Appendix C

# Petrov-Diakonov representation of $W_{4q}$

We note that the integral

$$\int d\mu(g)d\mu(g_2)d\mu(g'')d\mu(g''')\,\langle g,\nu_1|\Gamma_1|g',\nu_1\rangle\langle g,\nu_2|\Gamma_2|g',\nu_2\rangle \\ \times\langle g'',\nu_{G'}|\Gamma_{G'}|g',\nu_{G'}\rangle\langle g'',\nu_3|\Gamma_3|g''',\nu_3\rangle\langle g'',\nu_4|\Gamma_4|g''',\nu_4\rangle\langle g,\nu_G|\Gamma_G|g''',\nu_G\rangle\ . \tag{C.1}$$

is nonzero and proportional to $W_{4q}$ if and only if $\nu_G=\nu_{G'}$, $\nu_3+\nu_4+\nu_G=\nu_1+\nu_2+\nu_G=0$. Here, we used the group coherent states [95, 88] $|g,\nu\rangle = g|\nu\rangle$, with $|\nu\rangle$ being weight vectors of the fundamental representation, and the formula (the normalization of the Haar measure is $\int d\mu(g)=1$)

$$\int d\mu(g) g_{aa'}g_{bb'}g_{cc'} = \frac{1}{3!}\epsilon_{abc}\epsilon_{a'b'c'} \quad , \quad g\in SU(3)\ . \tag{C.2}$$

Then, a possible choice to accompany the holonomies $\{\Gamma_1,\Gamma_3\}$, $\{\Gamma_2,\Gamma_4\}$, $\{\Gamma_G,\Gamma_{G'}\}$ in Eq. (C.1) is given by $\nu_1=\nu_3=\omega_1$, $\nu_2=\nu_3=\omega_2$), $\nu_G=\nu_{G'}=\omega_3$, respectively, where $\omega_1$, $\omega_2$, $\omega_3$ are the three (ordered) fundamental weights of $\mathfrak{su}(3)$. Next, for each factor in Eq. (C.1), we can use the Petrov-Diakonov (PD) representation [89]

$$\langle g_{\rm f},\nu|\Gamma_\gamma|g_{\rm i},\nu\rangle \propto \int [dg(s)]\; e^{i\int ds\,{\rm Tr}\left(\left(g^{-1}Ag+ig^{-1}\partial_s g\right)\nu\cdot T\right)} \quad , \quad A=\frac{dx_\mu}{ds}A_\mu\ , \tag{C.3}$$

where $\Gamma_\gamma$ is an holonomy, and the measure $[dg(s)]$ integrates over paths $g(s)$ defined on $\gamma$ (parametrized by $x(s)$), with initial and final conditions $g_{\rm i}$ and $g_{\rm f}$, respectively. In the exponent of the PD representation of $W_{4q}$ thus obtained, the six line integrals can be replaced by five integrals along the loops $\gamma_k^c$, $k=1,\ldots,5$, after extending $[dg(s)]\to[d\tilde{g}(s)]$, which also integrates over group elements defined on the dotted lines. Indeed, because of the weight distribution, the additional integrals along $\gamma_L$ and $\gamma_R$ are canceled

because of the property $\omega_1 + \omega_2 + \omega_3 = 0$. A further extension of the paths in the group to configurations $\tilde{U}(x)$ such that $\tilde{g}(s) = \tilde{U}(x(s))$, and the Stokes' theorem, finally lead to

$$W_{4q} \propto \int [D\tilde{U}] e^{\frac{i}{2}\int d^4x \mathrm{Tr}\left(\tilde{U}^{-1}\mathcal{Y}_{\mu\nu}\tilde{U}\, J_{\mu\nu}\right)} \quad , \quad \mathcal{Y}_{\mu\nu}(\tilde{U}, g) = \epsilon_{\mu\nu\rho\sigma} D_\rho(\tilde{L})(A_\sigma - \tilde{L}_\sigma) \; , \qquad \text{(C.4)}$$

where $\tilde{L}_\mu \equiv i\tilde{U}\partial_\mu \tilde{U}^{-1}$ and $J_{\mu\nu}$ is given by Eq. (5.58).

# Appendix D

# Non-Abelian diffusion

Center vortices in 3 dimensions and monopoles in 4 dimensions are propagated along worldlines in Euclidean spacetime. Then, the corresponding ensembles will naturally involve the building block $Q$ associated to a worldline with length $L$ that starts at $x_0$ with orientation $u_0$ and ends at $x$ with final orientation $u$. This is given by

$$Q(x,u,x_0,u_0,L) = \int [dx(s)]_{x_0,u_0}^{x,u}\, e^{-S(\gamma)}\, \mathrm{D}\big(\Gamma_\gamma[b_\mu]\big)\ , \tag{D.1}$$

$$\Gamma_\gamma[b_\mu] = P\{e^{i\int_\gamma dx_\mu b_\mu}\}\ , \tag{D.2}$$

where $S(\gamma)$ is a vortex effective action, and an interaction with a general non-Abelian gauge field $b_\mu$ was considered. We are interested in the specific form

$$S(\gamma) = \int_0^L ds\, \left(\frac{1}{2\kappa}\dot{u}_\mu\dot{u}_\mu + \mu\right) \quad , \quad u_\mu(s) = \frac{dx_\mu}{ds}\ , \tag{D.3}$$

which corresponds to tension $\mu$ and stiffness $1/\kappa$. These objects were extensively studied in [56, 81]. In what follows, we review the results obtained.

For the simplest center-vortex worldlines in 3d, D is the defining $SU(N)$ representation, while for monopole worldlines in 4d, D corresponds to the adjoint. To derive a diffusion equation for this object, the paths were discretized into $M$ segments of length $\Delta L = L/M$. In this case, the path ordering was obtained from

$$P\{e^{-\int_0^L ds H(x(s),u(s))}\} = e^{-H(x_M,u_M)\Delta L}\dots e^{-H(x_1,u_1)\Delta L}, \tag{D.4}$$

where $H(x,u) = -i\mathrm{D}(u_\mu b_\mu(x))$. The relation between the building block $Q_M$ associated to a discretized path containing $M$ segments of length $\Delta L$ and that associated with a path of length $L-\Delta L$ is given by:

$$Q_M(x,u,x_0,u_0,L) = \int d^n x' d^{n-1}u' e^{-\mu\Delta L}\psi(u-u')\times$$
$$e^{-\mu\Delta L}e^{-H(x,u)\Delta L}\delta(x-x'-u\Delta L)\, Q_{M-1}(x',x_0,u',u_0)\ , \tag{D.5}$$

with

$$\psi(u-u') = \mathcal{N} e^{-\frac{1}{2\kappa}\Delta L\left(\frac{u-u'}{\Delta L}\right)^2} \tag{D.6}$$

arising from the discretization of the stiffness term. It acts like an angular distribution in velocity space, which tends to bring $u'$ close to $u$. Expanding Eq.(D.5) to first order in $\Delta L$, and taking the limit $\Delta L \to 0$, the diffusion equation

$$\left(\partial_L - \frac{\kappa\sigma}{2}\hat{L}_u^2 + \mu + u_\mu(\partial_\mu - i\mathrm{D}(b_\mu)\right) Q(x,u,x_0,u_0,L) = 0\ , \tag{D.7}$$

was obtained, to be solved with the initial condition

$$Q(x,u,x_0,u_0,0) = \delta(x-x_0)\delta(u-u_0)I_{\mathscr{D}}\ . \tag{D.8}$$

$\mathscr{D}$ is the dimension of the quark representation D and $\hat{L}_u^2$ is the Laplacian on the sphere $S^{n-1}$. The constant $\sigma$ is given, in $n$ spacetime dimensions, by

$$\sigma = \frac{\sqrt{\pi}}{2^{n-3}}\frac{\Gamma\left(\frac{n-2}{2}\right)\Gamma\left(\frac{n+1}{2}\right)}{\Gamma^2\left(\frac{n-1}{2}\right)\Gamma\left(\frac{n-3}{2}\right)}\left(\frac{4\Gamma(n-3)}{\Gamma\left(\frac{n-3}{2}\right)} - \frac{\Gamma(n-1)}{\Gamma\left(\frac{n+1}{2}\right)}\right)\ . \tag{D.9}$$

For the cases considered in this thesis ($n = 3, 4$), $\sigma = 1, 2/\pi$, respectively. In the limit of small stiffness, there is practically no correlation between $u$ and $u_0$, which allowed for a consistent solution of these equations with only the lowest angular momenta components:

$$Q(x,u,x_0,u_0,L) \approx Q_0(x,x_0,L) \quad , \quad \partial_L Q_0(x,x_0,L) = -OQ_0(x,x_0,L)\ , \tag{D.10}$$
$$O = -\frac{2}{(n-1)\sigma\kappa n}(\partial_\mu - iD(b_\mu))^2 + \mu \quad , \quad Q_0(x,x_0,0) = \frac{1}{\Omega_{n-1}}\delta(x-x_0)\ , \tag{D.11}$$

$\Omega_{n-1}$ being the solid angle of $S^{n-1}$. This implies,

$$Q(x,u,x_0,u_0,L) \approx \langle x|e^{-L\mathcal{O}}|x_0\rangle\ . \tag{D.12}$$

Then, in this limit, we also have

$$\int_0^\infty dL\, du\, du_0 \int [Dx]_{x_0,u_0}^{x,u}\, e^{-S(\gamma)}\,\mathrm{D}(\Gamma[b]) = \int_0^\infty dL\, du\, du_0\, Q(x,u,x_0,u_0,L)$$
$$\approx \langle x|O^{-1}|x_0\rangle \quad , \quad O\,G(x,x_0) = \delta(x-x_0)\, I_{\mathscr{D}}\ . \tag{D.13}$$

# Bibliography


[1] K. G. Wilson, *Confinement of quarks*, Phys. Rev. D **10** (1974) 2445.

[2] G. S. Bali, *QCD forces and heavy quark bound states*, Phys. Rep. **343** (2001) 1.

[3] G. 't 'Hooft, *On the phase transition towards permanent quark confinement*, Nucl. Phys. B **138** (1978) 1.

[4] F. M. Stokes, W. Kamleh and D. B. Leinweber, *Visualizations of coherent center domains in local Polyakov loops*, Ann. Phys. **348** (2014) 341.

[5] M. Lüscher and P. Weisz, *Quark confinement and the bosonic string*, JHEP **7** (2002) 049.

[6] B. Lucini, M. Teper, and U. Wenger, *Glueballs and k-strings in SU(N) gauge theories: Calculations with improved operators*, JHEP **6** (2004) 012.

[7] A. Athenodorou and M. Teper, *SU(N) gauge theories in 2+1 dimensions: glueball spectra and k-string tensions*, JHEP **2** (2017) 015.

[8] Athenodorou, A.; Teper, M. *On the mass of the world-sheet 'axion'in SU(N) gauge theories in 3+ 1 dimensions*, Phys. Lett. B **771** (2017) 408.

[9] P. Cea, L. Cosmai, F. Cuteri and A. Papa, *Flux tubes in the QCD vacuum*, Phys. Rev. D **95** (2017) 114511.

[10] R. Yanagihara, T. Iritani, M. Kitazawa, M. Asakawa, and T. Hatsuda, *Distribution of stress tensor around static quark–anti-quark from Yang–Mills gradient flow*, Phys. Lett. B **789** (2019) 210.

[11] R. Yanagihara and M. Kitazawa, *A study of stress-tensor distribution around the flux tube in the Abelian–Higgs model*, Prog. Theor. Exp. Phys. **2019** (2019) 093B02; [Erratum-ibid: 2020 (2020) id.079201].

[12] S. Nishino, K. Kondo, A. Shibata, T. Sasago and S. Kato, *Type of dual superconductivity for the SU(2) Yang–Mills theory*, Eur. Phys. J. C **79** (2019) 774.

[13] G. S. Bali, *Casimir scaling of SU(3) static potentials*, Phys. Rev. D **62** (2000) 114503.

[14] S. Kratochvila and P. de Forcrand, *Observing string breaking with Wilson loops*, Nucl. Phys. B **671** (2003) 103.

[15] L. Del Debbio, M. Faber, J. Greensite, and Š. Olejník, *Center dominance and $Z_2$ vortices in SU(2) lattice gauge theory*, Phys. Rev. D **55** (1997) 2298.

[16] L. Del Debbio, M. Faber, J. Giedt, J. Greensite, and Š. Olejník, *Detection of center vortices in the lattice Yang-Mills vacuum*, Phys. Rev. D **58** (1998) 094501

[17] Ph. de Forcrand and M. Pepe, *Center vortices and monopoles without lattice Gribov copies*, Nucl. Phys. B **598**, (2001) 557.

[18] M. Faber, J. Greensite, and S. Olejník, *Direct Laplacian Center Gauge*, JHEP **1** (2001) 053.

[19] R. Golubich and M. Faber, *The Road to Solving the Gribov Problem of the Center Vortex Model in Quantum Chromodynamics*, Acta Phys. Polon. Suppl. **13** (2020) 59.

[20] M. Engelhardt and H. Reinhardt, *Center projection vortices in continuum Yang–Mills theory*, Nucl. Phys. B **567** (2000) 249.

[21] C. Alexandrou, P. de Forcrand and M. D'Elia, *The role of center vortices in QCD*, Nucl. Phys. A **663** (2000) 1031.

[22] P. de Forcrand and M. D'Elia, *Relevance of center vortices to QCD*, Phys. Rev. Lett. **82** (1999) 4582.

[23] R. Höllwieser, T. Schweigler, M. Faber and U. M. Heller, *Center vortices and chiral symmetry breaking in SU(2) lattice gauge theory*, Phys. Rev. D **88** (2013) 114505.

[24] S.M.H. Nejad, M. Faber and R. Höllwieser, *Colorful plane vortices and chiral symmetry breaking in SU(2) lattice gauge theory*, JHEP **10** (2015) 108.

[25] S. Deldar, Z. Dehghan, M. Faber, R. Golubich and R. Höllwieser, *Influence of Fermions on Vortices in SU(2)-QCD*, Universe **7** (2021) 130.

[26] D. Trewartha, W. Kamleh and D. Leinweber, *Evidence that centre vortices underpin dynamical chiral symmetry breaking in SU(3) gauge theory*, Phys. Lett. B **747** (2015) 373.

[27] D. Trewartha, W. Kamleh and D. Leinweber, *Connection between center vortices and instantons through gauge-field smoothing*, Phys. Rev. D **92** (2015) 074507.

[28] J. Gattnar, K. Langfeld, A. Schäfke and H. Reinhardt, *Center-vortex dominance after dimensional reduction of $SU(2)$ lattice gauge theory*, Phys. Lett. B **489** (2000) 251.

[29] M. Engelhardt, K. Langfeld, H. Reinhardt and O. Tennert, *Deconfinement in SU(2) Yang-Mills theory as a center vortex percolation transition*, Phys. Rev. D **61** (2000) 054504.

[30] R. Bertle, M. Engelhardt, and M. Faber, *Topological susceptibility of Yang-Mills center projection vortices*. Phys. Rev. D **64** (2001) 074504.

[31] J. Gattnar, C. Gattringer, K. Langfeld, H. Reinhardt, A. Schafer, S. Solbrig, and T. Tok, *Center vortices and Dirac eigenmodes in SU(2) lattice gauge theory*, Nucl. Phys. B **716** (2005) 105.

[32] J.M. Cornwall, *Quark confinement and vortices in massive gauge-invariant QCD*, Nucl. Phys. B **157** (1979) 392.

[33] G. Mack and V.B. Petkova, *Comparison of lattice gauge theories with gauge groups $Z_2$ and $SU(2)$*, Annals Phys. **123** (1979) 442.

[34] H.B. Nielsen and P. Olesen, *A quantum liquid model for the QCD vacuum: gauge and rotational invariance of domained and quantized homogeneous color fields*, Nucl. Phys. B **160** (1979) 380.

[35] J. C. Biddle, W. Kamleh and D. B. Leinweber, *Visualization of center vortex structure*, Phys. Rev. D **102** (2020) 034504.

[36] K. Langfeld, H. Reinhardt and O. Tennert, *Confinement and scaling of the vortex vacuum of SU(2) lattice gauge theory*, Phys. Lett. B **419** (1998) 317.

[37] P. Y. Boyko, M. I. Polikarpov and V. I. Zakharov, *Geometry of percolating monopole clusters*, Nucl. Phys. Proc. Suppl. **119** (2003) 724.

[38] V. G. Bornyakov, P. Y. Boyko, M. I. Polikarpov and V. I. Zakharov, *Monopole clusters at short and large distances*, Nucl. Phys. B **672** (2003) 222.

[39] K. Langfeld, *Vortex structures in pure lattice gauge theory*, Phys. Rev. D **69** (2004) 014503.

[40] J. Greensite, *An Introduction to the Confinement Problem*, 2nd ed.; Springer Nature Switzerland: Cham, Switzerland, 2020.

[41] B. Lucini and M. Teper, *Confining strings in gauge theories*, Phys. Rev. D **64** (2001) 105019.

[42] M. Faber, J. Greensite and Š. Olejník, *Casimir scaling from center vortices: Towards an understanding of the adjoint string tension*, Phys. Rev. D **57** (1998) 2603.

[43] J. Greensite, K. Langfeld, S. Olejník, H. Reinhardt and T. Tok, *Color screening, Casimir scaling, and domain structure in G(2) and SU(N) gauge theories*, Phys. Rev. D **75** (2007) 034501.

[44] M. Engelhardt and H. Reinhardt, *Center vortex model for the infrared sector of Yang–Mills theory—confinement and deconfinement*, Nucl. Phys. B **585** (2000) 591.

[45] M. Engelhardt, M. Quandt and H. Reinhardt, *Vortex model for the infrared sector of SU(3) Yang–Mills theory—confinement and deconfinement*, Nucl. Phys. B **685** (2004) 227.

[46] H. Reinhardt, *Topology of center vortices*, Nucl. Phys. B **628** (2002) 133.

[47] L. E. Oxman, *4d ensembles of percolating center vortices and chains*, PoS(Confinement2018) **336** (2019) 054.

[48] A.L.L. de Lemos, L.E. Oxman and B.F.I. Teixeira, *Derivation of an Abelian effective model for instanton chains in 3D Yang-Mills theory*, Phys. Rev. D **85** (2012) 125014.

[49] L. E. Oxman and H. Reinhardt, *Effective theory of the D=3 center vortex ensemble*, Eur. Phys. J. C **78** (2018) 177.

[50] Kleinert, H. *Gauge Fields in Condensed Matter. No. Bd. 2 in Gauge Fields in Condensed Matter*; World Scientific: Singapore, 1989.

[51] Kleinert, H. *Path Integrals in Quantum Mechanics, Statics, Polymer Physics, and Financial Markets*; World Scientific: Singapore, 2006.

[52] G. H. Fredrickson, *The Equilibrium Theory of Inhomogeneous Polymers*, 1st ed.; Clarendon Press: Oxford, UK, 2006; p. 452.

[53] Durhuus, B.; Ambjørn, J.; Jonsson, T. *Quantum Geometry: A Statistical Field Theory Approach*; Cambridge University Press: Cambridge, UK, 1997.

[54] J. F. Wheater, *Random surfaces: From polymer membranes to strings*, J. Phys. A **27** (1994) 3323.

[55] S. J. Rey, *Higgs mechanism for Kalb-Ramond gauge field*, Phys. Rev. D **40** (1989) 3396.

[56] L. E. Oxman, *4D ensembles of percolating center vortices and monopole defects: The emergence of flux tubes with N-ality and gluon confinement*, Phys. Rev. D **98** (2018) 036018.

[57] J. M. Cornwall, *Finding Dynamical Masses in Continuum QCD*, In Proceedings of the Workshop on Non-Perturbative Quantum Chromodynamics; K. A. Milton & M. A. Samuel, Eds.; Birkhäuser: Stuttgart, Germany, 1983.

[58] S. Deldar, *Potentials between static SU(3) sources in the fat-center-vortices model*, JHEP **1** (2001) 013.

[59] C. D. Fosco, A. Kovner, *Vortices and bags in dimensions*, Phys. Rev. D **63** (2001) 045009.

[60] I. I. Kogan, A. Kovner, *Monopoles, Vortices and Strings: Confinement and Deconfinement in 2+1 Dimensions at Weak Coupling*, arXiv:hep-th/0205026.

[61] L. E. Oxman and G. C. Santos-Rosa, *Detecting topological sectors in continuum Yang-Mills theory and the fate of BRST symmetry*, Phys. Rev. D **92** (2015) 125025.

[62] D. Fiorentini, D. R. Junior, L. E. Oxman, and R. F. Sobreiro, Renormalizability of the center-vortex free sector of Yang-Mills theory, Phys. Rev. D **101** (2020) 085007.

[63] D. Fiorentini, D. R. Junior, L. E. Oxman, R. F. Sobreiro, *Renormalizability of a first principles Yang-Mills center-vortex ensemble*, arXiv:2108.11361.

[64] I. M. Singer. Commun. *Some remarks on the Gribov ambiguity*, Math. Phys. **60** (1978) 7.

[65] D. Fiorentini, D. R. Junior, L. E. Oxman, G. M. Simões, R. F. Sobreiro, *Study of Gribov copies in a Yang-Mills ensemble*, Phys. Rev. D **103** (2021) 114010.

[66] A. Gorsky, M. Shifman, and A. Yung, *Non-Abelian Meissner effect in Yang-Mills theories at weak coupling*, Phys. Rev. D **71** (2005) 045010.

[67] A. Hanany and D. Tong, Vortices, *Instantons and branes*, JHEP **307**, **2003**, 037.

[68] R. Auzzi, S. Bolognesi, J. Evslin, K. Konishi, and A. Yung, *Nonabelian superconductors: Vortices and confinement in N=2 SQCD*, Nucl. Phys. B **673** (2003) 187.

[69] M. Shifman and A. Yung, N*on-Abelian string junctions as confined monopoles*, Phys. Rev. D **70** (2004) 045004.

[70] A. Hanany and D. Tong, *Vortex strings and four-dimensional gauge dynamics*, JHEP **404** (2004) 066.

[71] V. Markov, A. Marshakov, A. Yung, *Non-Abelian vortices in N= 1* gauge theory*, Nucl. Phys. B **709** (2005) 267.

[72] A. P. Balachandran, S. Digal, T. Matsuura, *Semisuperfluid strings in high density QCD*, Phys. Rev. D **73** (2006) 074009.

[73] M. Eto, Y. Isozumi, M. Nitta, K. Ohashi, N. Sakai, *Moduli space of non-Abelian vortices*, Phys. Rev. Lett. **96** (2006) 161601.

[74] M. Eto, K. Konishi, G. Marmorini, M. Nitta,K. Ohashi, W. Vinci, N. Yokoi, *Non-Abelian vortices of higher winding numbers*, Phys. Rev. D **74** (2006) 065021.

[75] E. Nakano, M. Nitta, T. Matsuura, *Non-Abelian strings in high-density QCD: Zero modes and interactions* , Phys. Rev. D **78** (2008) 045002.

[76] J. Ambjorn, J. Giedt and J. Greensite, *Vortex Structure vs. Monopole Dominance in Abelian-Projected Gauge Theory*, JHEP **2** (2000) 033.

[77] J. Greensite, R. Höllwieser, *Double-winding Wilson loops and monopole confinement mechanisms*, Phys. Rev. D **91** (2015) 054509.

[78] A. S. Kronfeld, M. L. Laursen, G. Schierholz, and U.-J. Wiese, *Monopole condensation and color confinement*, Phys. Lett. B **198** (1987) 516.

[79] M. N. Chernodub, F. V. Gubarev, M. I. Polikarpov, and A. I. Veselov, *Monopoles in the Abelian projection of gluodynamics*, Prog. Theor. Phys. Suppl. **131** (1998) 309.

[80] A. Di Giacomo, B. Lucini, L. Montesi, and G. Paffuti, *Color confinement and dual superconductivity of the vacuum. I*, Phys. Rev. D **61** (2000) 034503.

[81] L. E. Oxman, G. C. Santos-Rosa and B. F. I. Teixeira, *Coloured loops in 4D and their effective field representation*, J. Phys. A **47** (2014) 305401.

[82] M. Quandt, H. Reinhardt and M. Engelhardt, *Center vortex model for the infrared sector of Yang-Mills theory: Vortex free energy*, Phys. Rev. D **71** (2005) 054026.

[83] L. E. Oxman, *Confinement of quarks and valence gluons in SU(N) Yang-Mills-Higgs models*, JHEP **3** (2013) 038.

[84] H. Reinhardt and M. Engelhardt, *Center vortices in continuum Yang-Mills Theory*, in Proceeding of the 4th International Conference in Quark confinement and the hadron spectrum, Vienna, Austria, July 3-8, 2000.

[85] Y. Nambu, *Strings, monopoles, and gauge fields*, Phys. Rev. D **10** (1974) 4262.

[86] S. Mandelstam, *Vortices and quark confinement in non-Abelian gauge theories*, Physics Reports **23** (1976) 245.

[87] John R. Klauder and Bo-Sture Skagerstam, *Coherent States: Applications in Physics and Mathematical Physics*, World Scientific, 1985.

[88] A. Perelemov, *Generalized Coherent States and Their Applications*; Springer: Berlin/Heidelberg, Germany, 1986.

[89] D. Diakonov and V. Petrov, *A formula for the Wilson loop*, Phys. Lett. B **224** (1989) 131.

[90] Kei-Ichi Kondo, *Abelian magnetic monopole dominance in quark confinement*, Phys. Rev. D **58** (1998) 105016.

[91] Kei-Ichi Kondo and Yutaro Taira, *Non-Abelian Stokes Theorem and Quark Confinement in $SU(N)$ Yang-Mills Gauge Theory*, Prog. Theor. Phys. **104** (2000) 1189.

[92] M. Creutz, *On invariant integration over $SU(N)$*, Journal of Mathematical Physics **19** (1978) 2043.

[93] M. Hamermesh, *Group Theory and its Applications to Physical Problems*, Dover, 1989.

[94] R. Gilmore, *Lie Groups, Lie Algebras, and Some of Their Applications* (Dover Publications, 2006).

[95] Wei-Min Zhang, Da Hsuan Feng and Robert Gilmore, *Coherent states: theory and some applications*, Rev. Mod. Phys. **62** (1990) 867.

[96] A. P. Balachandran, P. Salomonson, B. Skagerstam and J. Winnberg, *Classical description of a particle interacting with a non-Abelian gauge field*, Phys. Rev. D **15** (1977) 2308.

[97] R. Auzzi and S. P. Kumar, *Non-Abelian k-vortex dynamics in $\mathcal{N} = 1^*$ theory and its gravity dual*, JHEP **12** (2008) 77.

[98] S. Maedan, Y. Matsubara, and T. Suzuki, *Abelian confinement mechanism and the QCD vacuum*, Prog. Theor. Phys. **84** (1990) 130.

[99] Y. Koma, E. M. Ilgenfritz, H. Toki, and T. Suzuki, *Casimir scaling in a dual superconducting scenario of confinement*, Phys. Rev. D **64** (2001) 011501.

[100] Y. Koma, M. Koma, E. M. Ilgenfritz, and T. Suzuki, *Detailed study of the Abelian-projected SU (2) flux tube and its dual Ginzburg-Landau analysis*, Phys. Rev. D **68** (2003) 114504.

[101] M. Baker, J. S. Ball, and F. Zachariasen, *QCD flux tubes for SU (3)*, Phys. Rev. D **41** (1990) 2612.

[102] M. Baker, J. S. Ball, and F. Zachariasen, *Static heavy-quark potential calculated in the classical approximation to dual QCD*, Phys. Rev. D **44** (1991) 3328.

[103] M. Baker, N. Brambilla, H. G. Dosch, and A. Vairo, *Field strength correlators and dual effective dynamics in QCD*, Phys. Rev. D **58** (1998) 034010.

[104] D. Tong, *Monopoles in the Higgs phase*, Phys. Rev. D **69** (2004) 065003.

[105] D. Tong, *Quantum vortex strings: a review*, Ann. Phys. **324** (2009) 30.

[106] K. Konishi, *The Magnetic Monopoles Seventy-five Years Later*, Lect. Notes Phys. **737** (2008) 471.

[107] A. Armoni and M. Shifman, *Remarks on stable and quasi-stable k-strings at large N*, Nucl. Phys. B **671** (2003) 67.

[108] K. Konishi and L. Spanu, *Non-Abelian vortex and confinement*, Int. J. Mod. Phys. A **18** (2003) 249.

[109] M. A. C. Kneipp and P. Brockill, *BPS string solutions in non-Abelian Yang-Mills theories and confinement*, Phys. Rev. D **64** (2001) 125012.

[110] M. A. C. Kneipp, *BPS $Z_N$ string tensions, sine law and Casimir scaling, and integrable field theories*, Phys. Rev. D **76** (2007) 125010.

[111] J. Greensite and Š. Olejník, *k-string tensions and center vortices at large N*, J. High Energy Phys. **09** (2002) 039.

[112] H. J. de Vega, F. A. Schaposnik, *Vortices and electrically charged vortices in non-Abelian gauge theories*, Phys. Rev. D **34** (1986) 3206.

[113] N. Manton and P. Sutcliffe, *Topological Solitons*, (Cambridge University Press, 2004)

[114] L. E. Oxman and D. Vercauteren, *Exploring center strings in and relativistic Yang-Mills-Higgs models*, Phys. Rev. D **95** (2017) 025001.

[115] M. Eto, T. Fujimori, S. Gudnason, K. Konishi, M. Nitta, K. Ohashi, and W. Vinci, *Constructing non-Abelian vortices with arbitrary gauge groups*, Phys. Lett. B **669** (2008) 98.

[116] M. Shifman and A. Yung, *Constructing non-Abelian vortices with arbitrary gauge groups*, Phys. Rev. D **70** (2004) 025013.

[117] L. E. Oxman and G. M. Simões, *$k-$strings with exact Casimir law and Abelian-like profiles*, Phys. Rev. D **99** (2019) 016011.

[118] A. Hanany and D. Tong, *Vortex strings and four-dimensional gauge dynamics*, J. High Energy Phys. **04** (2004) 66.

[119] M. A. C. Kneipp, *Color superconductivity, Z(N) flux tubes, and monopole confinement in deformed N= 2* super Yang-Mills theories*, Phys. Rev. D **69** (2004) 045007.

[120] L. E. Oxman, *$SU(N) \to Z(N)$ dual superconductor models: the magnetic loop ensemble point of view*, EPJ Web Conf. **137** (2017) 03015.

[121] C. Alexandrou and G. Koutsou, *Static tetraquark and pentaquark potentials*, Phys. Rev. D **71** (2005) 014504.

[122] P. Bicudo, N. Cardoso, and M. Cardoso, *Colour flux-tubes in static pentaquark and tetraquark systems*, Prog. in Part. and Nuc. Phys. **67** (2012) 440.

[123] P. Bicudo, M. Cardoso, O. Oliveira, and P. J. Silva, *Lattice QCD static potentials of the meson-meson and tetraquark systems computed with both quenched and full QCD*, Phys. Rev. D **96** (2017) 074508.

[124] V. N. Gribov, *Quantization of Nonabelian Gauge Theories*, Nucl. Phys. B **139** (1978) 1.

[125] R. F. Sobreiro and S. P. Sorella, *Introduction to the Gribov ambiguities in Euclidean Yang-Mills theories*, In *13th Jorge Andre Swieca Summer School on Particle and Fields Campos do Jordao, Brazil, January 9-22, 2005.*

[126] D. Zwanziger, *Local and Renormalizable Action From the Gribov Horizon*, Nucl. Phys. B **32** (1989) 513.

[127] D. Dudal, J. A. Gracey, S. P. Sorella, N. Vandersickel, and H. Verschelde, *A Refinement of the Gribov-Zwanziger approach in the Landau gauge: Infrared propagators in harmony with the lattice results*, Phys. Rev. D **78** (2008) 065047.

[128] D. Dudal, S. P. Sorella, and N. Vandersickel, *The dynamical origin of the refinement of the Gribov-Zwanziger theory*, Phys. Rev. D **84** (2011) 06503.

[129] M.A.L. Capri, V.E.R. Lemes, R.F. Sobreiro, S.P. Sorella, and R. Thibes, *The Influence of the Gribov copies on the gluon and ghost propagators in Euclidean Yang-Mills theory in the maximal Abelian gauge*, Phys. Rev. D **72** (2005) 085021.

[130] M.A.L. Capri, V.E.R. Lemes, R.F. Sobreiro, S.P. Sorella, and R. Thibes, *A Study of the maximal Abelian gauge in SU(2) Euclidean Yang-Mills theory in the presence of the Gribov horizon*, Phys. Rev. D **74** (2006) 105007.

[131] M.A.L. Capri, A.J. Gomez, M.S. Guimaraes, V.E.R. Lemes, and S.P. Sorella, *Study of the properties of the Gribov region in SU(N) Euclidean Yang-Mills theories in the maximal Abelian gauge*, J. Phys. A **43** (2010) 245402.

[132] R.F. Sobreiro and S.P. Sorella, *A Study of the Gribov copies in linear covariant gauges in Euclidean Yang-Mills theories*, Journal of High Energy Physics **06** (2005) 054.

[133] M.A.L. Capri, A.D. Pereira, R.F. Sobreiro, and S.P. Sorella, *Non-perturbative treatment of the linear covariant gauges by taking into account the Gribov copies*, Eur. Phys. Jour. C **75** (2015) 479.

[134] M.A.L. Capri, D. Fiorentini, A.D. Pereira, R.F. Sobreiro, S.P. Sorella, and R.C. Terin, *Aspects of the refined Gribov-Zwanziger action in linear covariant gauges*, Annals Phys. **376** (2017) 40.

[135] A. D. Pereira and R. F. Sobreiro, *On the elimination of infinitesimal Gribov ambiguities in non-Abelian gauge theories*, Eur. Phys. Jour. C **73** (2013) 2584.

[136] M.A.L. Capri, D. Dudal, D. Fiorentini, M.S. Guimaraes, I.F. Justo, A.D. Pereira, B.W. Mintz, L.F. Palhares, R.F. Sobreiro, and S.P. Sorella, *Exact nilpotent nonperturbative BRST symmetry for the Gribov-Zwanziger action in the linear covariant gauge*, Phys. Rev. D **92** (2015) 045039.

[137] M. A. L. Capri, D. Dudal, D. Fiorentini, M. S. Guimaraes, I. F. Justo, A. D. Pereira, B. W. Mintz, L. F. Palhares, R. F. Sobreiro, and S. P. Sorella, *Local and BRST-invariant Yang-Mills theory within the Gribov horizon*, Phys. Rev. D **94** (2016) 025035.

[138] M. A. L. Capri, D. Fiorentini, and S. P. Sorella, *Gribov horizon and non-perturbative BRST symmetry in the maximal Abelian gauge*, Phys. Lett. B **751** (2015) 262.

[139] J. D. Länge, M. Engelhardt, and H. Reinhardt, *Energy density of vortices in the Schrödinger picture*, *Phys. Rev. D* **68** (2003) 025001.

[140] Daniel Zwanziger, *Nonperturbative Modification of the Faddeev-popov Formula and Banishment of the Naive Vacuum*, *Nucl. Phys. B* **209** (1982) 336.

[141] G. Dell'Antonio and D. Zwanziger, *Every gauge orbit passes inside the Gribov horizon*, Commun. Math. Phys. **138** (1991) 291.

[142] Pierre van Baal, *More (thoughts on) gribov copies*, Nucl. Phys. B **369** (1992) 275.

[143] Ph. de Forcrand, J.E. Hetrick, A. Nakamura, and M. Plewnia, *Gauge fixing on the lattice*, Nuclear Physics B - Proceedings Supplements **20** (1991) 194.

[144] G. Dell'Antonio and D. Zwanziger, *Every gauge orbit passes inside the Gribov horizon*, *Communications in Mathematical Physics* **138** (1991) 291.

[145] J. Greensite, S. Olejník, and D. Zwanziger, *Center vortices and the Gribov horizon*, Journal of High Energy Physics **05** (2005) 070.

[146] A. Maas, *Instantons, monopoles, vortices, and the Faddeev-Popov operator eigenspectrum*, Nucl. Phys. A **790** (2007) 566c.

[147] H. Reinhardt and T. Tok, *Abelian and center gauge fixing in continuum Yang–Mills theory for general gauge groups*, Physics Letters B **500** (2001) 173.

[148] Jeroen C. Vink and Uwe-Jens Wiese, *Gauge fixing on the lattice without ambiguity*, Physics Letters B **289** (1992) 122.

[149] C. Ford, U.G. Mitreuter, T. Tok, A. Wipf, and J.M. Pawlowski, *Monopoles, polyakov loops, and gauge fixing on the torus*, Annals of Physics **269** (1998) 26.

[150] Peter W. Higgs, *Broken Symmetries and the Masses of Gauge Bosons*, Phys. Rev. Lett. **13** (1964) 508.

[151] H. J. de Vega, *Fermions and vortex solutions in abelian and non-abelian gauge theories*, Phys. Rev. D **18** (1978) 2932.

[152] C. D. Fosco, D. R. Junior, and L. E. Oxman, *Quantum effects due to a moving Dirichlet point*, Phys. Rev. D **101** (2020) 065014.

[153] D. R. Junior, L. E. Oxman, and G. M. Simões, *3D Yang-Mills confining properties from a non-Abelian ensemble perspective*, JHEP **1** (2020) 180.

[154] A. Maas, *On the spectrum of the Faddeev–Popov operator in topological background fields*, Eur. Phys. J. C **48** (2006) 179.